APPLICATION OF FIRE MONITORING BY USING FY-2C GEOSTATIONARY METEOROLOGICAL SATELLITE AND OTHER SATELLITE

Liu Cheng
National Satellite Meteorological Center China Meteorological Administration
Baishiqiao Road No.46, 100081
Beijing, China

Major Contents

Part 1. The Application of Fire Monitoring by using FY-2C Meteorological Satellite

1. General introduction of FY-2 geostationary satellite.
2. The method of hot spot detection by using FY-2C.
3. FY2C fire monitoring products generating and distribution
4. The application of fire monitoring by using FY-2C

Part 2. The Application of Fire Monitoring by using Meteorological Satellites in NSMC/CMA

1. Background
2. The fire information deriving
3. The operation and service of fire monitoring system
4. The aspects of applications in fire monitoring

1. General introduction of FY-2 series geostationary meteorological satellite

- **FY-2A/B: experiment series**
- FY-2A was launched on June 10, 1997
- FY-2B was launched on June 25, 2000

- **FY-2C/D/E/F/G: operational series**
- **FY-2 Op series is consists of FY-2C/D/E three satellites and 2 more satellites will be added (FY-2F&FY-2G) for connection to FY-4.**
- FY-2C was launched on October 19, 2004, located in 104.5°E. Now in the operational mode.
- FY-2D will be launched on December 8, 2006, and will be located in 86.5°E

Successful launch of FY-2C

FY-2C replaced FY-2B as primary operational spacecraft. The satellite is spin-stabilised and is stationed at 104.5°E. Its mission is to acquire visible, infrared and water vapour cloud images; transmitting S-VISSR images and low resolution images; data collection;space environment monitoring and it carries VISSR and SEM instruments and transmits 24 full-disc and 4 wind images per day.

The Op series is improved based on FY-2A/B with the major improvements on:

- 5 channel radiometers
- More products for widely use in meteorology and Environment
- More frequent observations during the main flooding season (June – August)
  - half-hourly image (48 images each day)

The characteristics of FY-2

FY-2A/B(E)			FY2C/D/E /F/G (O)		
Ch. No.	Wavelength (μm)	Resolution (km)	Ch. No.	Wavelength (μm)	Resolution (km)
1	0.5-1.05 (6 bits)	1.25	1	0.5-0.9 (8 bits)	1.25
2	6.3-7.6 (8 bits)	5	2	3.5-4.0 (10 bits)	5
3	10.5-12.5 (8 bits)	5	3	6.3-7.6 (8 bits)	5
			4	10.3-11.3 (10 bits)	5
			5	11.5-12.5 (10 bits)	5

FY2C First multiple channel composition image 2004/11/20/03:00z

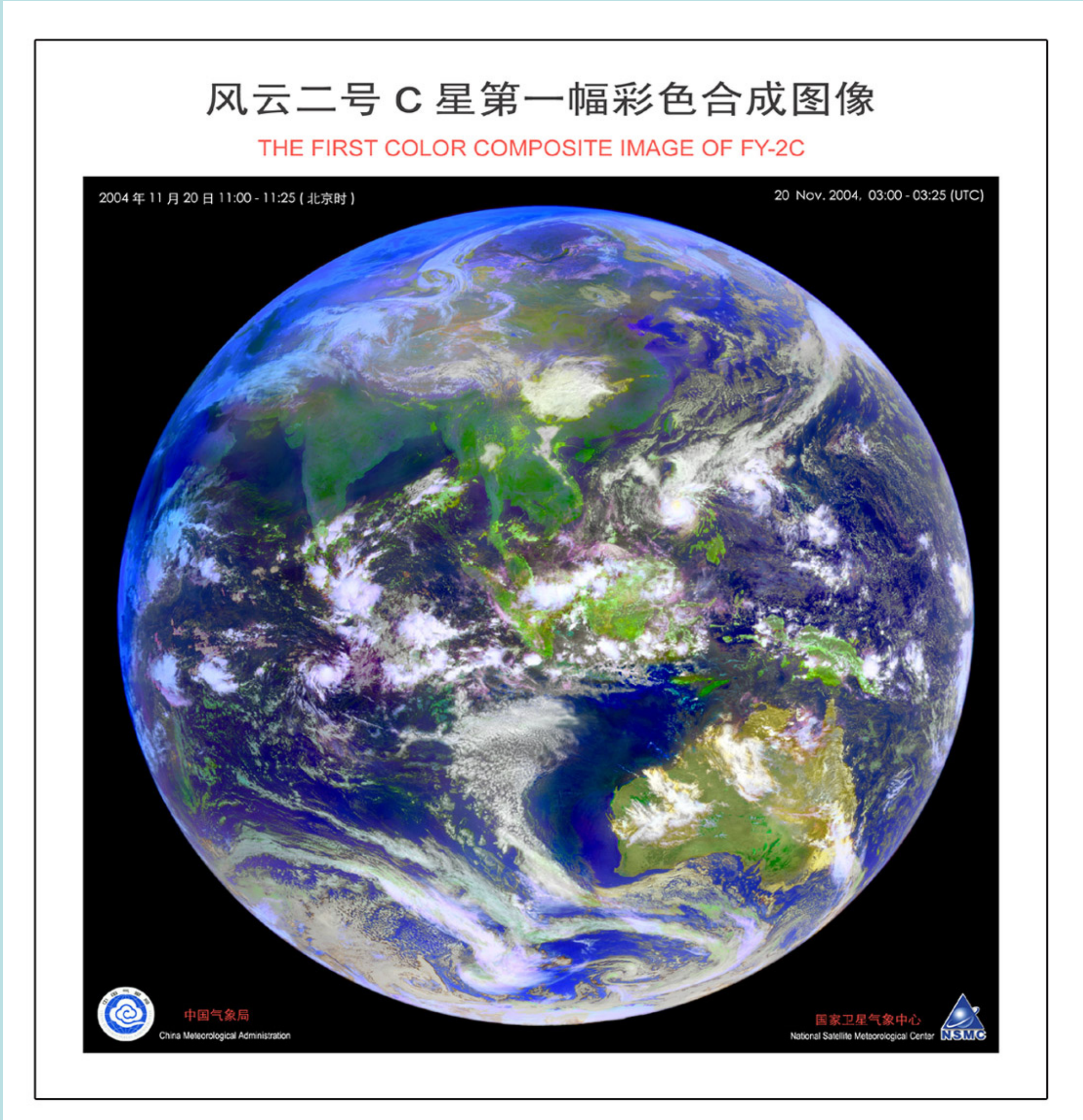

FY2C Visible channel image 2004/11/20/03:00z

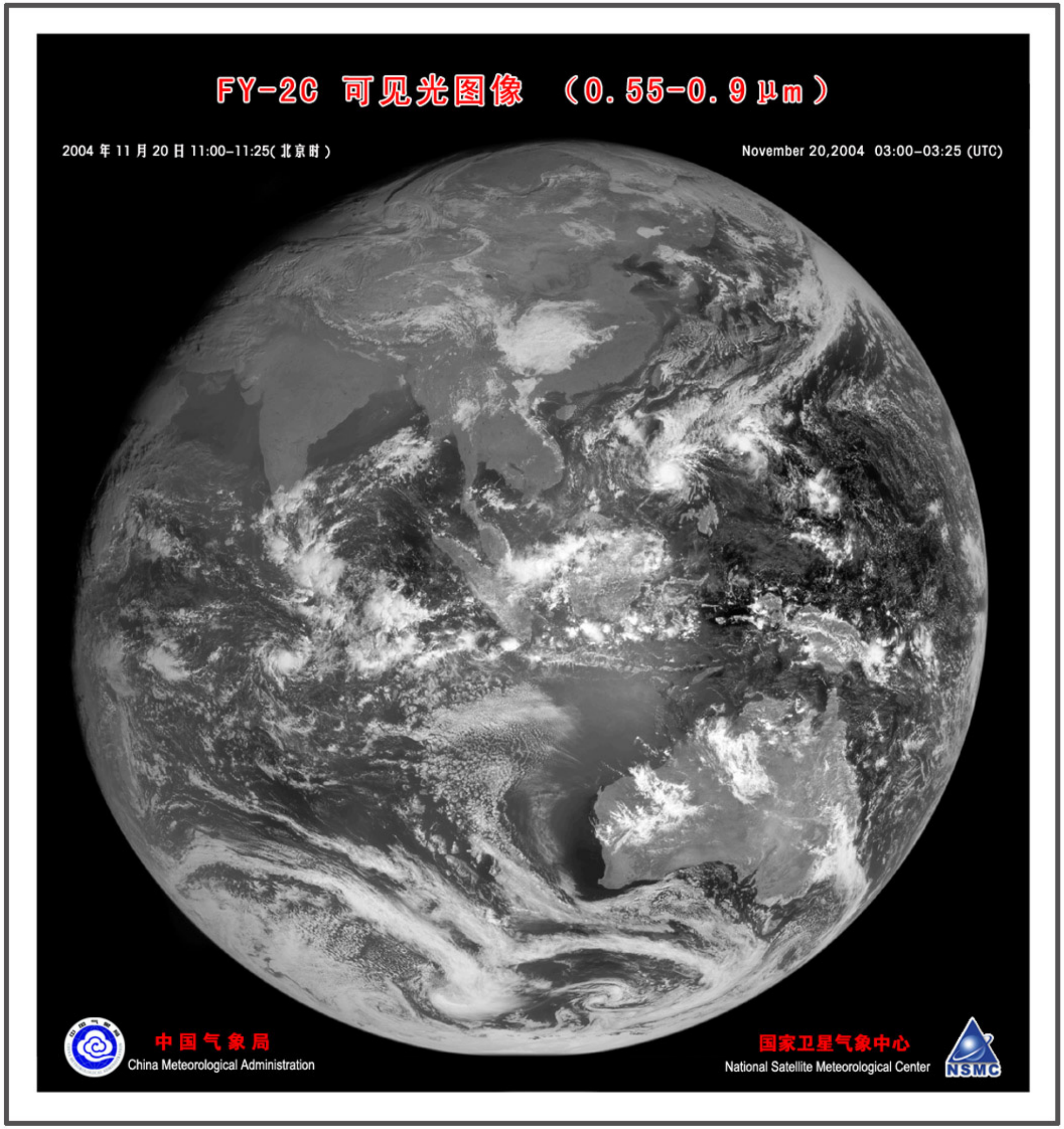

FY2C First far infrared channel image (10.3 – 11.3**μm**)
2004/11/20/03:00z

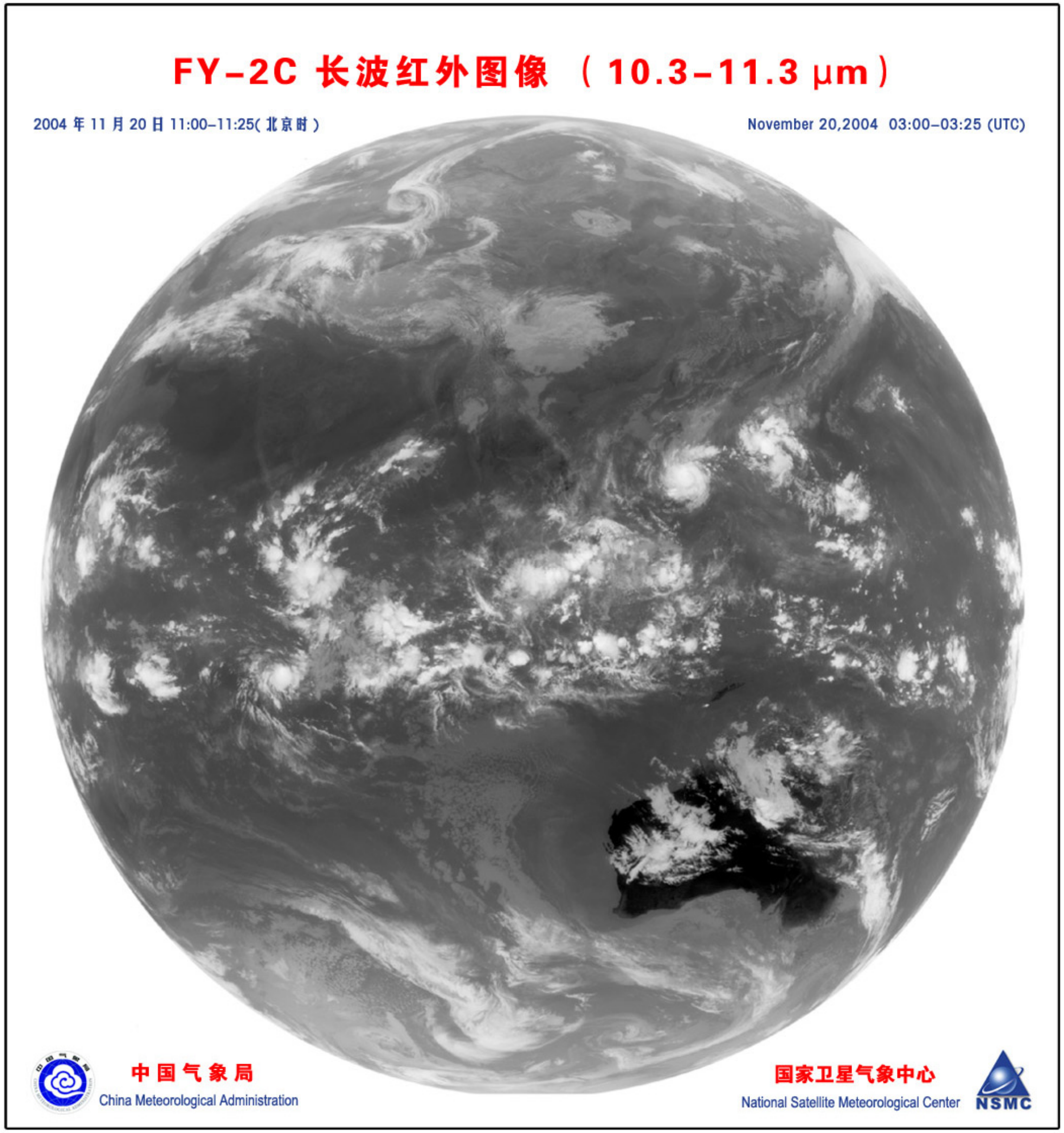

FY2C First far infrared channel image (11.5 – 12.5**μm**)
2004/11/20/03:00z

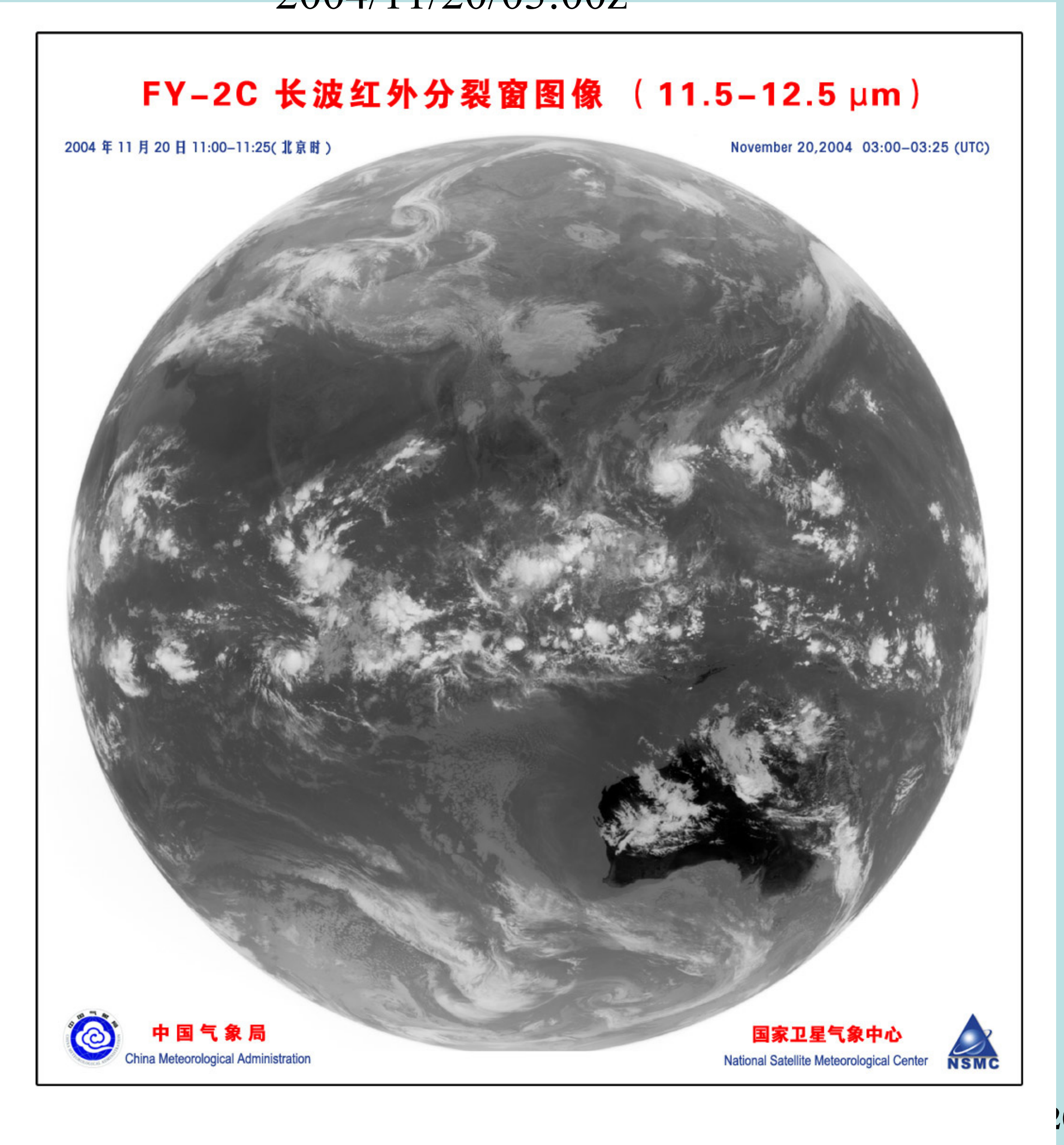

FY2C First water vapor channel image (6.3 – 7.6μm)
2004/11/20/03:00z

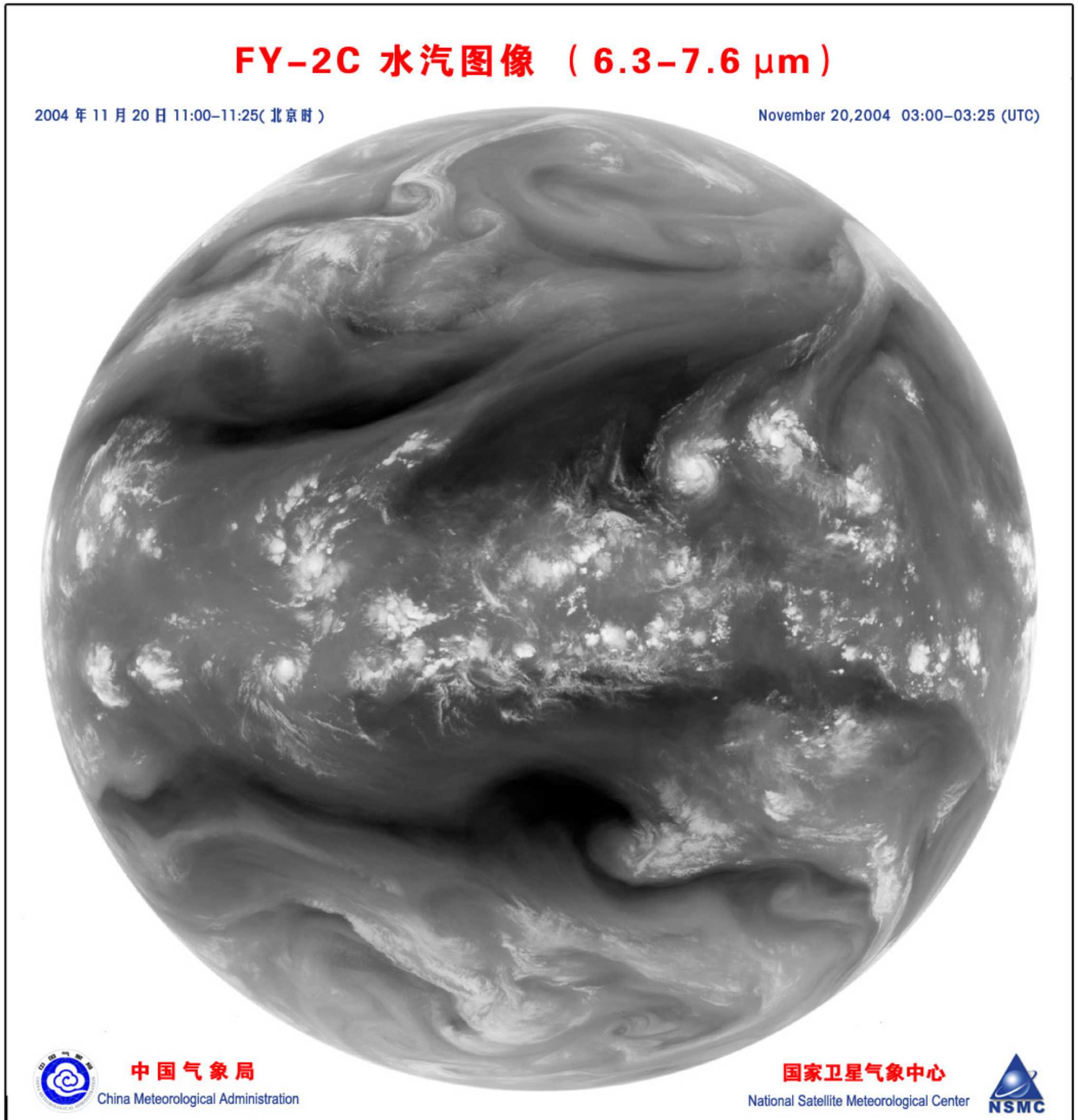

FY2C First mid. infrared channel image (3.5 – 4.0μm)
2004/11/20/03:00z

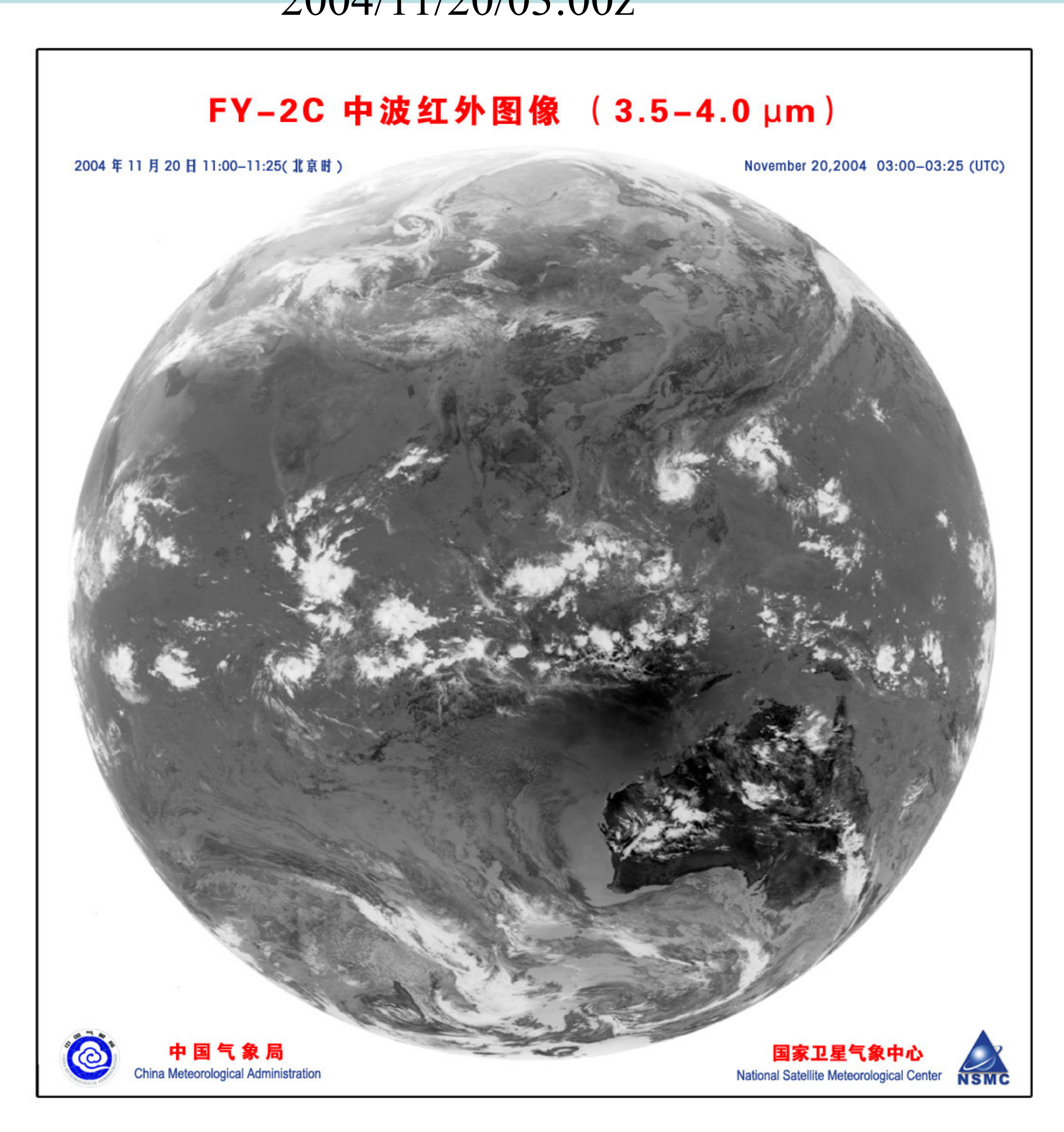

Products from FY2C

Name of Product	Coverage	Time/Day
Wind	50°N-50°S 55°E-155°E	4
SST	60°N-60°S 45°E-165°E	8
Upper Troposphere Humidity	60°N-60°S 45°E-165°E	8
ISCCP Data set	60°N-60°S 45°E-165°E	8
Precipitation Index	60°N-60°S 45°E-165°E	8
Precipitation Estimation	60°N-60°S 45°E-165°E	4
Cloud Classification	60°N-60°S 45°E-165°E	8
Cloud Amount	60°N-60°S 45°E-165°E	8
Humidity Profile from Cloud	50°N-50°S 55°E-155°E	8
Perceptible Water in Clear Sky Region	60°N-60°S 45°E-165°E	8
Outgoing Long wave Radiation	60°N-60°S 45°E-165°E	8
Solar Irradiance	60°N-60°S 45°E-165°E	1
Snow Cover	60°N-60°S 45°E-165°E	1
Sea Ice	60°N-60°S 45°E-165°E	1
Flood Monitoring	China	1
Soil Moisture	60°N-60°S 45°E-165°E	1
Fire Monitoring	China	24
Tropical Cyclone Position and Intensity	Western Pacific and India Ocean	24
Sand Storm Monitoring	China and Mongolia	8
Fog	China	24
TBB	60°N-60°S 45°E-165°E	8

Observation range in 105°E

(FY2C,operational position)

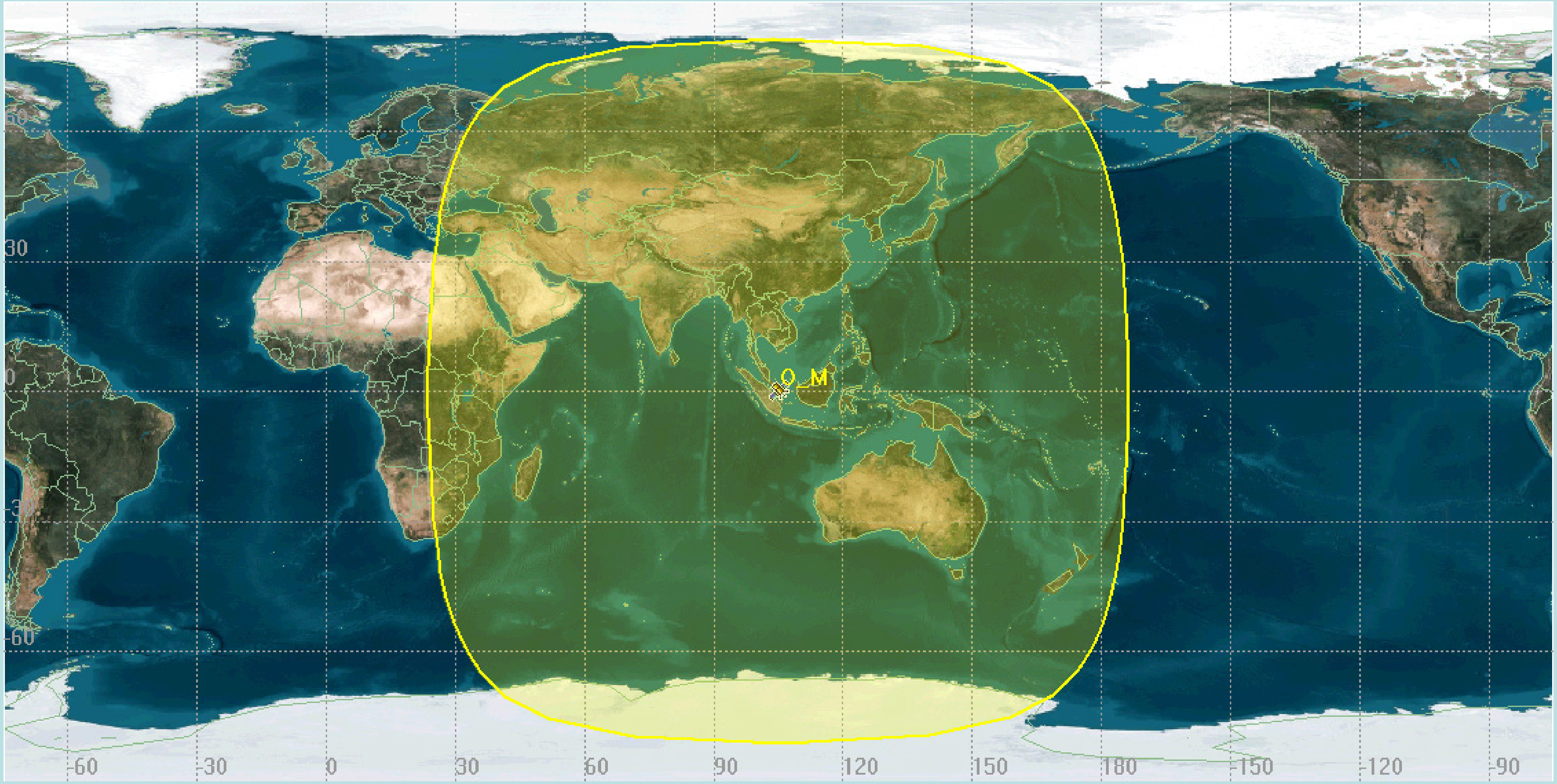

81°N ~ -81°S ，24°E ~ -174°W

Observation range in 86.5°E
(FY2D,backup position)

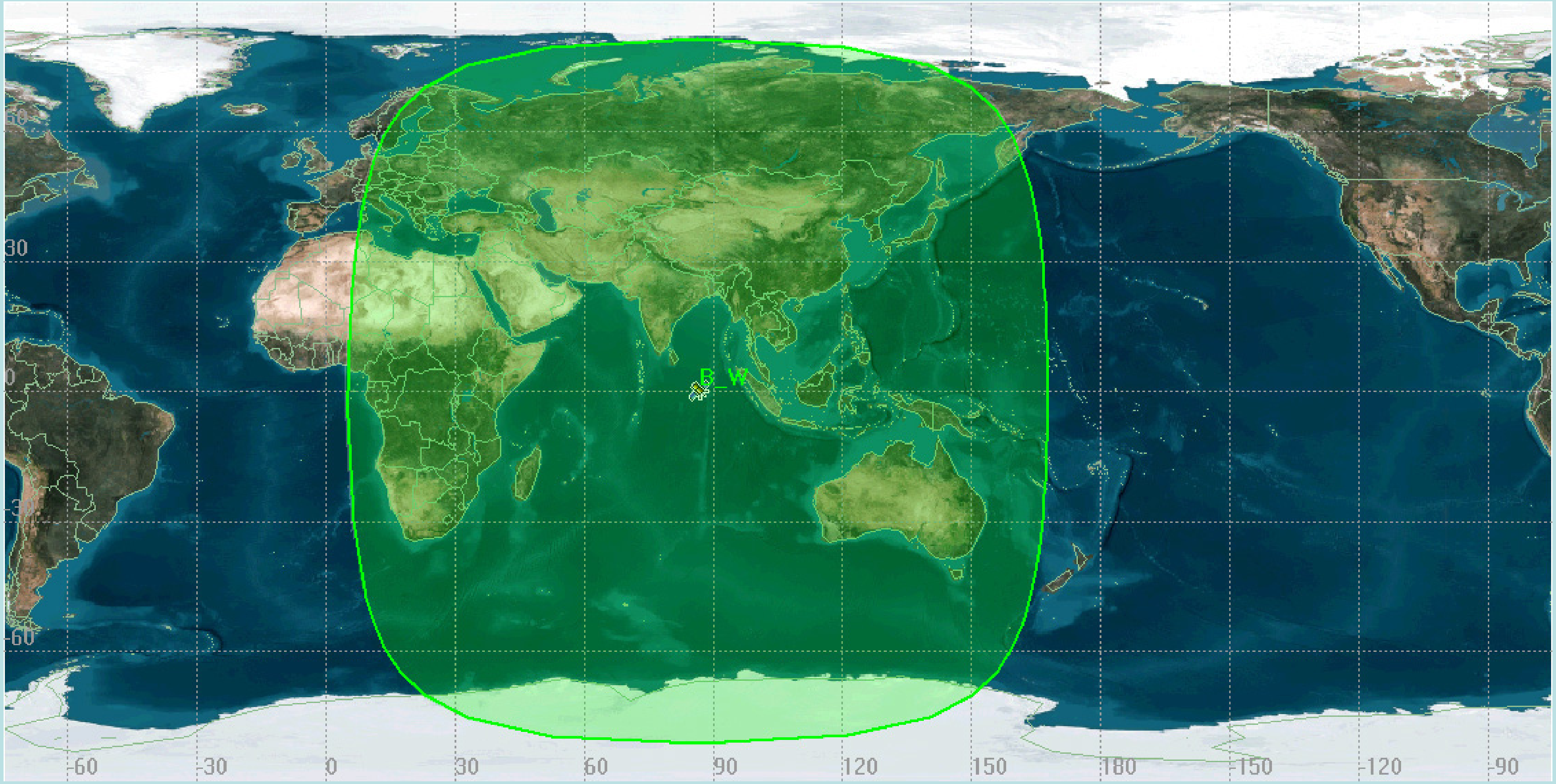

81°N ~ -81°S ，5°E ~ 167°

Two FY2C Satellite Observation Range

(105°和86.5°)

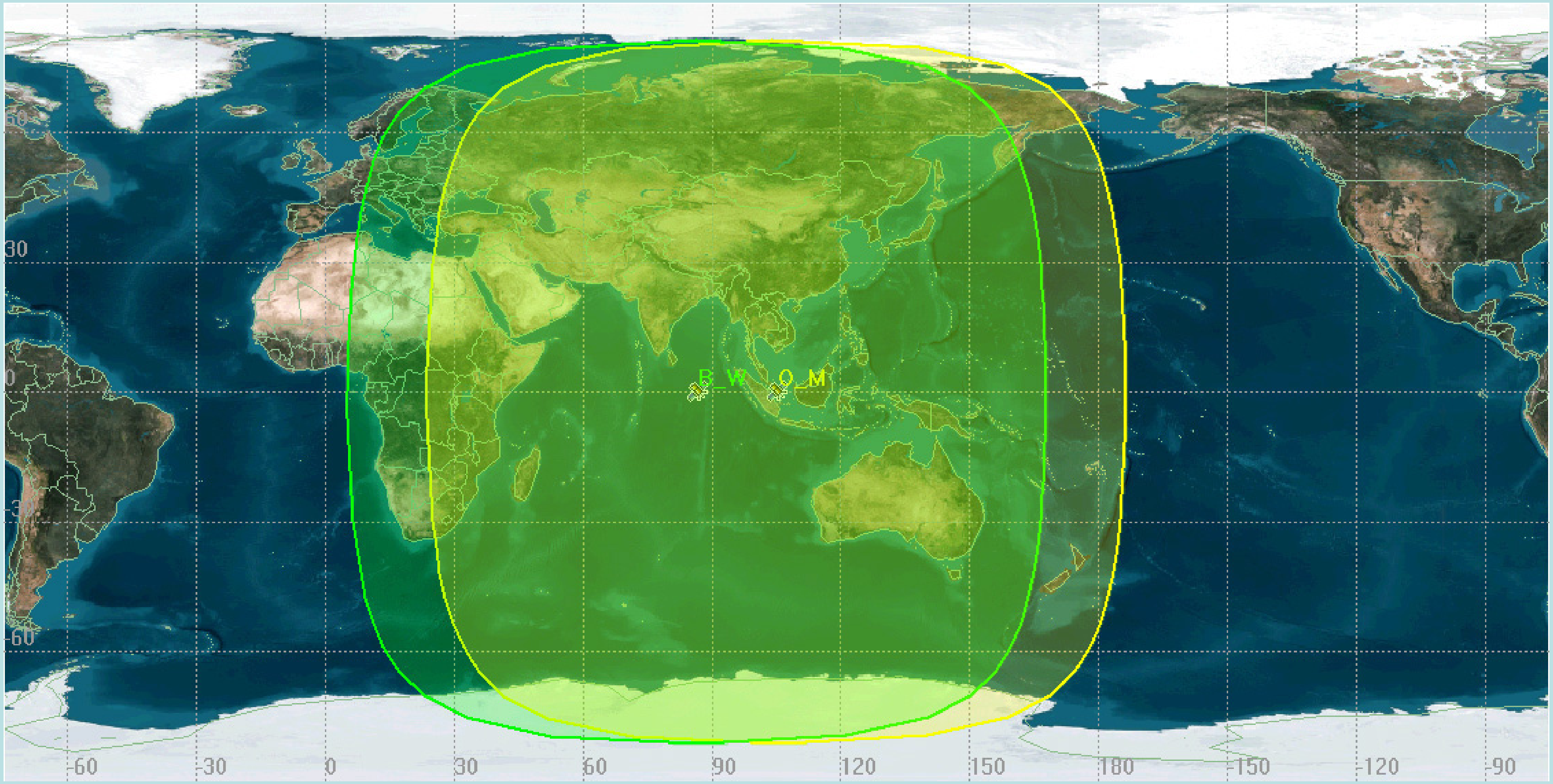

5°E ~ -174°W，about 181°，overlaped: 24°E ~ 167°E，about 143°

FY-2C S-VISSR Time Schedule

No.	Time (GT Time)	Format	No.	Time (GT Time)	Format
1	00:00	Disc	15	12:00	Disc
2	01:00	Disc	16	13:00	Disc
3	02:00	Disc	17	14:00	Disc
4	03:00	Disc	18	15:00	Disc
5	04:00	Disc	19	16:00	Disc
6	04:56	Disc	20	16:56	Disc
7	05:29	Northern Hemisphere	21	17:29	Northern Hemisphere
8	06:00	Disc	22	18:00	Disc
9	07:00	Disc	23	19:00	Disc
10	08:00	Disc	24	20:00	Disc
11	09:00	Disc	25	21:00	Disc
12	10:00	Disc	26	22:00	Disc
13	10:56	Disc	27	22:56	Disc
14	11:29	Northern Hemisphere	28	23:29	Northern Hemisphere

The FY-2 ground segment

- A Primary ground center (Beijing, NSMC)
- A Command and Data Acquisition Station (CDAS),
- An Main Data Processing Center (DPC),
- A System Operational Control Center (SOCC),
- Three Ranging Stations (One primary station and 3 secondary stations)
- Data Collection Platforms (133 DCPs)
- Medium-scale, Small-scale Data Utilization Stations (MDUS, SDUS)
- WEFAX stations, the communication system, etc.

The FY-2 ground segment

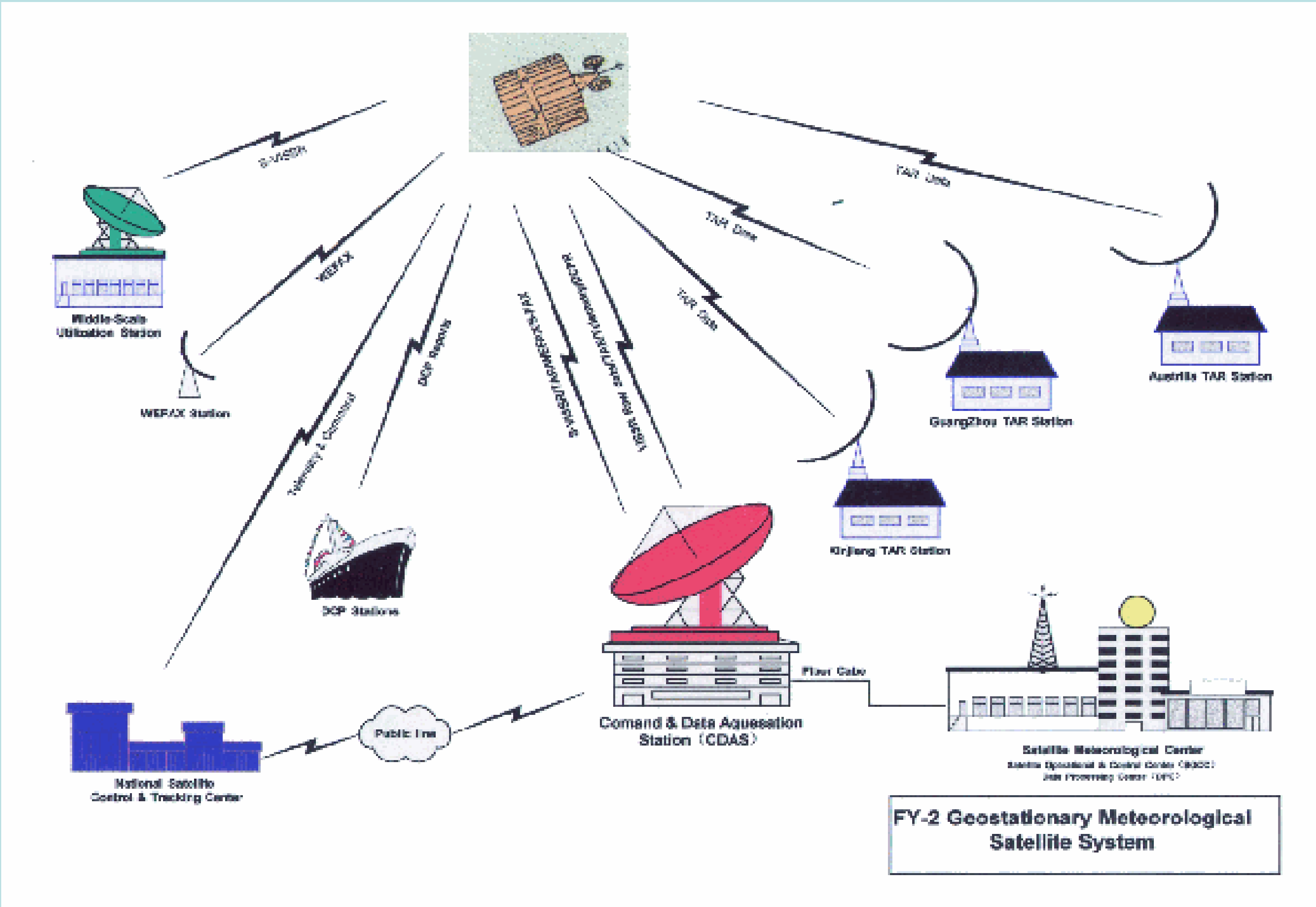

2. The method of hot spot detection by using FY-2C.

1) **Principle Theory**

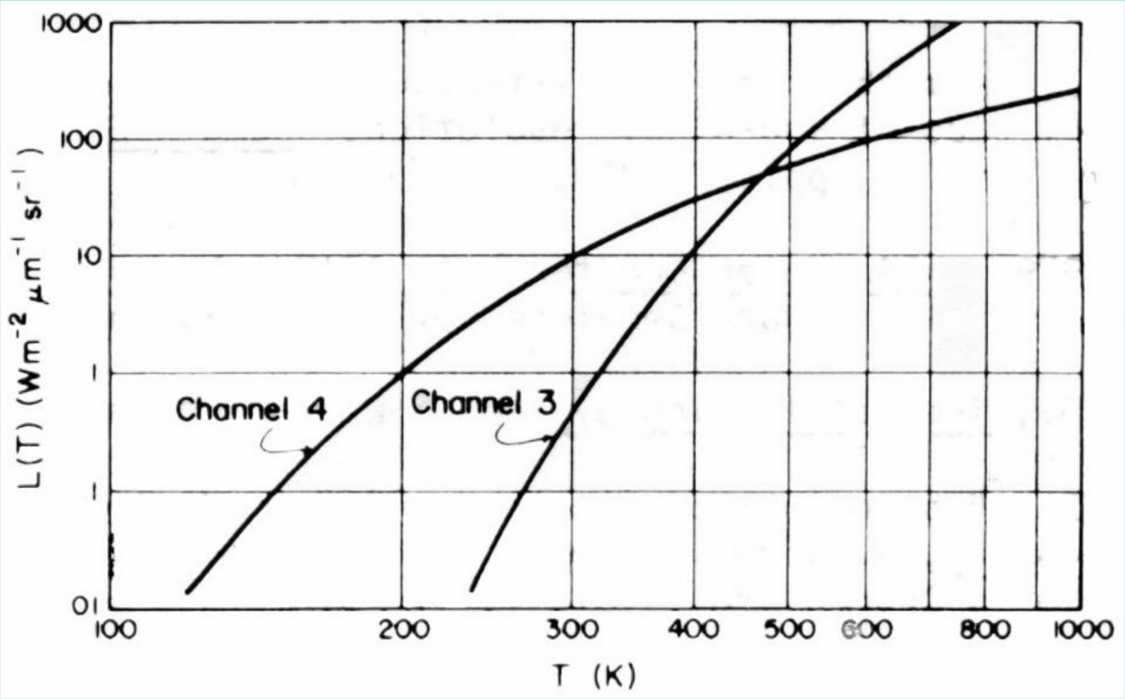

Fig. 2.1. Integrated Planck radiances for 3.8 μm and 11 μm channels of the NOA-6 AVHRR, as calculated by integrating Planck's (Dozzer,1982)

Fig. 2.1 shows that in the same temperature increment, the radiance increment of the mid. Infrared channel (3.7 μ_m) is much bigger than that of thermal infrared channel (11 μ_m). FY-2C channel 2 and 4 are in the central wavelength around 3.7 μ_m and 11 μ_m .

Assuming the radiance of mixed pixel (containing a fire spot) is expressed as below (Dozzer,1982):

$$N_{imix} = P * N_{ihi} + (1 - P) N_{ibg} \qquad (1)$$

$$= P * \frac{C_1 V_i^3}{e^{C_2 V_i / T_{hi}} - 1} + (1 - P) * \frac{C_1 V_i^3}{e^{C_2 V_i / T_{bg}} - 1}$$

The difference of brightness temperature $\triangle Ti$ between mixed pixel and background in CH3,CH4 and CH5 can be expressed as:

$$\Delta T_i = T_{imix} - T_{iB} = \frac{C_2 V_i}{Ln\left(1 + \frac{C_1 V_i^3}{N_{imix}}\right)} - \frac{C_2 V_i}{Ln\left(1 + \frac{C_1 V_i^3}{N_{iB}}\right)}$$

$$= \frac{C_2 V_i}{Ln\left(1 + \frac{C_1 V_i^3}{P(N_{ihi} - N_{iB}) + N_{iB}}\right)} - \frac{C_2 V_i}{Ln\left(1 + \frac{C_1 V_i^3}{N_{iB}}\right)} \qquad (2)$$

When the sub-pixel size is up to only 1% in the condition of T_{hi} = 500K and T_{bg} = 290K, the △Ti in CH2 is already up to about 40K. There is also a increment in CH4 and CH5, but is much smaller than that in CH3, and when the sub-pixel size is up to about 12%, the △Ti is up to about 40K.

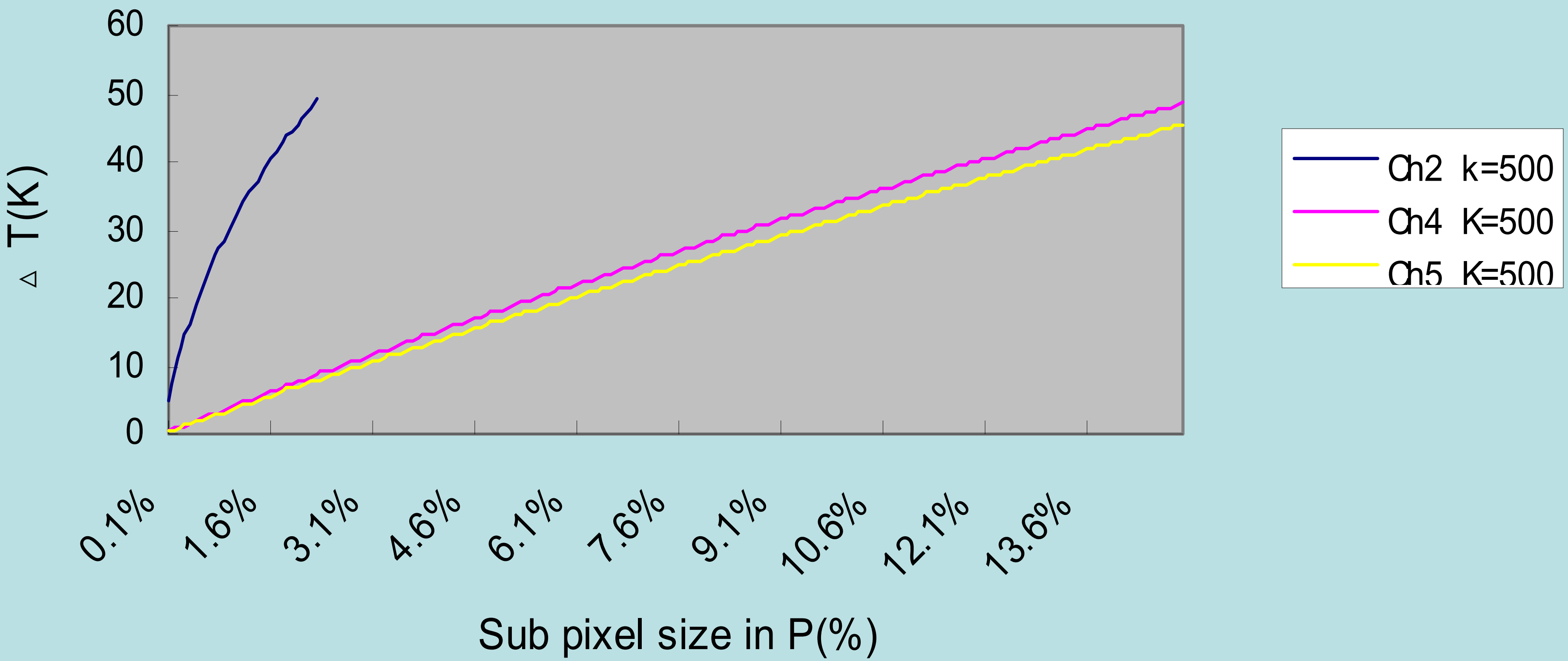

Fig.2.2 The difference of brightness temperature between mixed pixel and background along with sub-pixel size and temperature of fire spot changing in CH2, CH4 and CH5。

Fig.2.3 shows when temperature in an active fire getting higher, the temperature increment in Ch.2 will be much higher tan that of Ch.4,5.

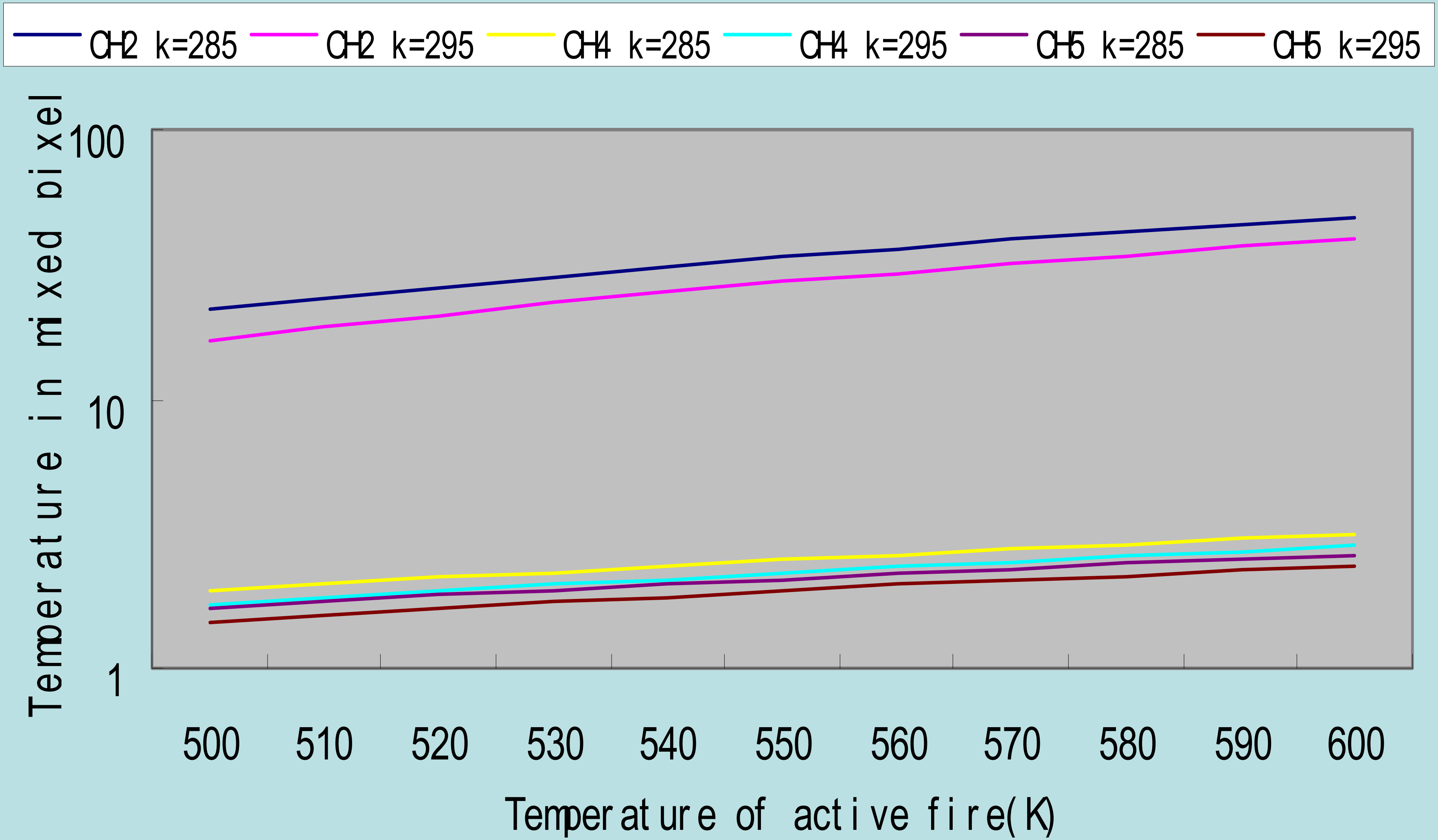

Fig.2.3 The relationship curve of temperature increment of a mixed pixel in channel 2,4,5 following the temperature increasing of fire spot within the pixel in the condition of same size (p=0.5%) and same temperature in the background.

Fig.2.4 shows that when temperature increase from lower range, the count value in Ch2 changed much slower than that of Ch.4 and Ch.5, until it reached to around 290K, then it changed much faster than Ch.4 and Ch.5.

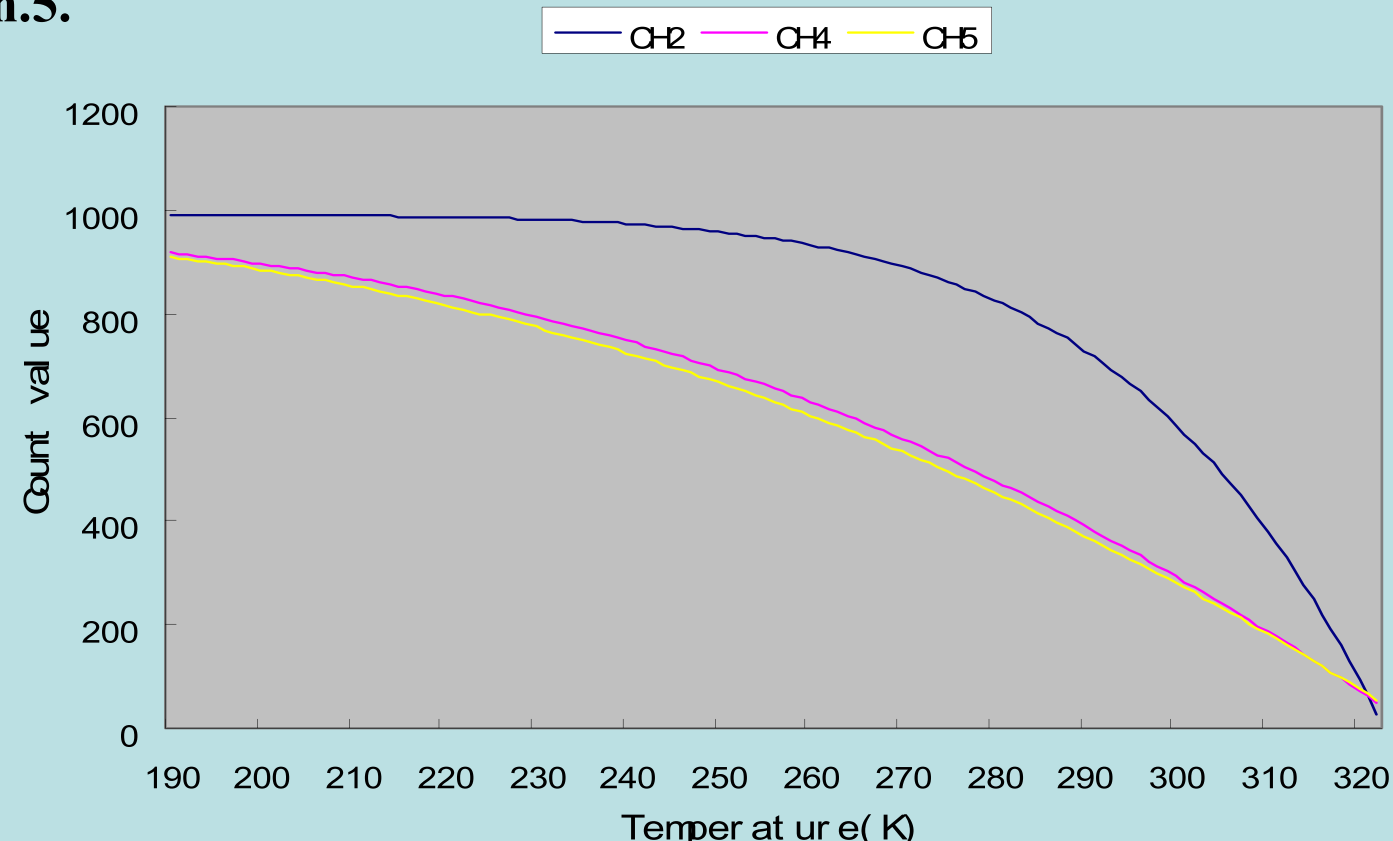

Fig. 2.4 The relationship curve of count value of channel 3,4,5 following black body temperature derived from Plank's Function.

Channel 2 (Mid. Infrared channel) is very sensitive to hot spot, and can be used as major channel in hot spot detection.

The Sensitivity of FY2C CH2 to Fire Spot

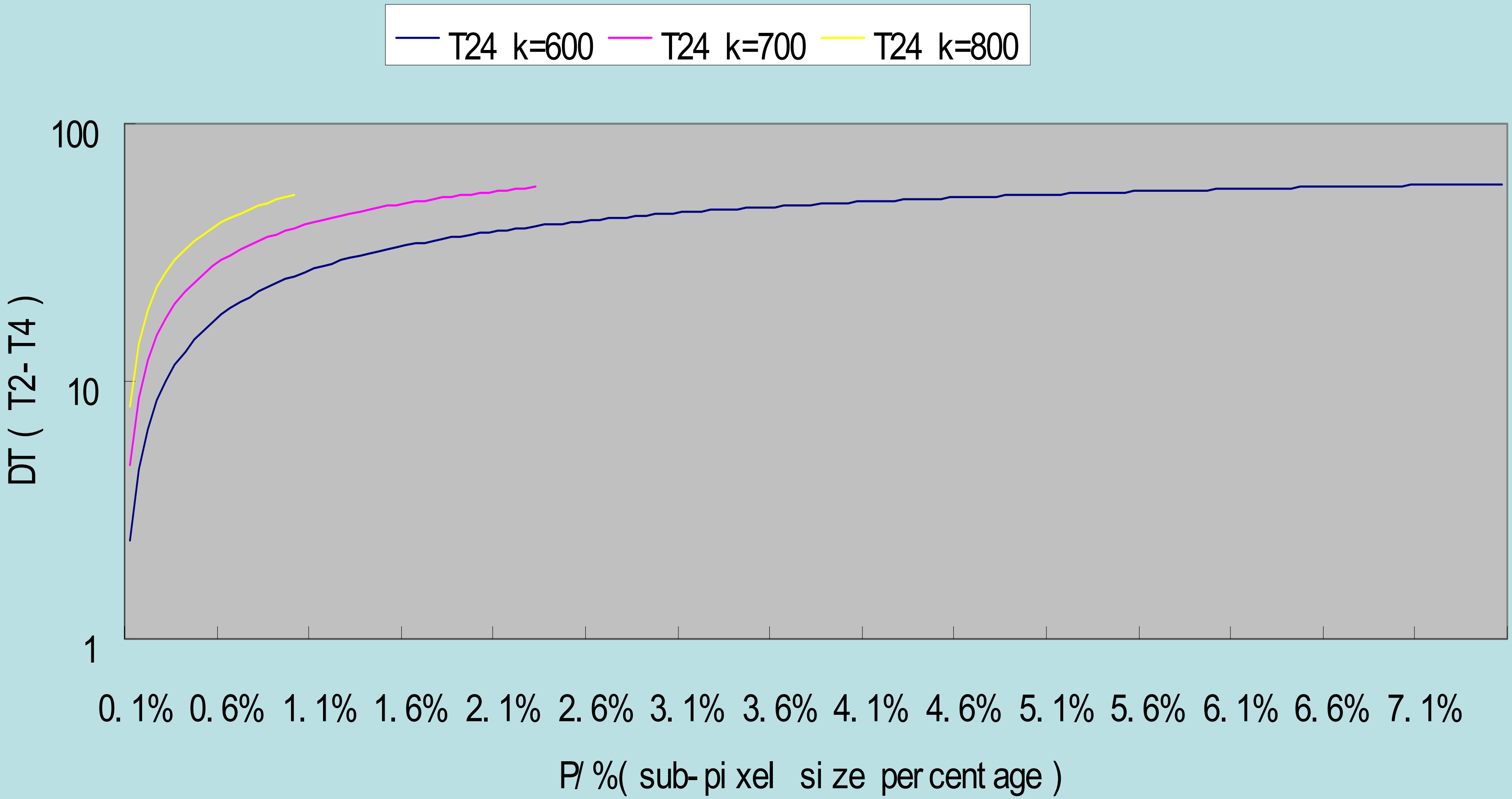

Fig.2.5 The difference of blackbody temperature between FY2C CH.2 and CH.4 along with the sub-pixel size (P) and temperature (600K,700K,800K) of hot spot .

0.1% of sub-pixel size occupied within a pixel with fire temperature in 600K, or 0.05% in 700k, can be founded theoretically by using threshold of T_{34} in 5K.

2) The method of hot spot detection by using FY2C data

- **Select a portion data from disc image**
- The whole disc image is divided into 14 regions which cover all the
- land area in the full disc image.
- Each region is 400 * 500 pixels.
- Searching hot spot pixel by pixel

- **Evaluate the background temperature in a searched pixel**

  Delete the cloud in a 7 * 7 pixels window around the searched pixel.
- Calculate the average of T2, T4 and the difference between T2
- and T4 as T2bg , T4bg , T24bg.

- ● **discern hot spot pixel**
    - ● $T2 > T2bg + \triangle Th_2$, and
    - ● $T24 > T24bg + \triangle Th_{24}$
- here $\triangle Th_2$ and $\triangle Th_{24}$ is threshold.

- ● **delete cloud contaminate**
- In a daytime image, as solar radiation reflection influence, little amount of cloud in a pixel may not be checked out but may cause brightness temperature in channel 2 goes up to certain level.
- ● $CH1 > CH1bg + 10\%$,
- ● $T4 < T4bg - 5K$
- here CH1 is reflectance of channel 1, CH1bg is average of channel in a window.

- • Evaluate the sub-pixel size and temperature for each detected hot pixel.
- • Calculate the energy emitted from the hot spot considering it as blackbody
- • Generate a fire pixel information file.

Considering the effect of analyzing to the result of sub-pixel size of hot spot evaluation, the fire intensity level is defined to six levels according to the energy emitted from the hot spot which can be calculated as following:

$$FN=S\cdot\sigma T^4 \quad (\sigma=5.6693\times10^{-8}\ (w\cdot m^{-2}\cdot K^{-4}))$$

- here S is the size of the hot spot evaluated, T is the temperature evaluated.
- The unit of FN is w, as the number of FN is too big, we use 10^6w as unit.
- level 1: ＜ 200
- level 2 : 201-400
- level 3 : 401-1000
- level 4 : 1000-3000
- level 5 : 3000 - 8000
- level 6 : ＞ 8000
- This level can be adjusted according the different features of vegetation coverage and it is may be different between forest and grassland region.

FY2C Whole disc image

2006/05/28/04:56z

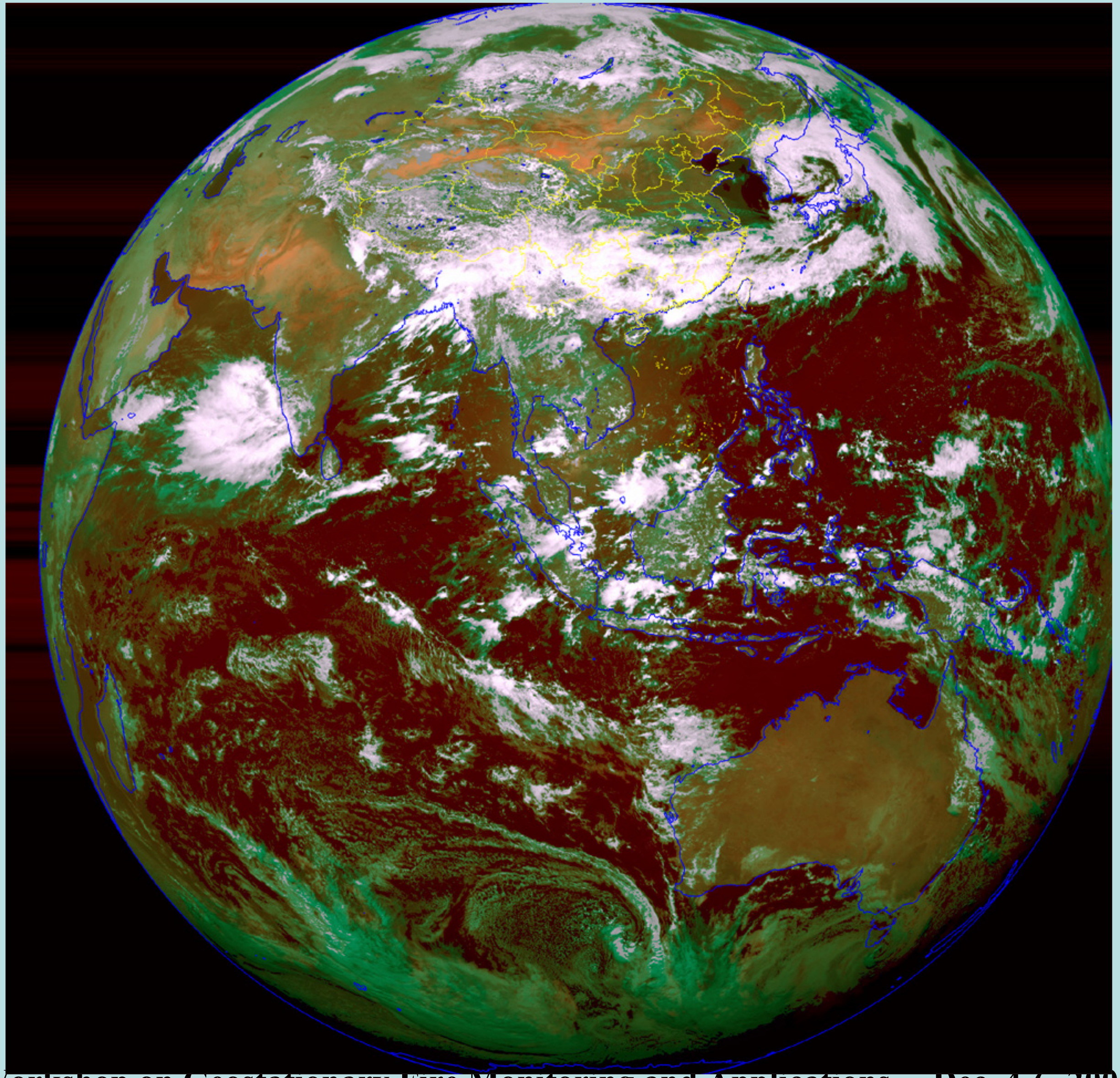

FY2C Regional image (Indonesia and Malaysia)
2006/05/28/04:56z

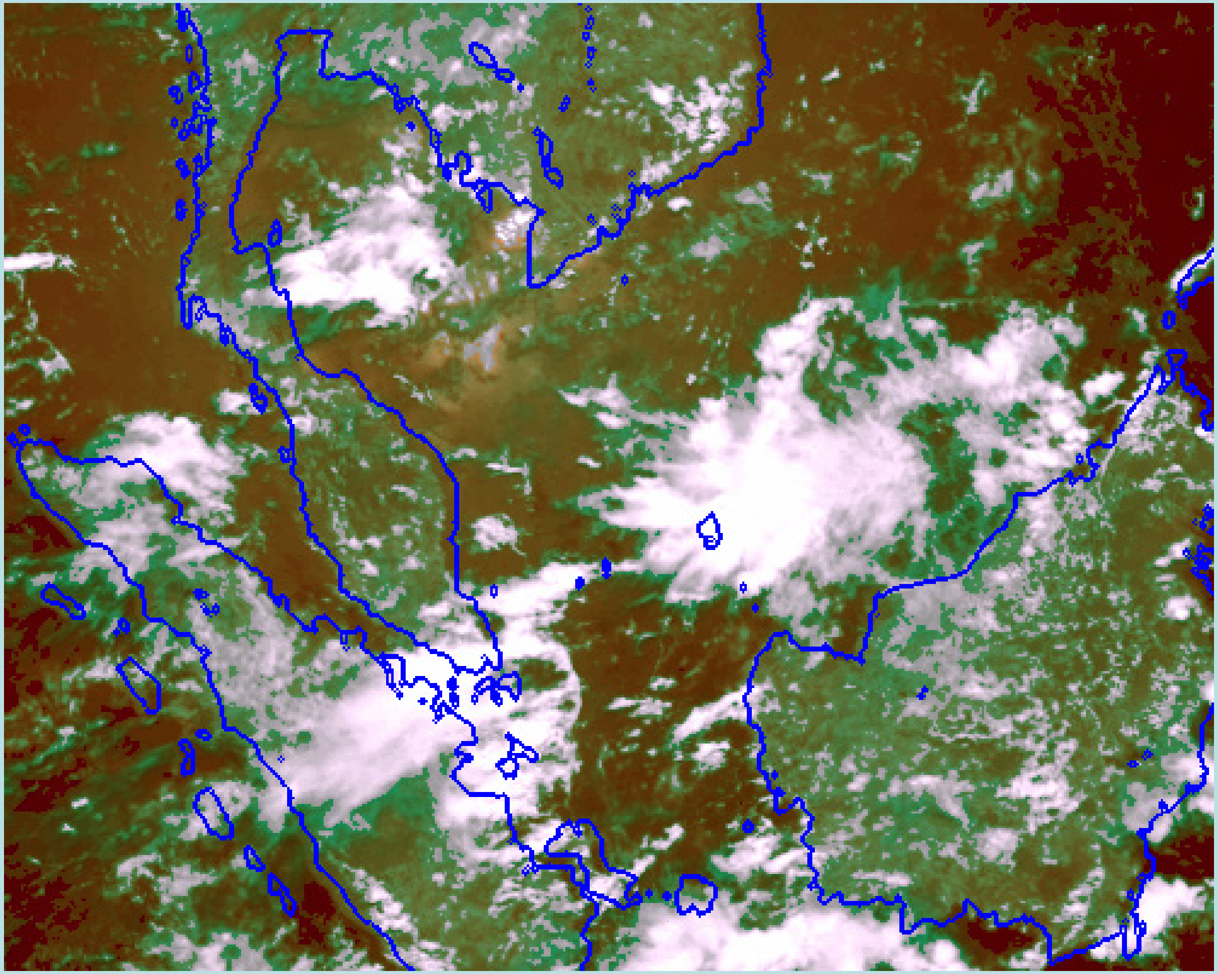

FY2C Regional image (North and Northeast part of China) 2006/05/28/04:56z

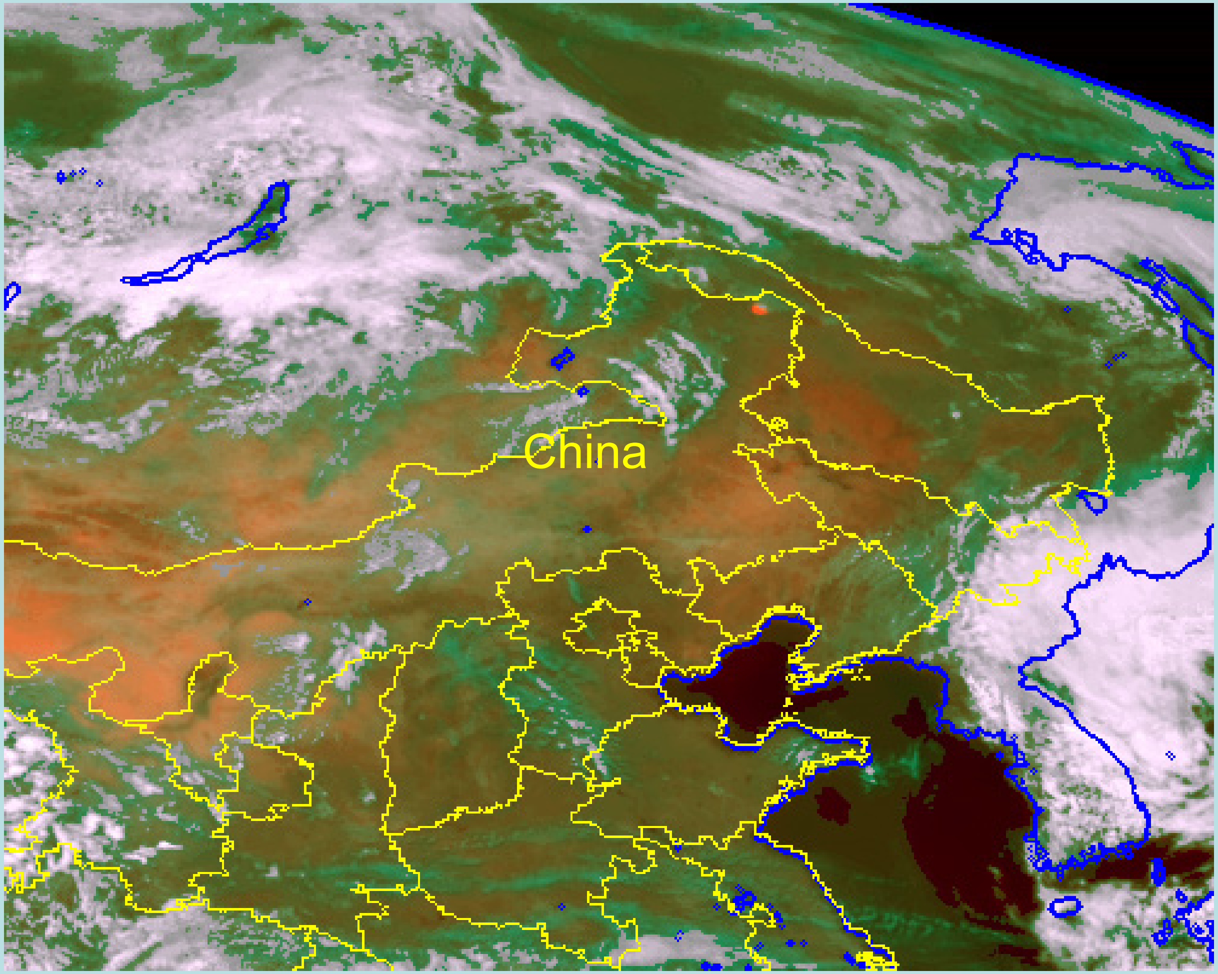

The detected fire pixel is marked by red color

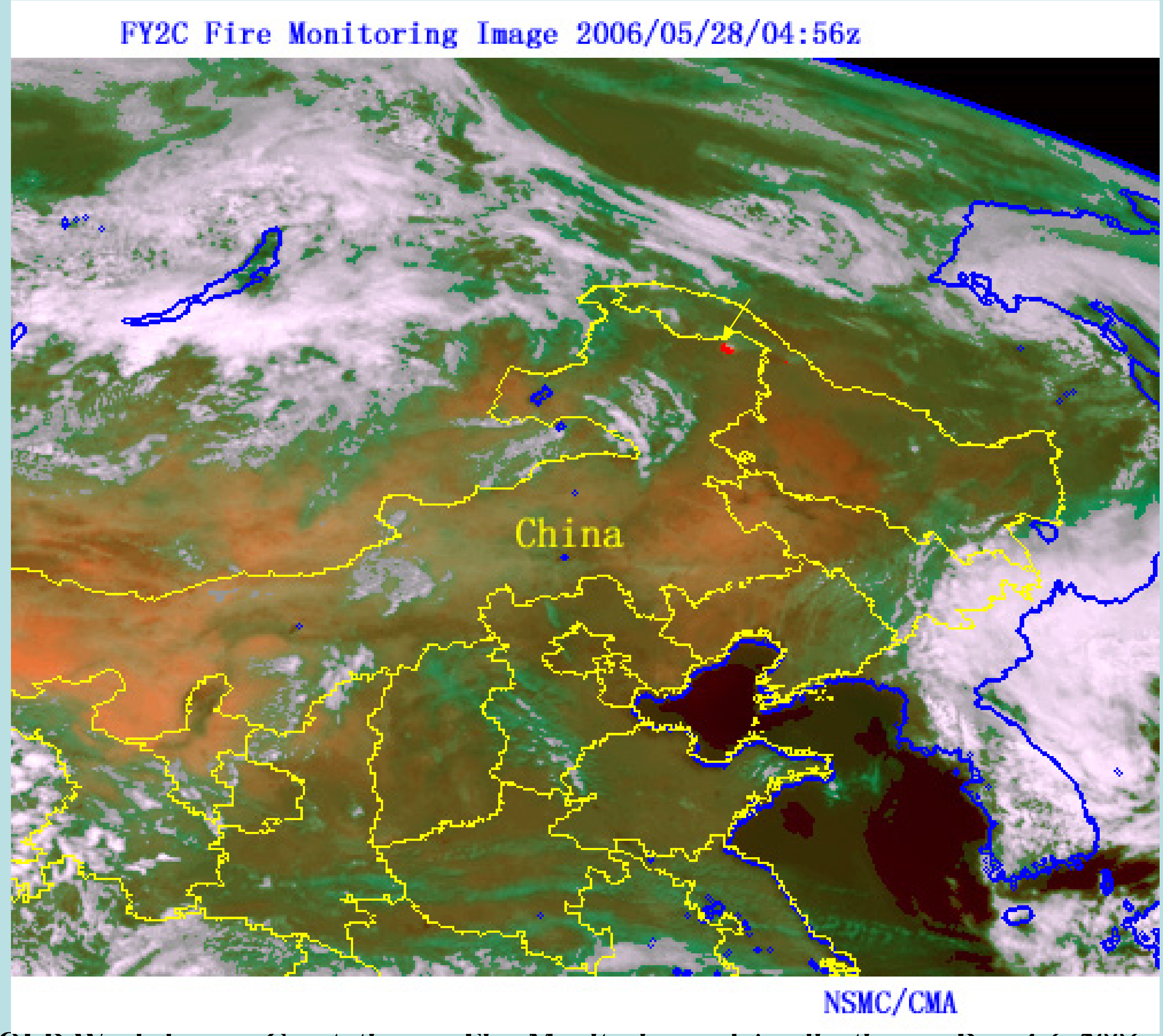

FY2C detected hot spot pixel information list

2006/05/28//4:56z)

Pixel No.	Lat.	Long.	Region No.	County No.	Land Utilization Type	Size of Pixel (km^2)	Percentage in the Pixel	Temp. of fire spot (K)	Emitted energy as black body (MW)
0	51.16	124.58	0	152127	22	62.108	0.000349	623	186.280487
1	51.06	124.47	0	152127	22	62.246	0.001944	527	530.076050
2	51.08	124.55	0	152127	22	62.304	0.000635	650	356.322601
3	50.98	124.43	0	152127	22	62.355	0.003126	507	734.294006
4	50.98	124.51	0	152127	22	61.584	0.008504	460	1333.972046
5	50.98	124.58	0	152127	22	61.584	0.022354	395	1908.233643
6	50.98	124.66	0	152127	22	62.355	0.011578	416	1228.275635
7	50.88	124.52	0	152127	6	62.491	0.020076	414	2099.118652
8	50.88	124.44	0	152127	22	61.718	0.005792	483	1110.445068
9	50.88	124.37	0	152127	22	61.718	0.002781	490	564.967529
10	50.79	124.48	0	152127	42	61.843	0.002140	533	545.253174
11	50.90	124.62	0	152127	6	62.464	0.021717	408	2134.528564
12	50.90	124.70	0	152127	22	61.695	0.011884	422	1330.003174
13	50.90	124.79	0	152127	42	61.695	0.003439	459	535.905273
14	50.90	124.87	0	152127	42	62.464	0.002386	438	312.993530
15	50.79	124.66	0	152127	6	62.600	0.011081	423	1259.539307
16	50.79	124.57	0	152127	6	69.556	0.008866	444	1369.627808
17	50.56	126.52	1	232601	3	62.926	0.000772	489	157.649872

3. FY2C fire monitoring products generating and distribution

FY2C Whole disc image 2006/05/28/06:00z

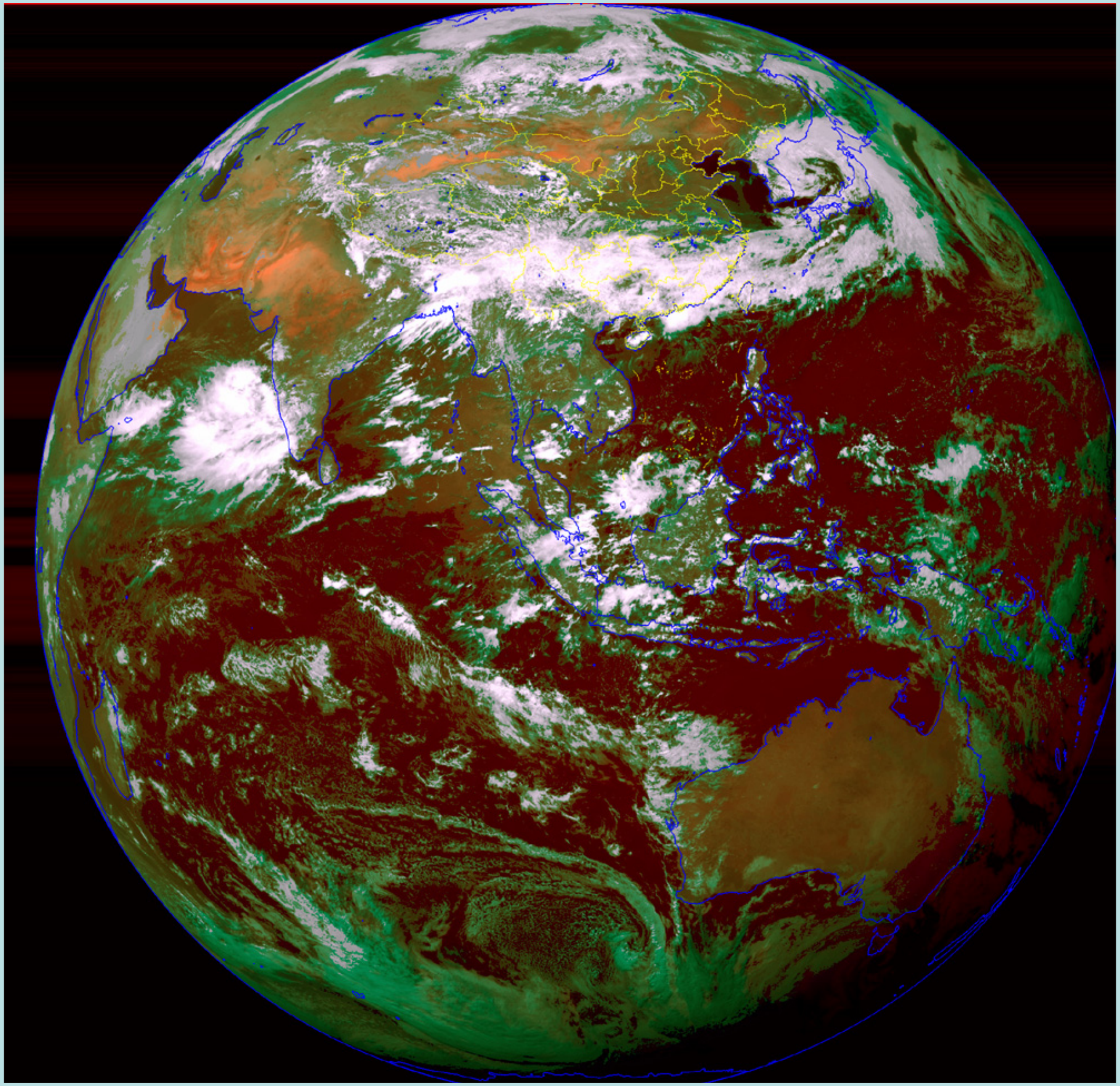

In current operatonal mode, NSMC only monitor the region in China area. When the important fire event happened, we also make some products displayed in TV weather program.

Processing the regional portion data in China range

FY2C CH2 Raw data 2006/05/28/06:00Z

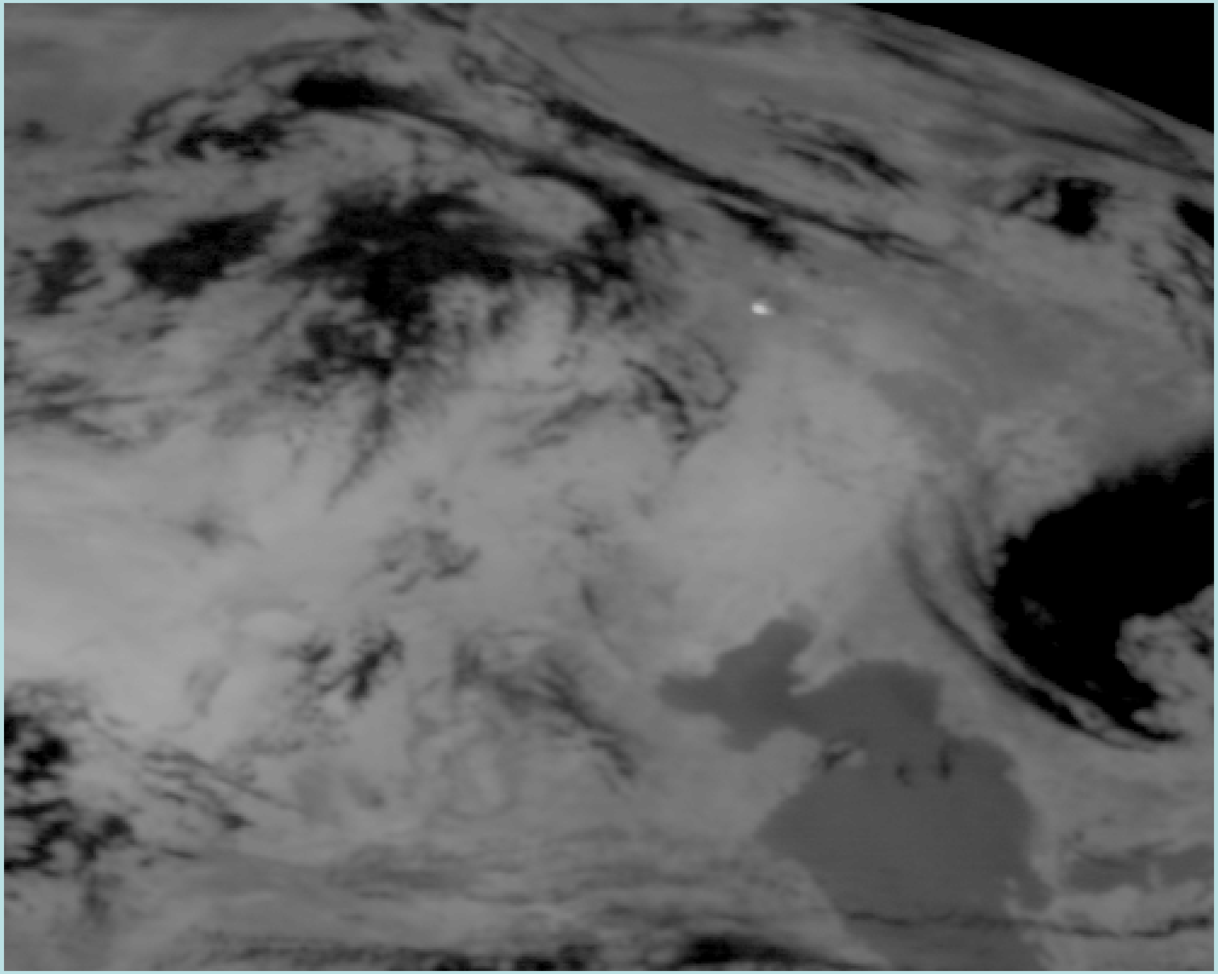

FY2C multiple channel enhancement and composition Image (Ch2,1,1)

2006/05/28/06:00Z

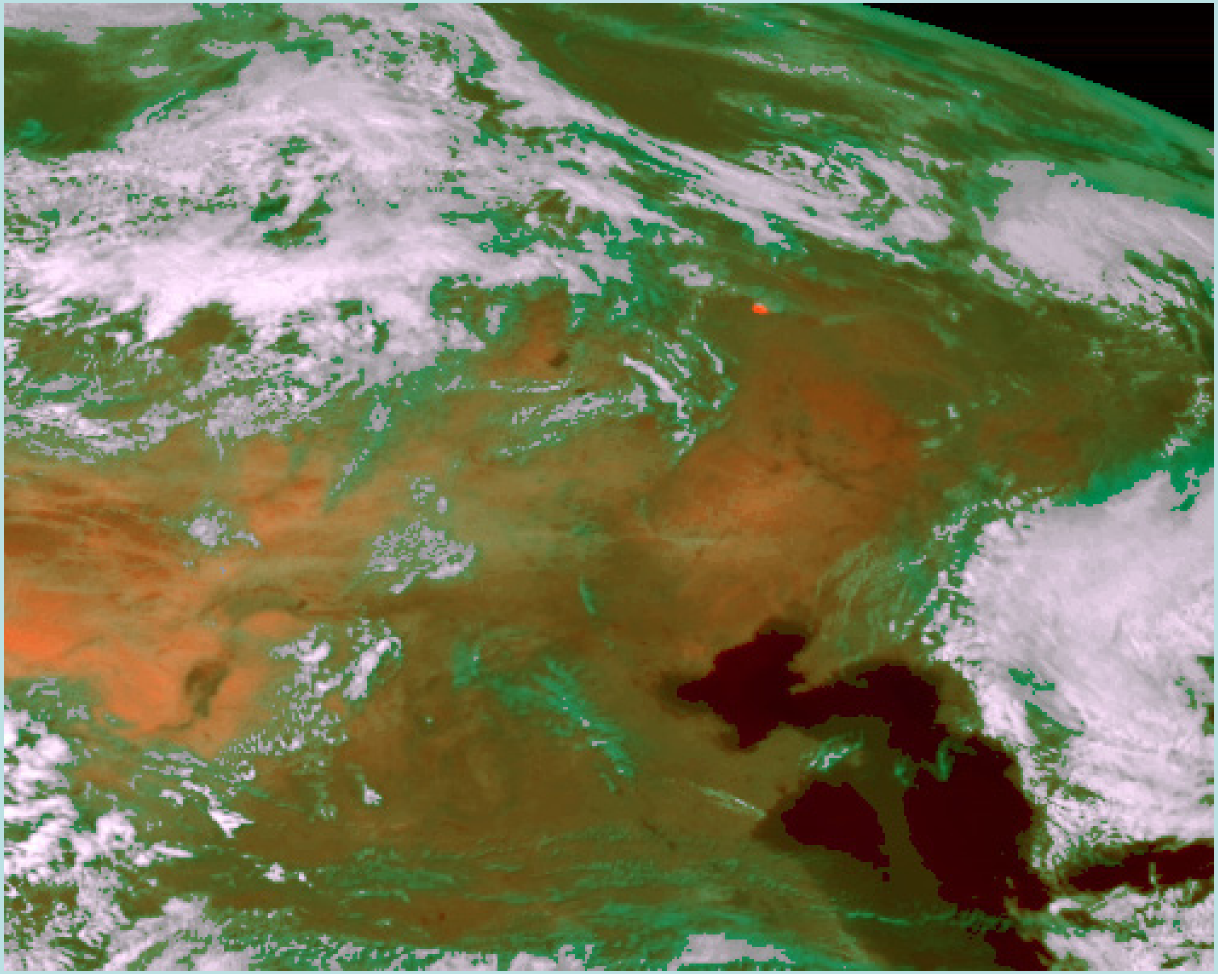

FY2C Hot spot detectetion

2006/05/28/06:00Z

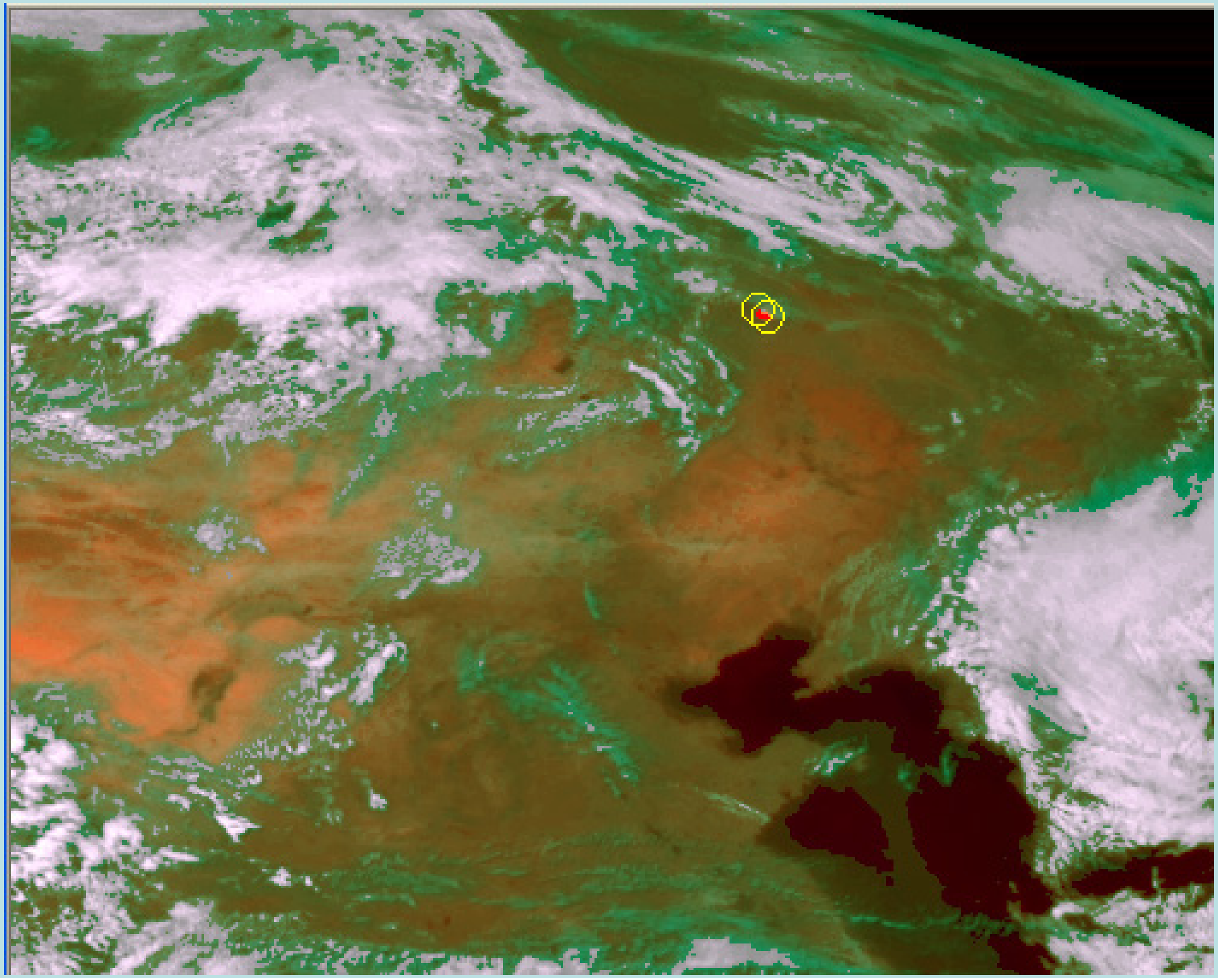

FY2C Fire monitoring product image generating and distributed by VAST System
2006/05/28/06:00z

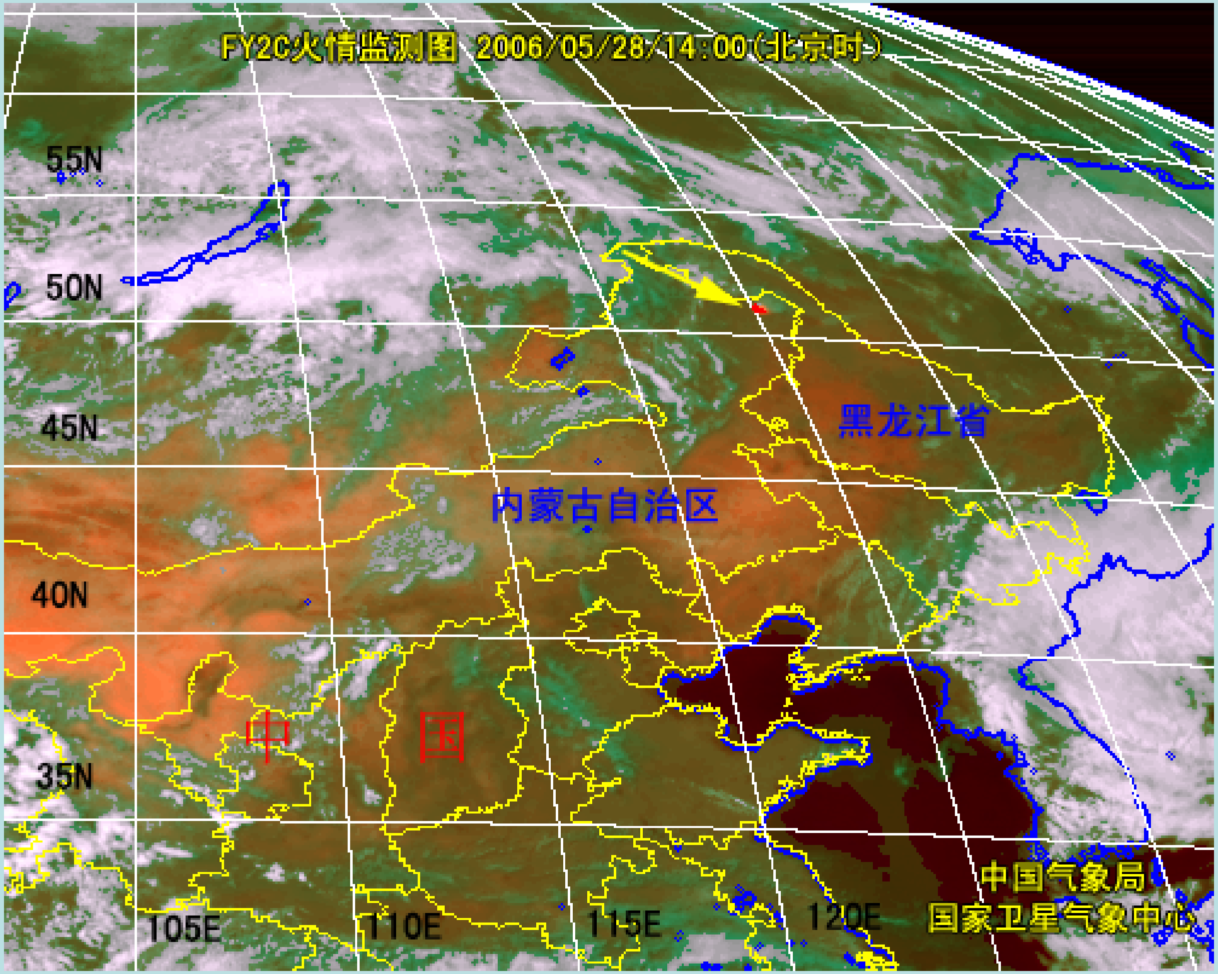

FY2C Fire monitoring information list distributed by VAST System

When fire event happened, generate the fire monitoring image and fire monitoring information list.and distributed by VAST System.

FY-2C气象卫星火情监测信息表
(FY2C Fire monitoring information list)

观测时间（北京时）：2006/05/28/14:00　　国气象局国家卫星气象中心制作

火区序号 Region No.	纬度 Lat.	经度 Long.	像元数 No. of pixels	土地利用类型（%） Land utilization type			所在行政区域 Administrative region			备注
				草地	林地	其他	省	地	县	
1	50.98	124.67	15	80	20	0	内蒙古自治区	呼伦贝尔盟	鄂伦春自治旗	

4. Application examples

FY2C monitored some big forest fire in recent years.

FY2C Daxinxlanling Fire Monitoring
in 1 km resolution
2006/05/25/00-09z

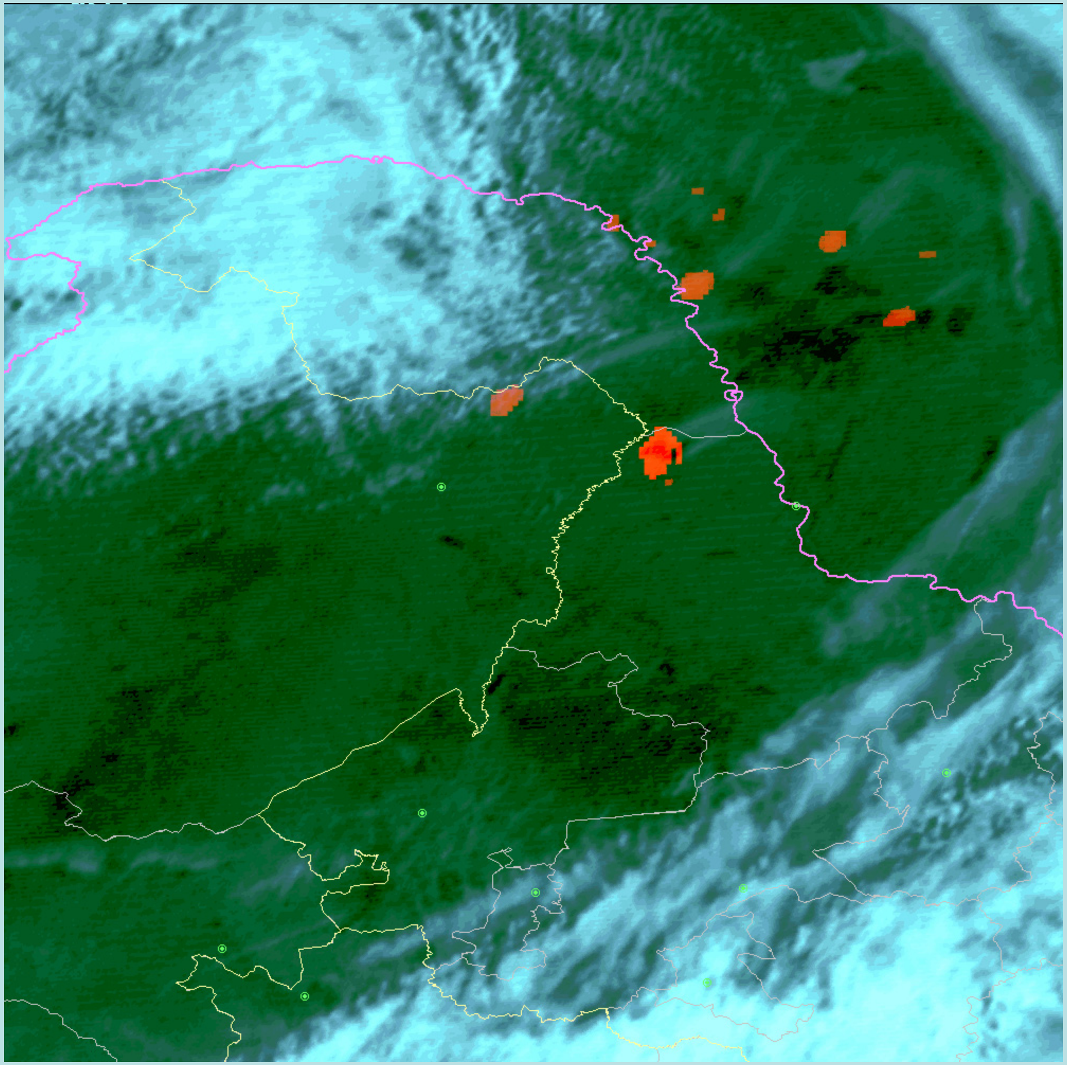

FY2C Daxinganling fire monitoring images

2006/10/28/01:00z-09:00z)

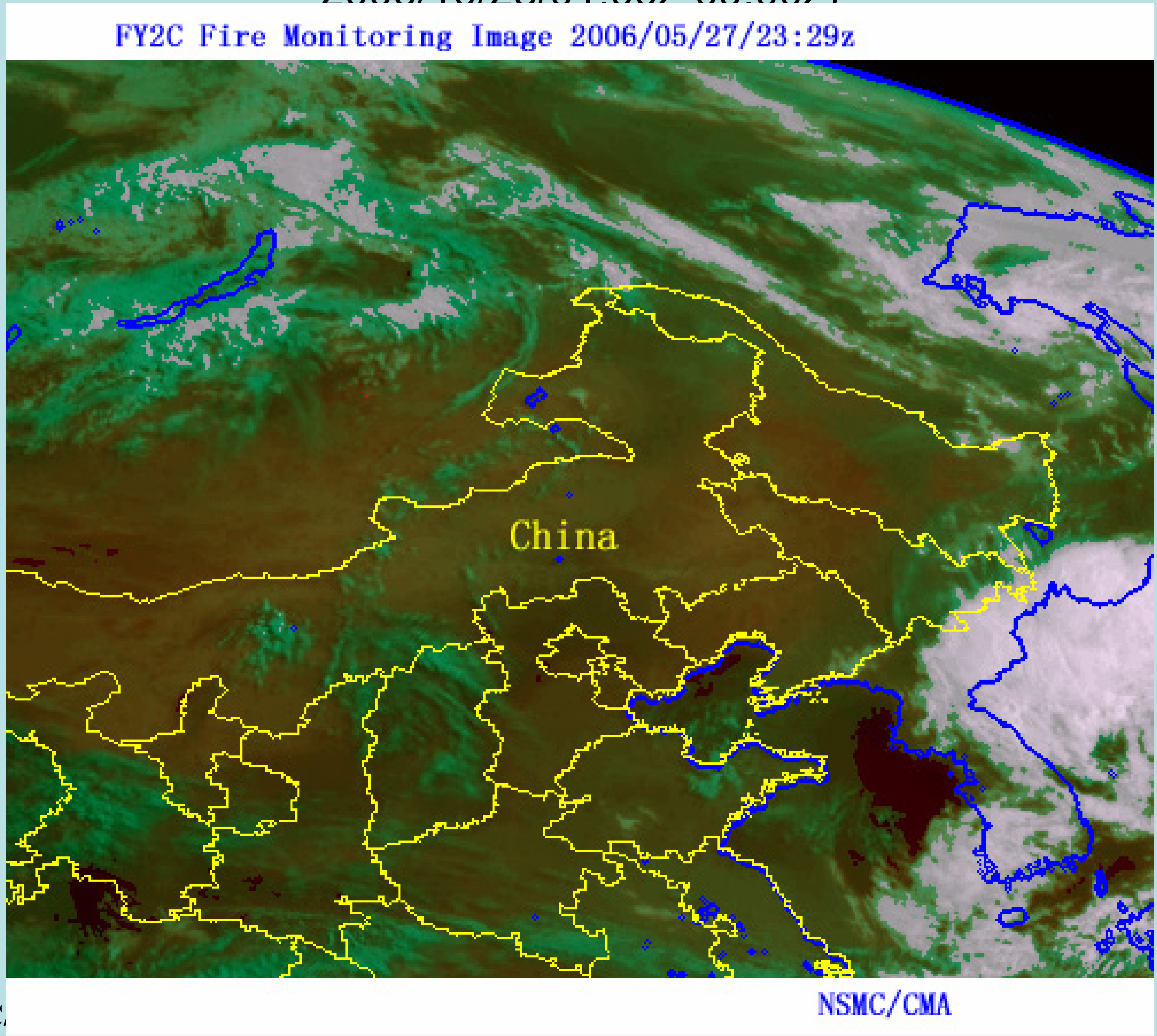

FY-2C Fire Intensity Image

2006/10/28/01:00z-09:00z)

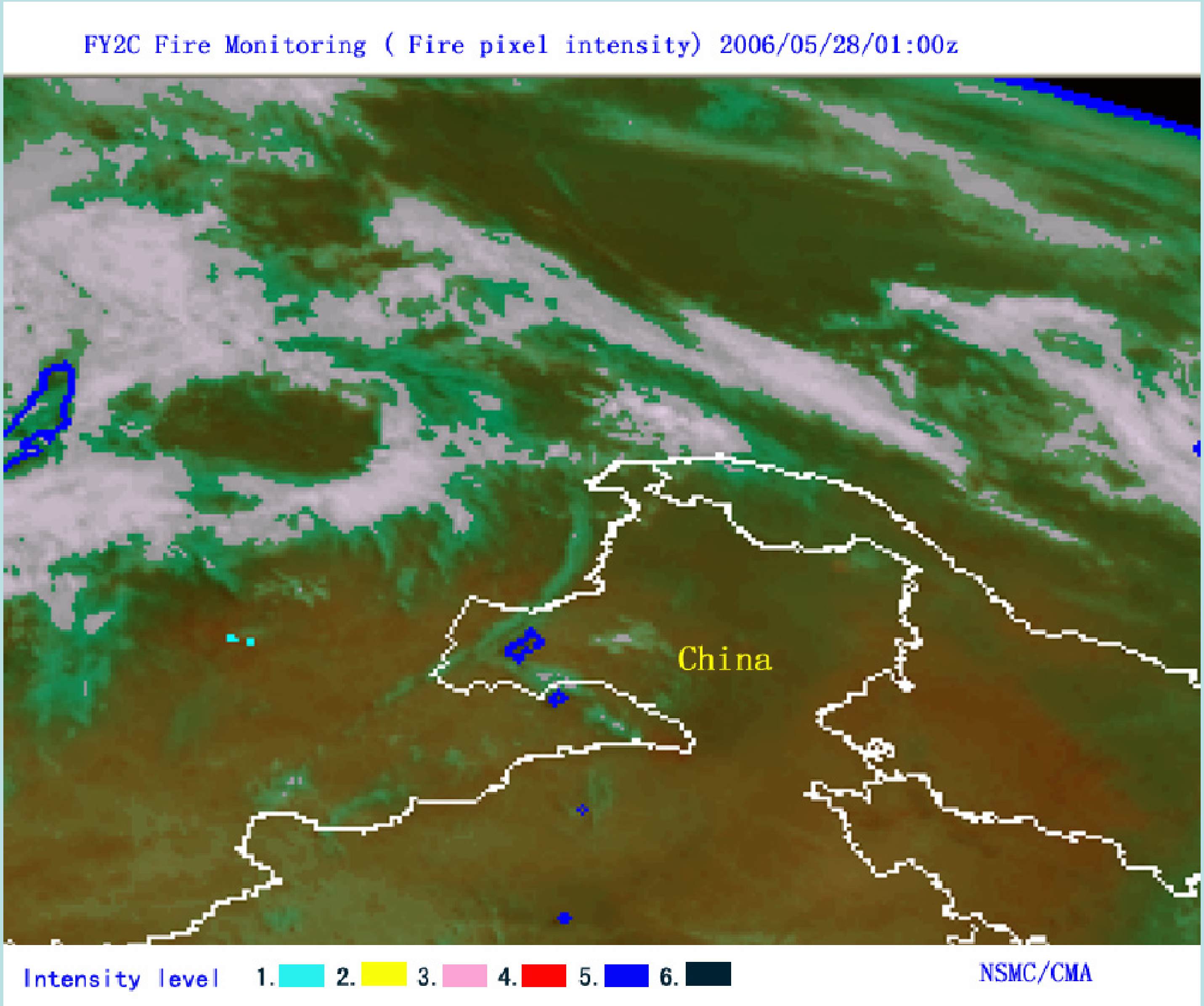

FY2C Indonesia fire monitoring images (2005/08/07—08/10)

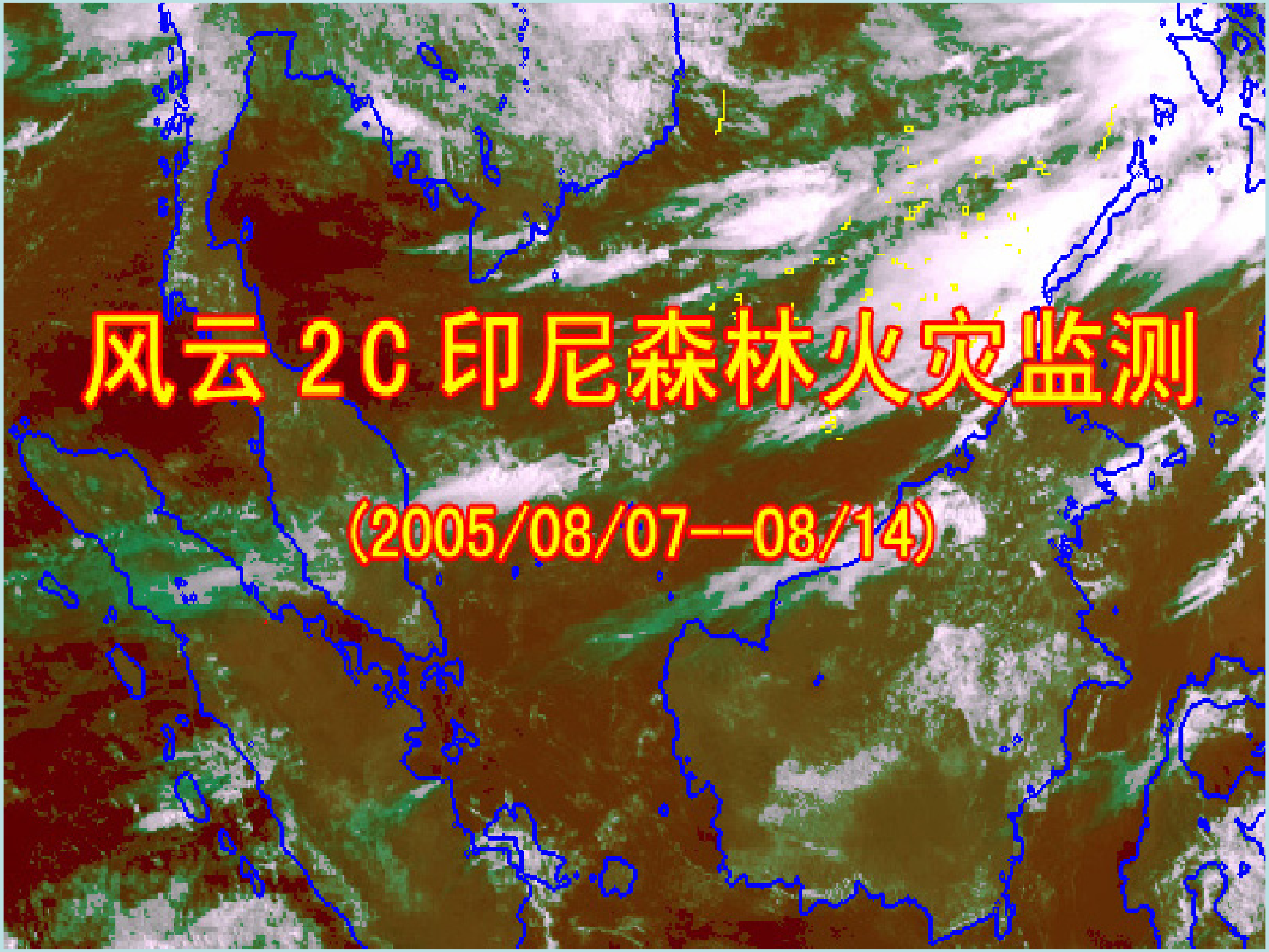

FY2C Indonesia fire monitoring

2006/10/04-07

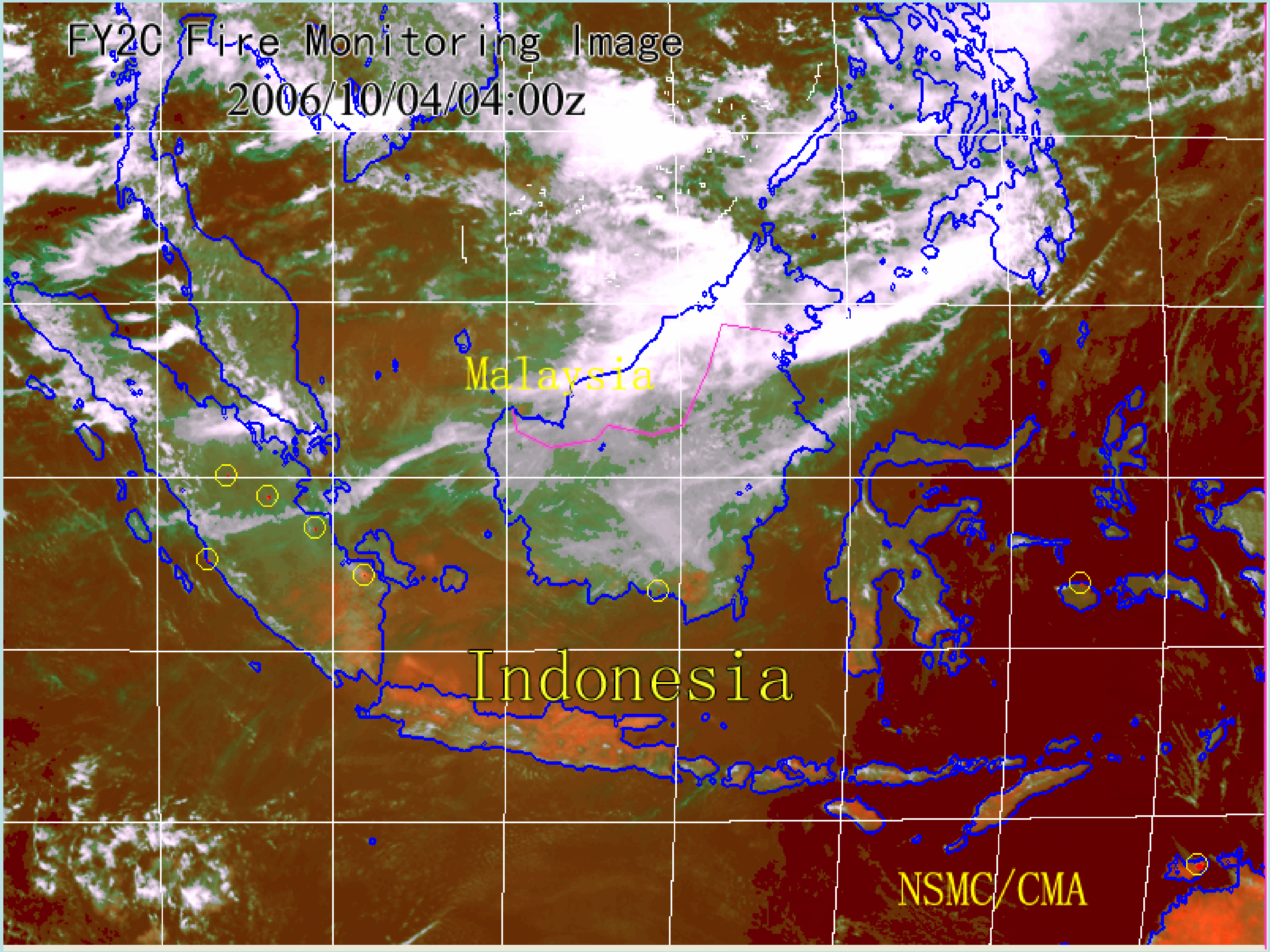

FY2C Indonesia fire monitoring
2006/10/10-14

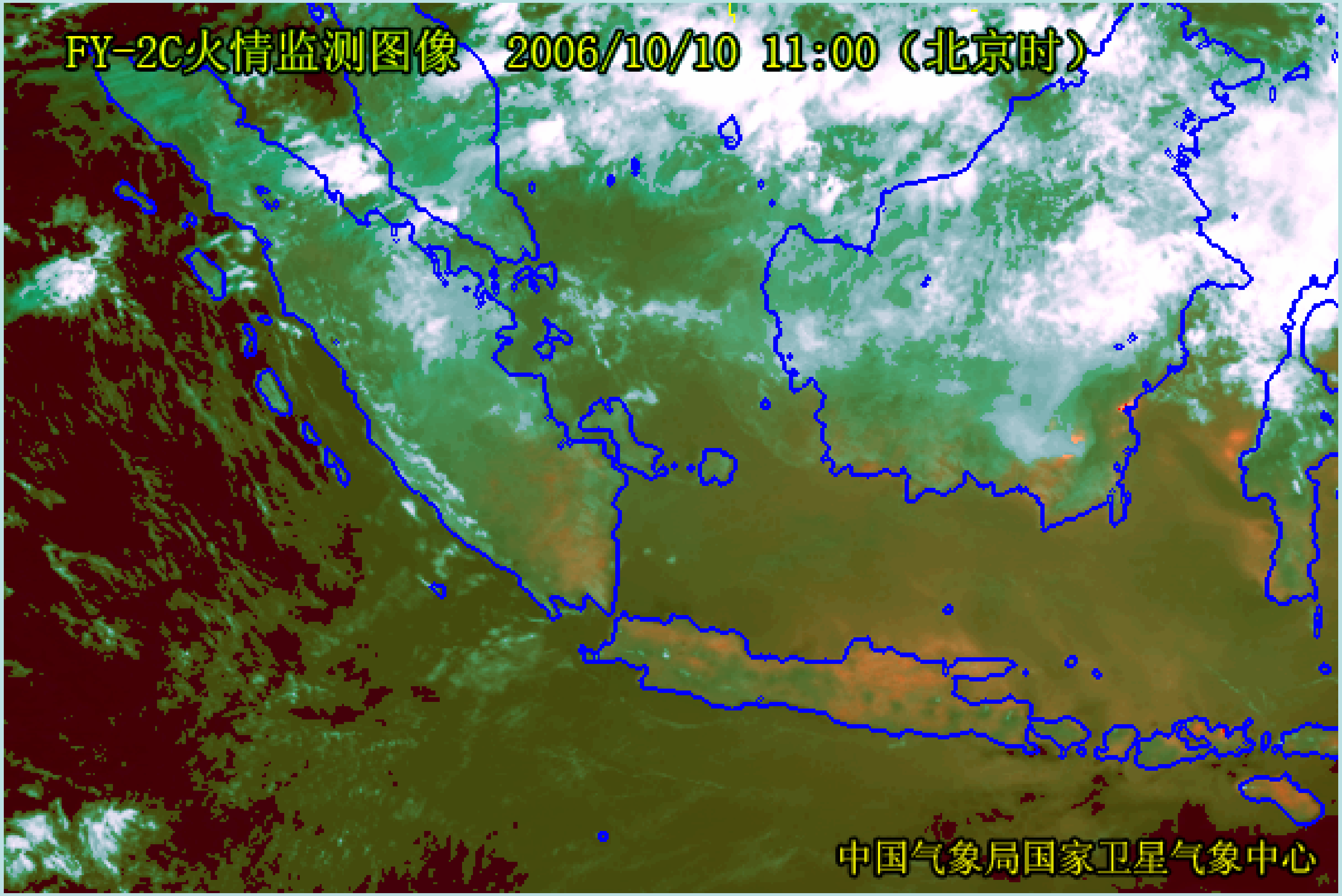

Part 2 The Application of Fire Monitoring by using Meteorological Satellites by NSMC/CMA

1. Background
2. The fire information deriving
   1) The method of hot spot detection
   2) Sub-pixel size of hot spot evaluation
   3) The validation for sub-pixel size evaluation
3. The operation and service of fire monitoring system
4. The aspects of applications in fire monitoring

1. The Background of Forest Fire Monitoring in China

The percentage of forest coverage in territory of China is about 12%, it is in the number of 131 in the world.

The average of forest area to the large population is very small, only about 0.12 hectare / person, it is in the number less than 136 in the world.

Forest resource in China is very valuable. In view of China's national condition, meteorological satellite is one of the efficient method to monitor the forest fire in the large area of China.

CMA started to develop the software for monitoring forest fire by using polar orbiting meteorological satellite data from the middle of 1980's.

The forest region are distributed in the widely area of China. The major forest region are in the northeast part and southwest part, where the population are quite few, especially in the nature forest area.

Fig. 1.1 Land Utilization Map of China

The first time we detected fire was in April 11, 1986

Fig. 1.2 shows a grassland fire located in the North Part of China. The fire prevention department were very interested in this ability. CMA provided the fire monitoring information by using meteorological satellite since then.

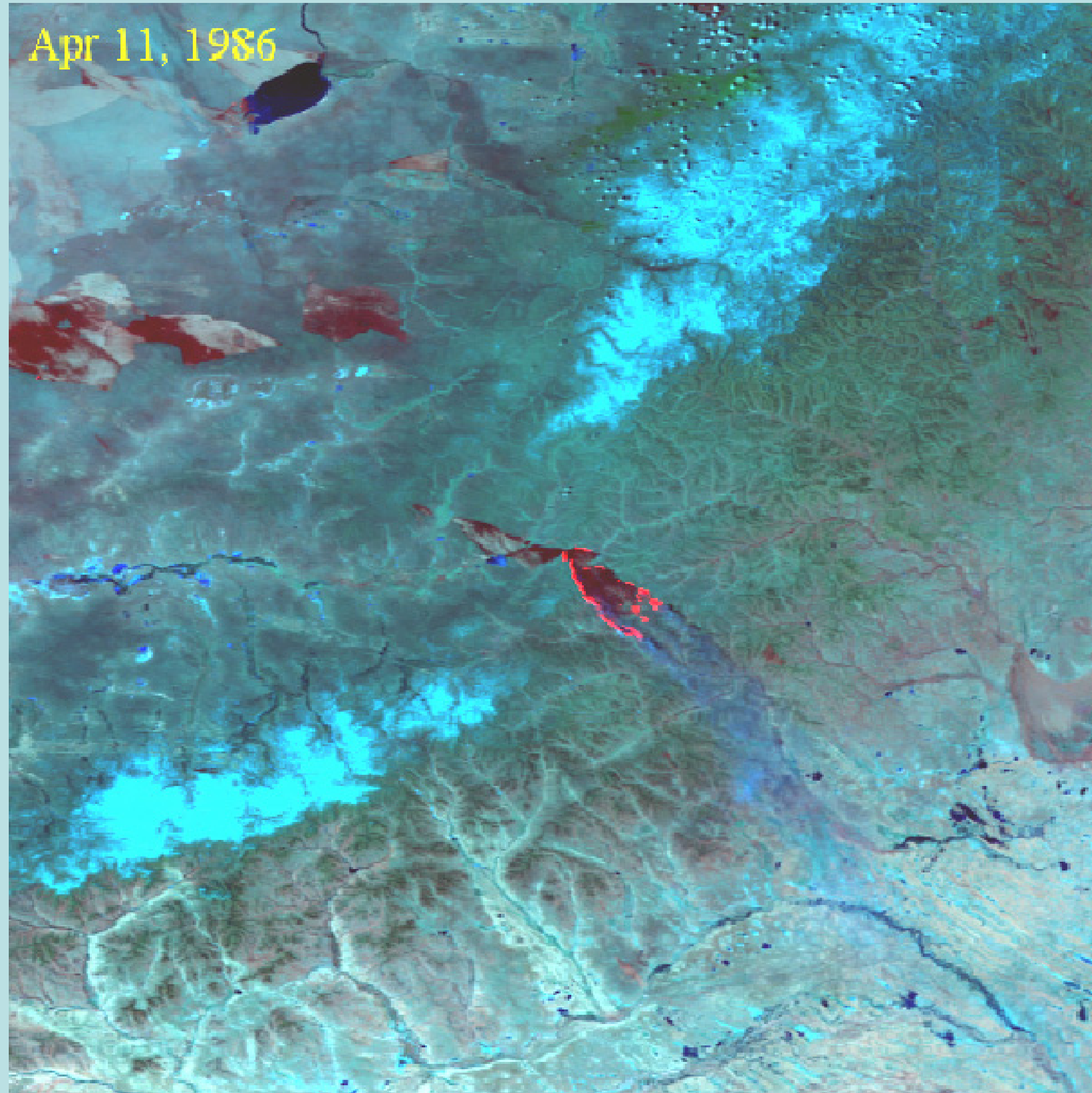

Fig. 1.2 grass land fire monitoring NOAA-7 AVHRR CH.3,2,1 April 11, 1986

In May of 1987, there was a huge forest fire happened in the Northeast Part of China. During the period of fighting the fire,CMA/NSMC use NOAA data to monitor and report all information about the fire to the related government. (see Fig. 1.3 and 1.4)

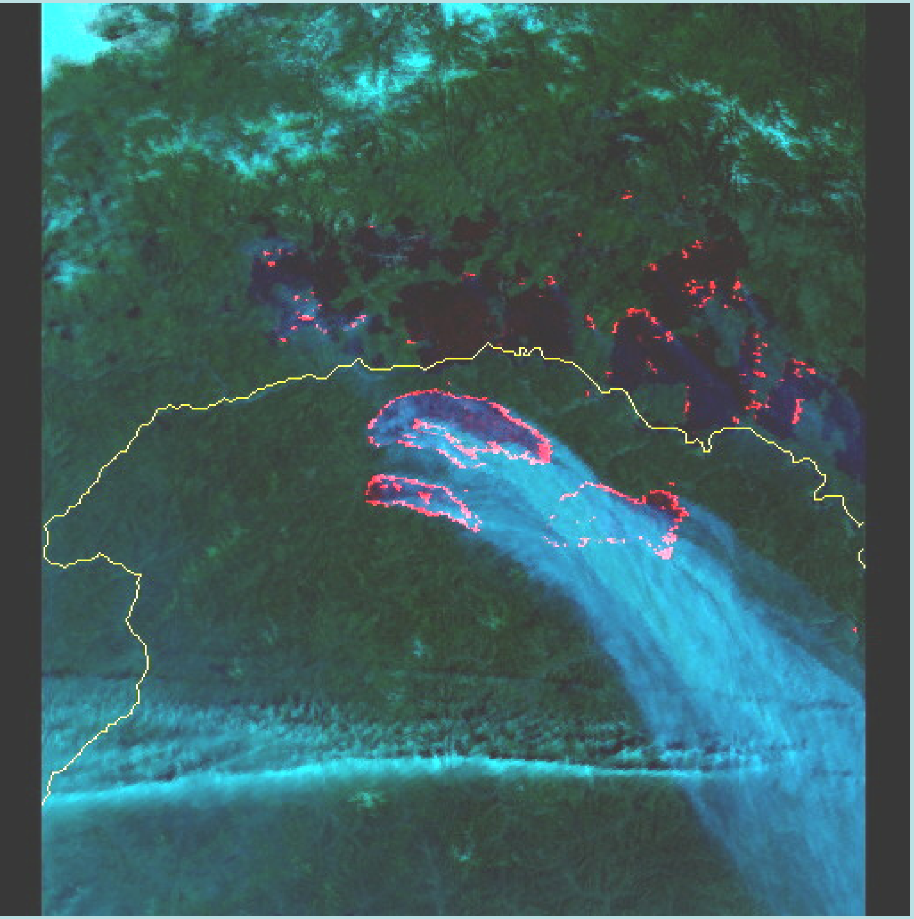

Fig. 1.3 In the morning of May 8, 1987

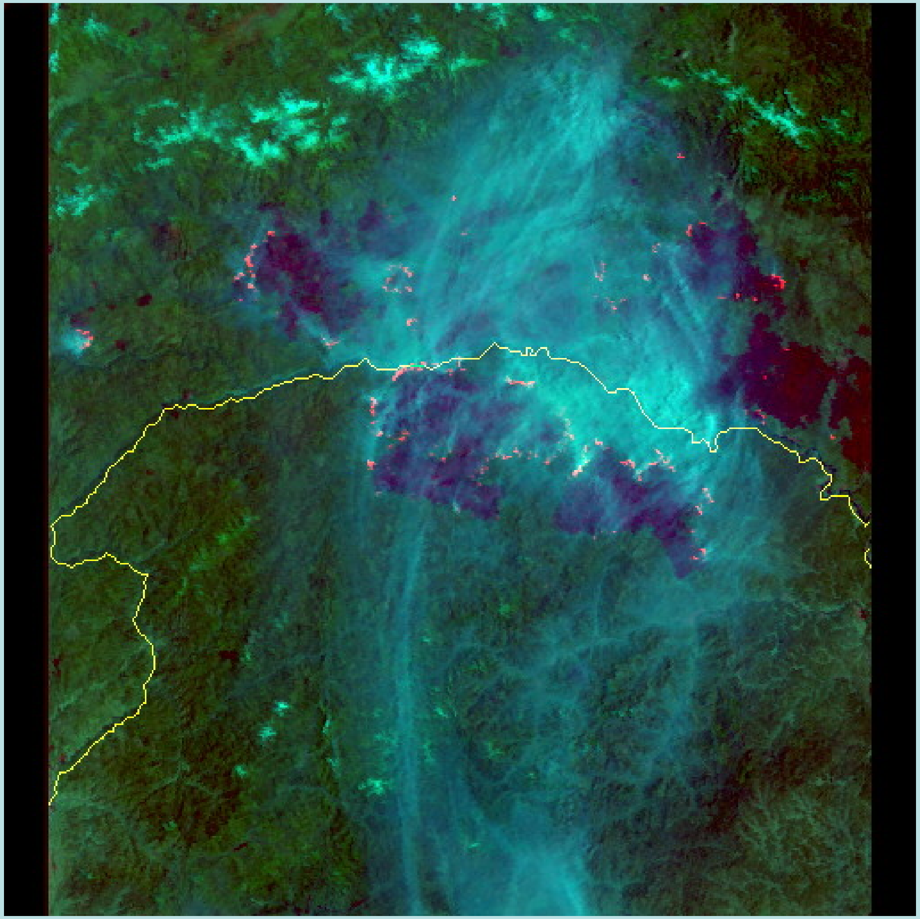

Fig. 1.4 the afternoon of May 20, 1987

From 1987, the forest fire monitoring became more operational.

From 1988, CMA started to provide grassland fire information to national grassland fire prevention department in operational mode.

One branch of people in NSMC are specially for fire monitoring by using meteorological satellite data. Averagely, we provided more than 10000 fire spots each year in recent years.

From 1990's, more provincial weather service established the meteorological satellite data receiving and processing system and one of the major task in these systems are for forest and grassland fire monitoring in their province.

2. The Fire Information Deriving

1) The method of hot spot detection

(1) Select a portion of pixels from the regional image to process

- Automatic searching in regional image in 5º*5º latitude and longitude range.
- Select a portion of pixels from a regional image to process as we consider there should be little amount of pixels containing fire spot. 5% pixels in highest brightness temperature of mid-infrared channel in a regional image are selected. (we also can use threshold temperature, but it is quite complicated).
- Searching hot spot pixel by pixel.

(2) Evaluate the background temperature in a searched pixel

- Delete the cloud in a window around the searched pixel, 7 * 7 pixels size.
- Delete the possible hot spot pixel in the window in the condition:

  T3 > T3max - 3K

  T34 > 15K (can be adjusted)

  Here T3 is brightness temperature of channel 3 in the checked pixel in a window ,T3max is the maximum brightness temperature of channel 3 in the window. T34 is the difference of T3 and T4.

- Calculate the average and standard deviation of T3, T4 and the difference between T3 and T4 as T3bg ,δT3bg , T4bg ,δT4bg , T34bg ,δT34bg.

- **(3) discern hot spot pixel**
  - ● T3 ＞T3bg + 4δT3bg， and
  - ● **T34 ＞T34bg + 4**δT34bg
- **when** δT3bg、δT43bg less than 2，set to 2K。

- **(4) delete cloud contaminate**
- In a daytime image, as solar radiation reflection influence, little amount of cloud in a pixel may not be checked out but may cause brightness temperature in channel 3 goes up to certain level.
- ● CH1 ＞ CH1bg + 10% ，
- ● T4 ＜T4bg - 5K
- here CH1 is reflectance of channel 1, CH1bg is average of channel in a window.

Example of automatic searching in a mixed cloud region condition (2006/06/30/13) (before searching)

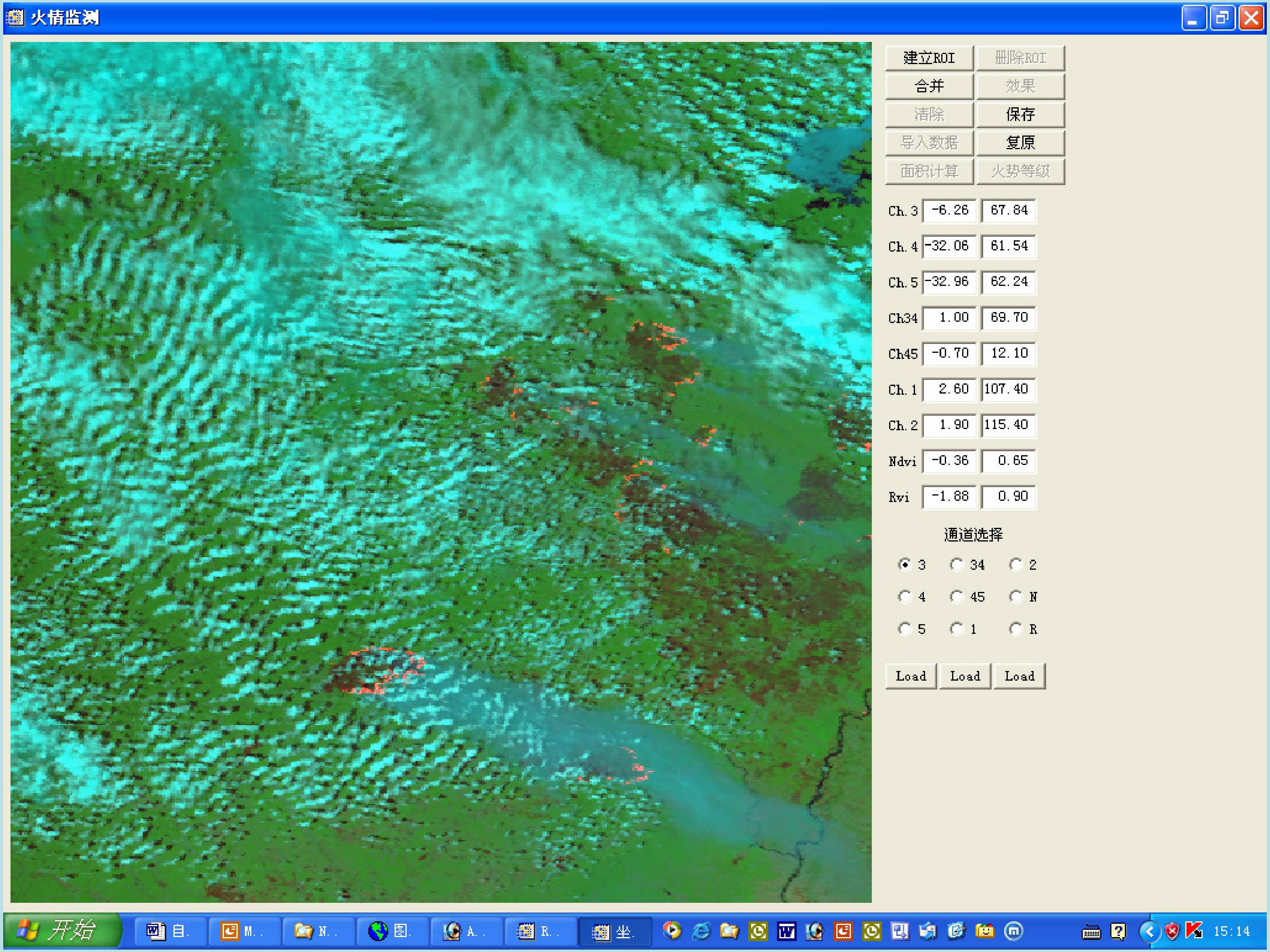

Fig. 2.1 Three channel composition (CH 3,2,1) to show the fire spots with bright red color.

Example of automatic searching in a mixed cloud region condition
(After searching, white color is a mark for selected pixel)

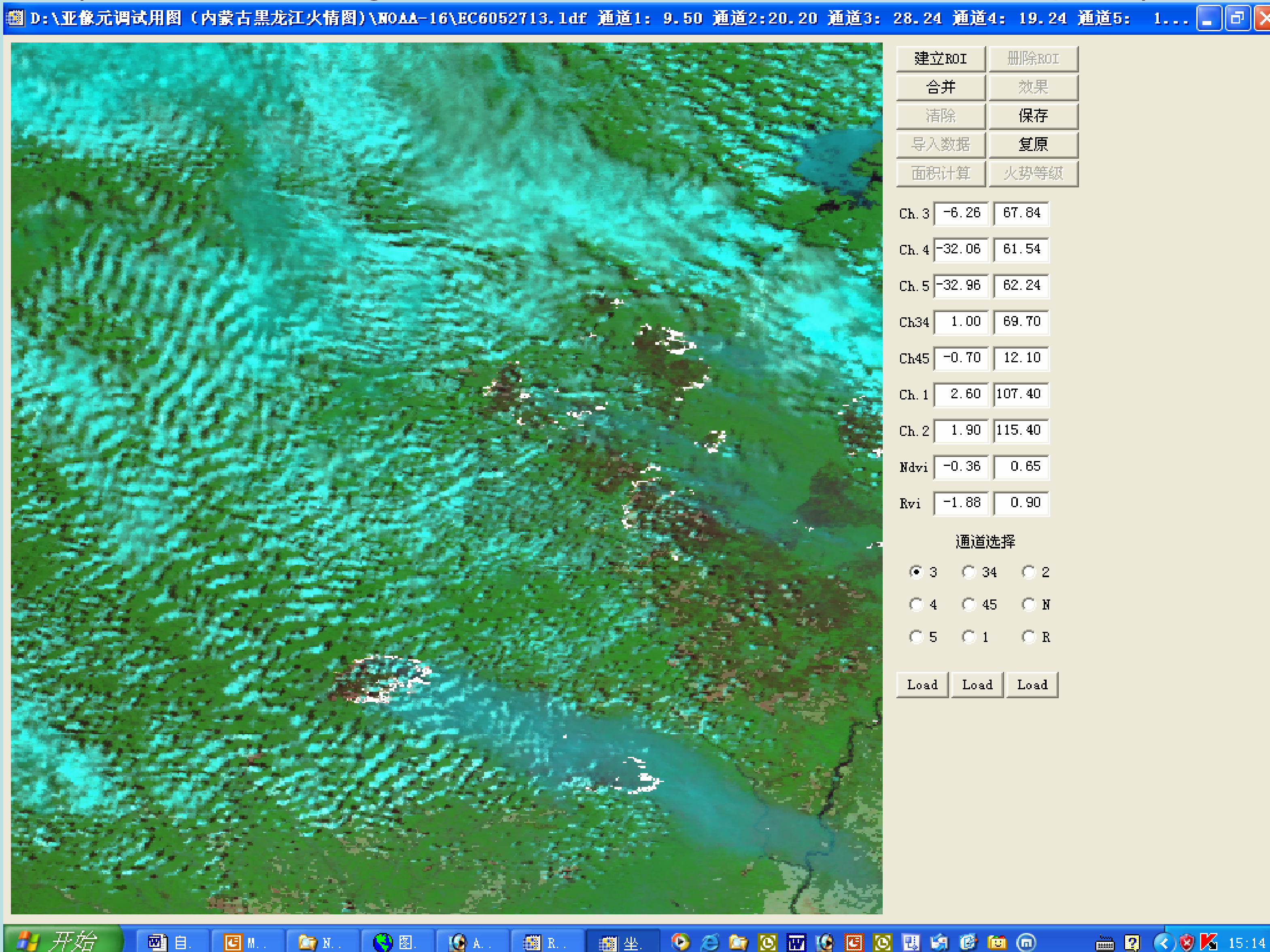

Fig. 2.2 After automatic searching, the white color represent the fire spot detected.

A portion of hot spot information list for all the pixels detected

EC6052713.lis - 记事本

文件(F) 编辑(E) 格式(O) 查看(V) 帮助(H)

679	97	0.7792	0.167	1299	3	340.90	295.80	26.3	303.44	292.64	1	0	33
680	97	0.7792	0.063	491	2	322.30	293.60	26.2	302.46	292.09	1	0	37
681	97	0.7794	0.067	519	2	325.40	295.50	20.3	306.73	293.08	1	0	35
682	97	0.7794	0.093	722	2	330.50	293.80	24.0	306.69	293.56	1	0	33
683	97	0.7794	0.092	716	2	330.50	293.80	24.0	306.98	293.84	1	0	32
684	97	0.7794	0.037	290	1	318.80	291.60	24.8	307.22	293.83	1	0	32
685	97	0.7794	0.074	574	2	326.90	293.40	23.2	306.81	293.80	1	0	30
686	97	0.7794	0.092	717	2	330.20	294.60	23.6	306.33	293.93	1	0	31
687	97	0.7794	0.062	483	2	323.20	291.70	26.2	304.60	294.26	1	0	29
688	97	0.7794	0.062	482	2	323.20	291.70	26.2	304.61	293.87	1	0	31
689	97	0.7794	0.166	1293	3	340.90	293.50	26.5	303.77	293.28	1	0	34
690	97	0.7795	0.056	437	2	322.80	296.90	18.7	306.27	293.20	1	0	37
691	97	0.7795	0.039	305	2	318.70	296.10	20.0	306.32	293.34	1	0	34
692	97	0.7795	0.039	304	2	318.70	296.10	20.0	306.39	293.56	1	0	34
693	97	0.7795	0.081	631	2	328.00	295.30	20.6	306.11	293.77	1	0	33
694	97	0.7795	0.098	760	2	331.10	293.90	24.8	306.07	293.86	1	0	32
695	97	0.7795	0.120	939	2	334.80	293.20	23.5	305.62	293.63	1	0	30
696	97	0.7795	0.121	946	2	334.80	293.20	23.5	305.25	293.78	1	0	31
697	97	0.7795	0.164	1281	3	340.90	295.40	25.3	304.44	293.91	1	0	30
698	97	0.7795	0.078	606	2	326.10	293.80	26.1	303.56	294.18	1	0	30
699	97	0.7797	0.038	299	1	318.70	292.20	25.8	306.63	292.51	1	0	41
700	97	0.7797	0.078	606	2	327.50	295.40	19.3	306.41	293.32	1	0	39
701	97	0.7797	0.070	543	2	325.90	295.30	15.7	306.47	294.25	1	0	34
702	97	0.7797	0.160	1244	3	340.90	297.50	14.9	306.41	294.45	1	0	34
703	97	0.7797	0.084	654	2	328.70	294.60	19.3	306.39	294.10	1	0	35
704	98	0.7782	0.057	443	2	324.00	297.60	18.9	307.96	297.64	1	0	47
705	98	0.7784	0.045	350	2	321.60	299.20	18.8	308.53	297.71	1	0	47
706	99	0.7790	0.100	779	2	332.40	292.00	15.6	307.94	292.75	1	0	44
707	100	0.7792	0.129	1004	3	340.90	298.20	8.2	316.45	287.18	1	0	46
708	100	0.7792	0.130	1014	3	340.90	302.10	12.4	316.11	288.02	1	0	46
709	101	0.7792	0.074	575	2	327.40	292.90	18.0	307.71	293.42	1	0	43
710	101	0.7792	0.149	1164	3	340.20	294.90	18.2	308.31	293.62	1	0	43
711	101	0.7792	0.089	692	2	331.00	295.90	16.5	309.13	293.37	1	0	44
712	101	0.7792	0.038	298	1	320.80	296.60	17.9	309.72	293.11	1	0	44
713	101	0.7794	0.069	541	2	327.20	295.70	15.5	308.92	292.38	1	0	44
714	102	0.7794	0.026	202	1	320.60	292.70	14.6	313.48	291.82	1	0	44
715	103	0.7795	0.061	475	2	327.30	293.90	11.1	311.97	291.68	1	0	44
716	103	0.7795	0.063	490	2	327.30	293.90	11.1	311.37	291.06	1	0	42
717	104	0.7832	0.064	502	2	327.40	302.40	21.5	311.09	300.94	1	0	48

开始 启动 Internet Explorer 浏览器 查找并显示 Internet 上的信息和网站。 15:24

Table 2.1 fire pixel list generated by automatic searching which give the fire pixel number, fire region number, longitude and latitude etc.

Fire region information list

保存的文件可用Excel读入

文件

	火区编号	省份	地市	区县	中心纬度	中心经度	估算面积(平方米)	火区像元数
69	69				52.09	127.96	3412	5
70	70				52.04	126.82	5652	7
71	71	内蒙古自治区	呼伦贝尔盟	鄂伦春旗	51.46	125.08	1127	1
72	72	内蒙古自治区	呼伦贝尔盟	鄂伦春旗	51.43	124.95	15228	14
73	73	内蒙古自治区	呼伦贝尔盟	鄂伦春旗	51.45	125.13	9655	9
74	74	内蒙古自治区	呼伦贝尔盟	鄂伦春旗	51.44	125.22	1162	1
75	75	内蒙古自治区	呼伦贝尔盟	鄂伦春旗	51.43	125.27	8756	10
76	76	内蒙古自治区	呼伦贝尔盟	鄂伦春旗	51.39	125.31	4105	6
77	77	内蒙古自治区	呼伦贝尔盟	鄂伦春旗	51.34	125.34	14817	19
78	78	内蒙古自治区	呼伦贝尔盟	鄂伦春旗	51.36	124.84	1145	1
79	79	内蒙古自治区	呼伦贝尔盟	鄂伦春旗	51.28	125.26	22700	32
80	80	内蒙古自治区	呼伦贝尔盟	鄂伦春旗	51.32	125.18	8676	11
81	81	内蒙古自治区	呼伦贝尔盟	鄂伦春旗	51.30	125.08	625	2
82	82	内蒙古自治区	呼伦贝尔盟	鄂伦春旗	51.26	125.16	9871	13
83	83	内蒙古自治区	呼伦贝尔盟	鄂伦春旗	51.26	125.00	408	1
84	84	内蒙古自治区	呼伦贝尔盟	鄂伦春旗	51.26	125.11	565	1
85	85	内蒙古自治区	呼伦贝尔盟	鄂伦春旗	51.25	125.13	2180	3
86	86	内蒙古自治区	呼伦贝尔盟	鄂伦春旗	51.24	125.03	634	1
87	87	内蒙古自治区	呼伦贝尔盟	鄂伦春旗	51.18	125.00	43178	47
88	88	内蒙古自治区	呼伦贝尔盟	鄂伦春旗	51.24	125.26	636	2
89	89	内蒙古自治区	呼伦贝尔盟	鄂伦春旗	51.18	124.95	5436	8
90	90	内蒙古自治区	呼伦贝尔盟	鄂伦春旗	51.20	124.91	1088	1
91	91	内蒙古自治区	呼伦贝尔盟	鄂伦春旗	51.20	124.93	1047	1
92	92				51.07	128.00	3421	3
93	93	黑龙江省	黑河市	嫩江县	50.98	126.18	946	3
94	94	黑龙江省	黑河市	黑河市	50.86	126.56	10639	15
95	95	黑龙江省	黑河市	黑河市	50.83	126.53	807	2
96	96	黑龙江省	黑河市	黑河市	50.81	126.62	5272	7
97	97	黑龙江省	黑河市	黑河市	50.65	126.56	57517	73
98	98	黑龙江省	黑河市	黑河市	50.73	126.49	793	2
99	99	黑龙江省	黑河市	黑河市	50.69	126.46	779	1
100	100	黑龙江省	黑河市	黑河市	50.68	126.31	2019	2
101	101	黑龙江省	黑河市	黑河市	50.68	126.48	3272	5
102	102	黑龙江省	黑河市	黑河市	50.67	126.34	202	1
103	103	黑龙江省	黑河市	黑河市	50.66	126.36	965	2
104	104				50.44	127.38	502	1

Table 2.2 fire region list gives the fire region number, longitude and latitude,number of pixels in the region, etc.

2). Evaluating sub-pixel size of hot spot by using multiple channels of AVHRR

Recent years, the forest fire prevention department want more information from satellite remote sensing, like the intensity of a fire spot, not only the location.

According to the features of blackbody radiance in different thermal infrared band and the characteristics of AVHRR infrared channel (spatial resolution and dynamic range of brightness temperature), there is evident difference of radiance increment caused by fire spot in different AVHRR infrared channels. The difference of the size of hot spot detected by satellite can be different in a range of tens times, and temperature in several hundreds K.

When the difference of brightness temperature between CH3 and CH4 in a mixed pixel is increased from 8K to 35K, the hot spot sub-pixel size within a pixel will be increased from 0.002 to 0.18, almost ten times.(see. Fig. 4.1)

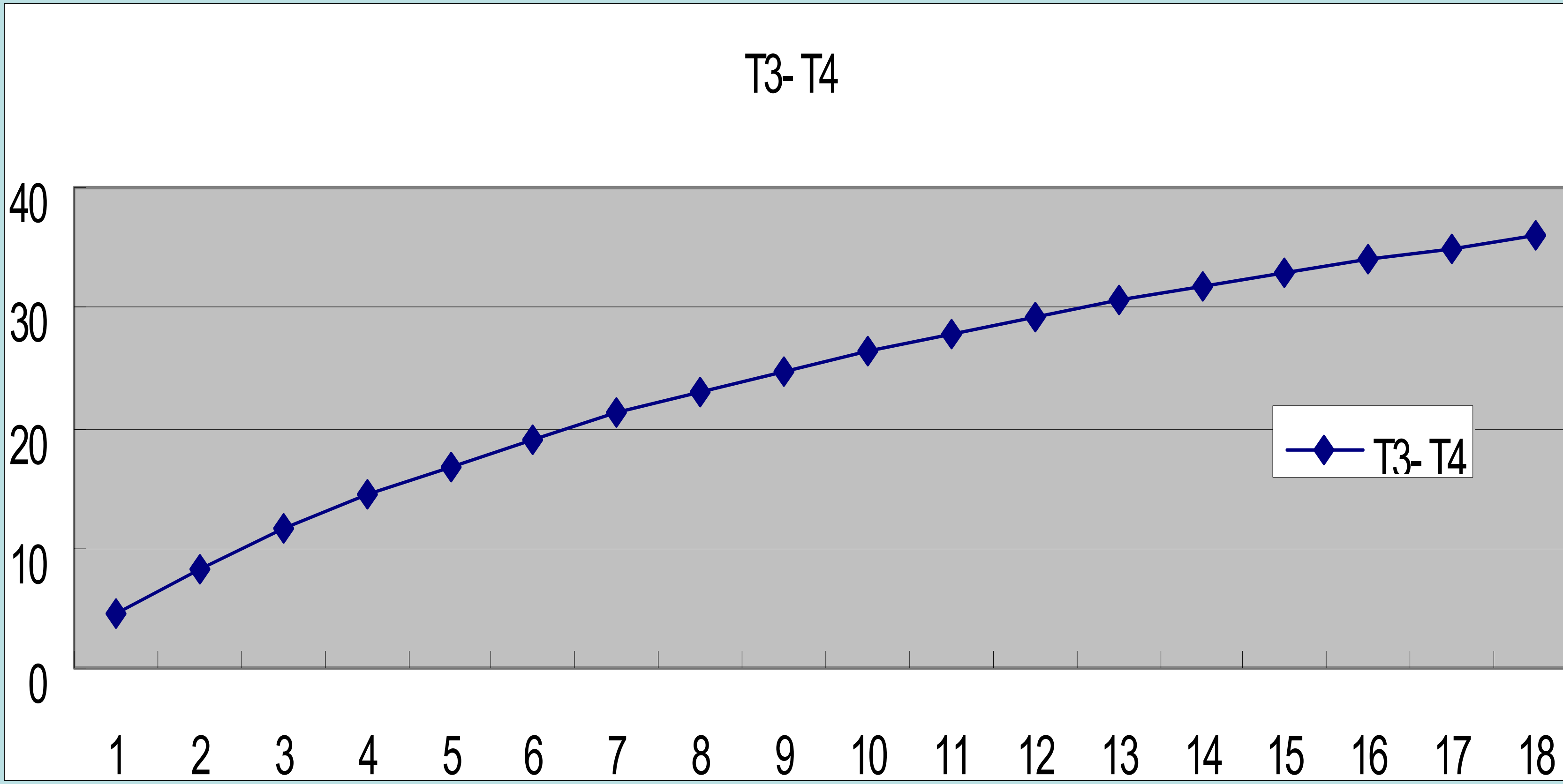

the ratio of sub-pixel size occupied within a pixel (‰)

Fig. 2.3 the temperature difference between CH3 and CH4 in a mixed pixel along with the size of fire spot increasing (assuming background temperature is 290K, fire temperature is 500K, 325K is upper limitation of CH3)

(1) Three ways of multiple channel combination in evaluating sub-pixel size and temperature:

- 3.7μm (mid-infrared) and 11μm (thermal infrared) channel

Using Newton's iteration method to solve the P (the percentage of hot spot sub-pixel size within a mixed pixel) and T_f(temperature of the fire).

- 1.6μm (near-infrared) and 11μm (thermal infrared) channel.

Deriving the emitted radiance from 1.6μm channel and using Newton's iteration method to solve the P and T_f with 11 μm channel.

- 11μm and 12μm (two thermal infrared) channel.

Establishing a relationship between the P, T_f and the difference of brightness temperature between the mixed pixel in CH4 and background, and the difference between CH4 and CH5 with background.

(2) The means of Presentation of Evaluation

Classification of fire intensity according to the hot spot sub-pixel evaluation

In daily forest and grassland fire monitoring by using remote sensing, the number of fire pixels (mixed pixel) is often up to tens or hundreds. If presenting evaluation result uses the means of table list, the analyzer will have much difficulty to realize the situation of fire condition. Using a figure can present various extent of sub-pixel evaluation in large area, and provide relevant qualitative information of fire condition.

Considering the effect of presentation, classification of fire extent can be five levels. Higher fire extent level means larger sub-pixel size and higher temperature of fire spot. The way of the classification should be according to the features of monitoring area.

Table 2.3 present one of the classification way of hot spot intensity which may be suitable for Northeast part of China.

Table 2.3 the definition of hot spot intensity

Intensity level / Sub-pixel size (km^2)	1	2	3	4	5
<3000	<600K	600K~750K	>750K		
3000 ~ 3500	<580K	580K~680K	680K~800K	>800K	
3500 ~ 6500	<500K	500K~630K	630K~720K	720K~850K	>850K
6500 ~ 10000	<500K	500K~600K	600K~700K	700K~800K	>800K
10000 ~ 20000	<500K	500K~580K	580K~650K	650K~750K	>750K
>20000	<500K	500K~550K	550K~630K	630K~700K	>700K

Table 2.4 sub-pixel evaluating results list
from the data of **NOAA-14 2001/10/05/15:47(lc)**

No.	Lat.	Long.	CH3mix	CH4mix	CH5mix	Tbg	P(%)	SIZE(M²)	T(K)	Intensity
0	49.49	125.10	320.90	282.90	281.30	278.53	0.84	6709	524	2
1	49.48	125.08	321.80	282.30	281.60	278.53	0.50	3995	590	2
2	49.48	125.09	321.80	282.30	281.60	278.53	0.50	3995	590	2
3	49.48	125.10	321.80	289.40	287.60	78.53	1.10	8796	680	3
4	49.48	125.11	321.80	287.20	285.60	278.53	0.70	5593	740	4
5	49.48	125.12	321.80	287.20	285.70	278.53	0.70	5593	740	4
6	49.47	125.09	321.80	283.60	282.90	278.53	0.60	4794	630	3
7	49.47	125.10	321.80	283.70	283.10	278.53	0.90	7191	540	2
8	49.47	125.11	321.80	283.70	283.10	278.53	0.90	7191	540	2
9	49.47	125.12	321.80	290.60	289.20	278.53	1.90	15182	570	2
10	49.47	125.13	314.70	281.20	279.90	278.53	0.45	3595	551	2
11	49.47	125.14	314.70	281.20	279.90	278.53	0.45	3595	551	2
12	49.46	125.12	321.80	282.30	281.90	278.53	0.50	3996	590	2
13	49.46	125.13	321.80	282.30	281.90	278.53	0.50	3996	590	2
14	49.46	125.14	316.10	280.10	279.70	278.53	0.31	2477	588	1

Table 2.4 presents NOAA-14 data hot spot sub-pixel evaluating in Northeast part of China 2001/10/05/15:47(lc) There are 15 fire pixels (mixed pixel) in the fire field, four of them (No. 0 , 10 , 11 , 14) using CH3 , CH4 data to do evaluation, others using CH4 and CH5 , as CH3 in those pixels are all saturated .The highest intensity is in No.4 and No.5, which are up to 4 intensity level.

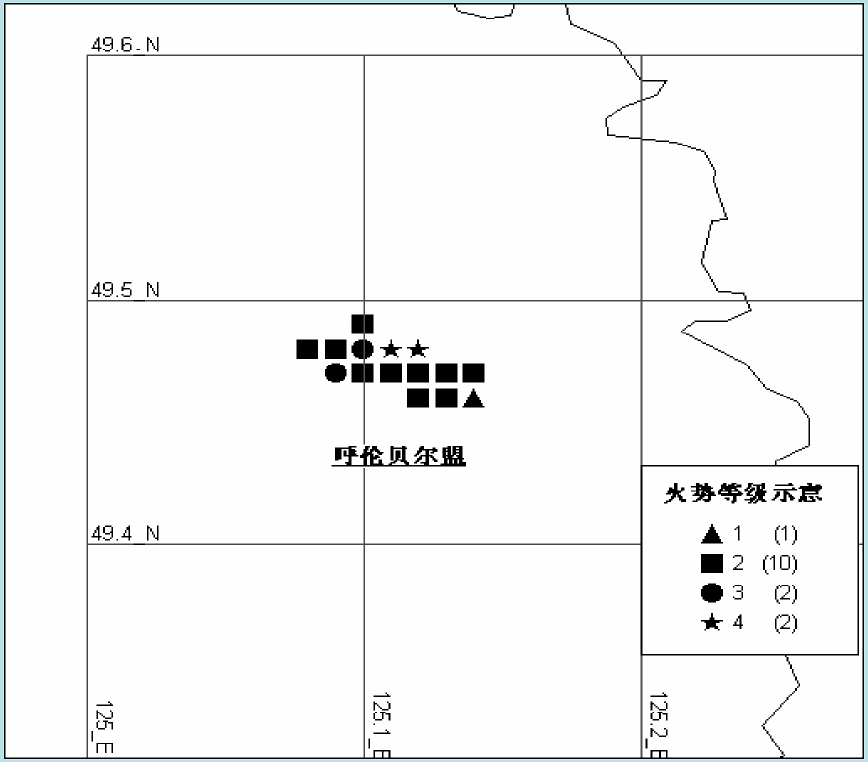

Fig. 2.4 Hot spot intensity figure

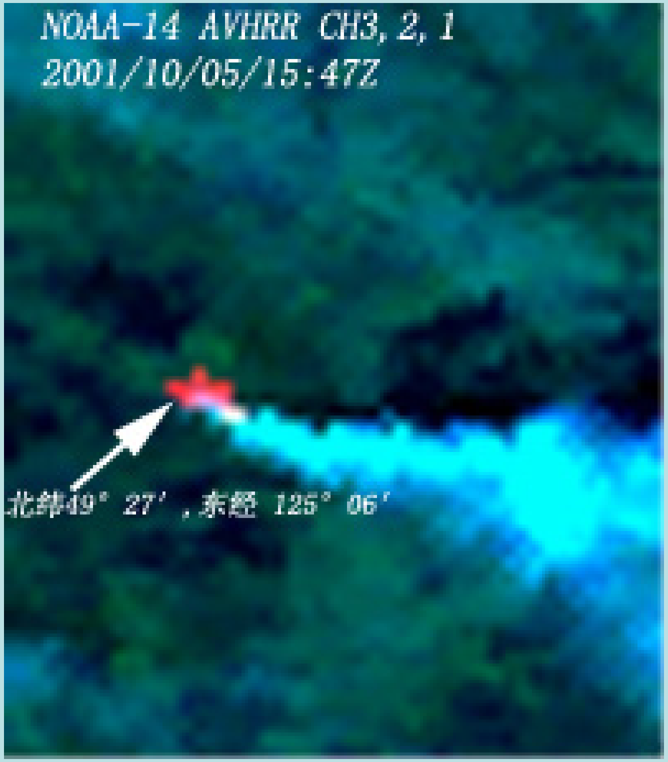

Fig. 2.5 NOAA-14 AVHRR CH3,2,1 2001/10/05/15:47

Fig. 2.4 presents the results of sub-pixel evaluation from the list in table 2.4. This fire region includes 15 pixels, upon them 4 pixels are calculated using CH3 and CH4, and the remainder all using CH4 and CH5 as CH3 is saturated.

The features analyzing to natural forest fire happened in the summer of 2002 using hot spot intensity (1)

The number of pixels with high intensity level in Inner Mongolia natural forest in the summer of 2002(Fig.4.7) is much less than in that of Northeast Part of China in October of 2001 (Fig.4.8). The features of this natural forest fire in summer is mainly under crown of trees, even under ground surface.

Fig. 2.6 NOAA-14 hot spot intensity 2002/08/14 /15:24 (LC)

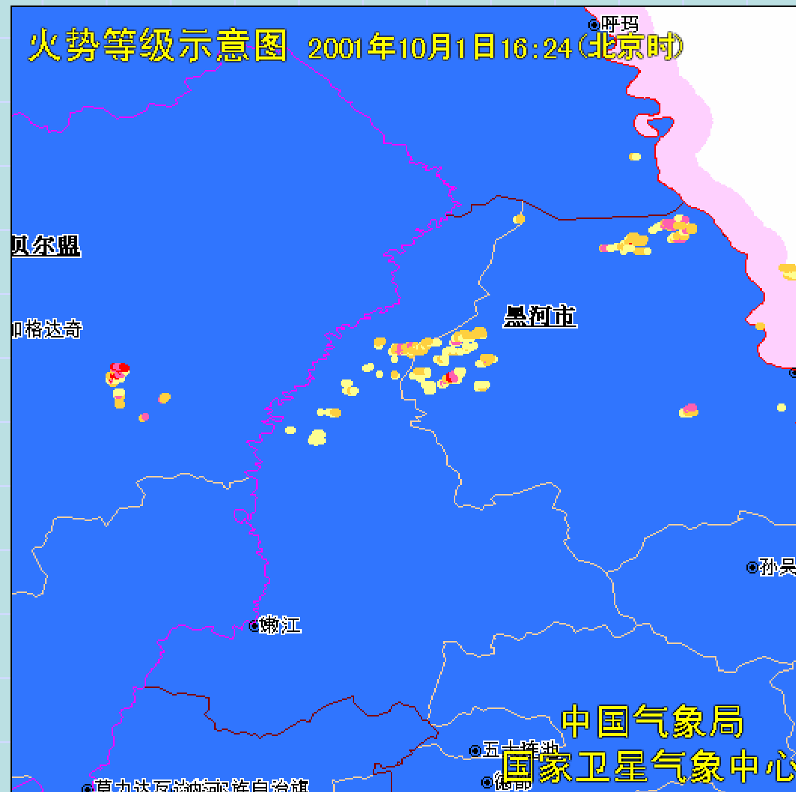

Fig. 2.7NOAA-14 hot spot intensity 2001/10/01/ 16:24(LC)

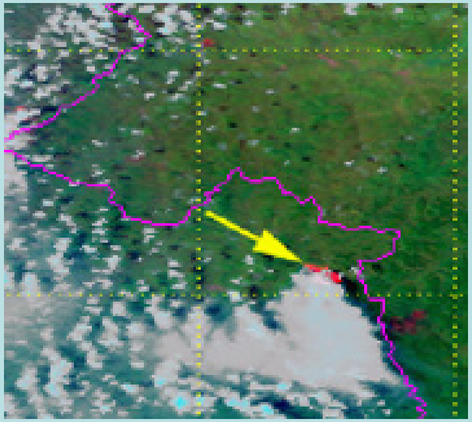

Fig. 2.8 NOAA-14 2002/08/14/ 15:24(LC)

The features analyzing to natural forest fire happened in the summer of 2002 using hot spot intensity (2)

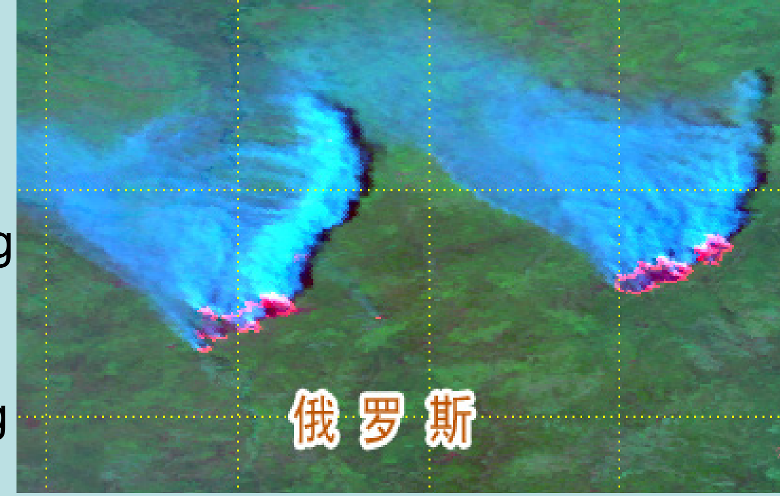

Fig. 2.9 NOAA-14 2002/08/12/ 16:11(LC)

Fig. 2.10 NOAA-14 hot spot intensity 2002/08/14/ 15:24(LC)

Fig. 2.11 NOAA-14 hot spot intensity 2002/08/12/ 16:11(LC)

The number of pixels with high intensity level in Inner Mongolia natural forest in Aug 14, 2002 is much less than in that of the Far-east forest region of Russia in same period. During the summer of 2002, the east part of Asia was very dry and the forest fire-dangerous level was very high.

Hot spot intensity map for Daxinganling Region forest fire monitoring in May 25, 2006

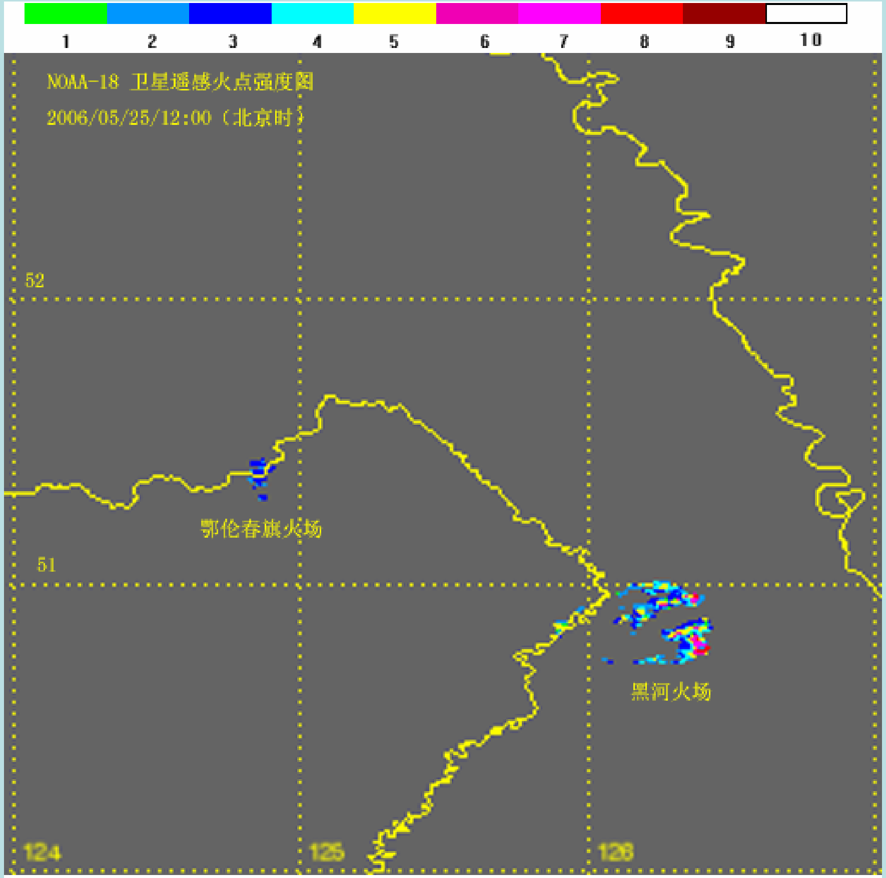

Fig.2.12 NOAA-18 hot spot intensity 2006/05/25/ 12:00(LC)

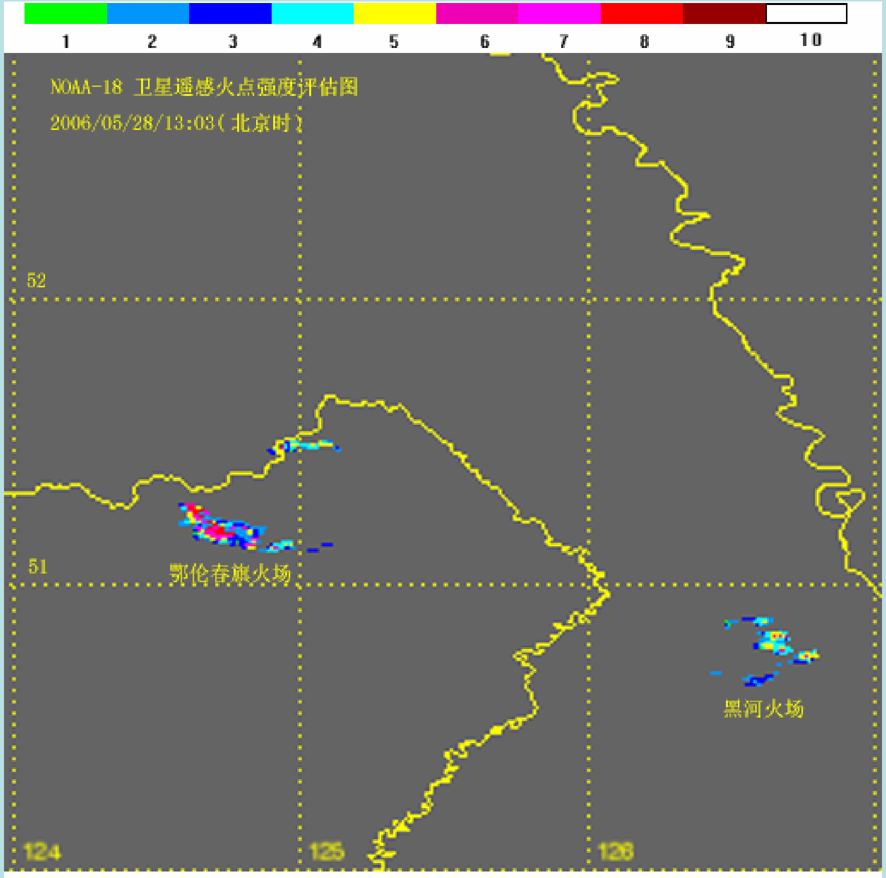

Fig. 2.13 NOAA-16 hot spot intensity 2006/05/25/ 13:03(LC)

3) The validation for sub-pixel size evaluation

- To validate the sensitivity and sub-pixel size evaluation to fire spot with meteorological and environment satellites, NSMC/CMA had a series of experiments by making man-made fire field observed simultaneously by FY-1D and EOS/MODIS and measured by some relative instruments in the late of October of 2005. The experiment site in a discarded airport located in Wu Ming County, Guang Xi Province (Fig. 2.14)

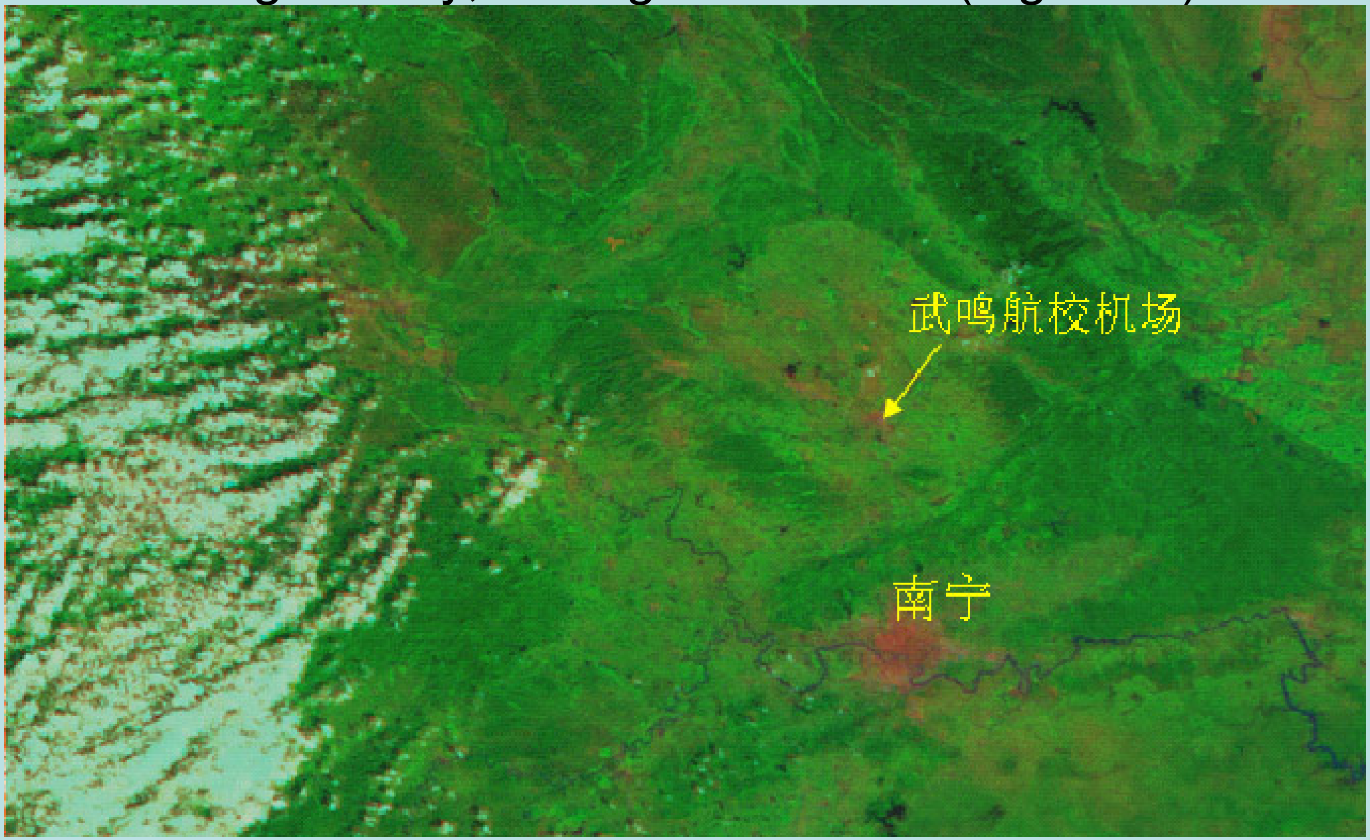

Fig. 2.14 EOS/MODIS CH.20，2，1 RGB，250m 2005/10/08/11:39（Beijing time）

The position of the airport in which the experiment site located (see Fig.2.15 and Fig.2.16).

Fig..2.15 The image is from google earth

Fig. 2.16 The picture is from a pilotless plane

The position of the experiment site

(The pictures are taken by a pilotless plane)

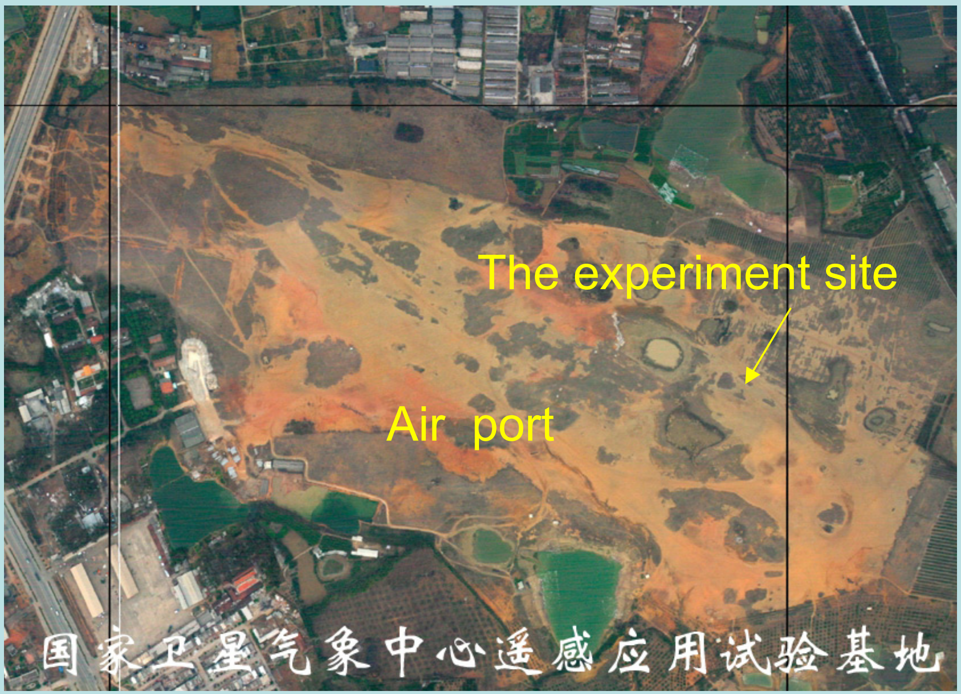

Fig. 2.17 The picture is taken from a pilotless plane before the experiment.

Fig. 2.18 The picture is taken from a pilotless plane during the experiment.

The man-made fire field is in circular shape with the size of 100 km^2 and 200 km^2 (Fig.2.19) , and was laid over firewood, branches and trunks in about 40-60 cm thick (Fig.2.20). It was burned just before the satellite pass over to get the maximum burning extent when satellite scanned it.

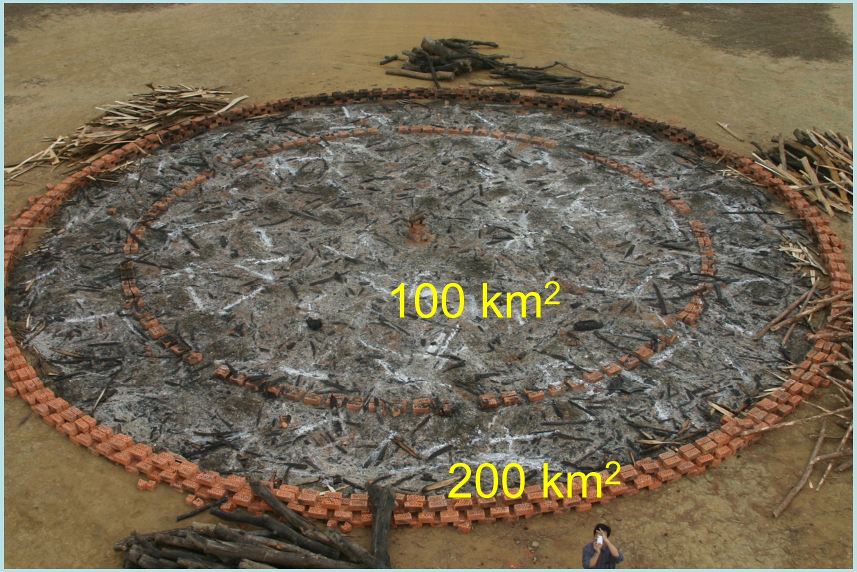

Fig. 2.19 The man-made fire field in the size of 100 km^2 and 200 km^2.

Fig.2.20 The man-made fire field was laid over firewood, branches and trunks .

To get the radiance from fire field when satellite passing over, the Thermal Imaging System, Boman middle-far infrared spectrometer and other relative instruments were used to measure the radiance in 3.5~4.0μm, 10.5~11.3μm, and 11.5~12.5μm channels at different height (from 0m,2.5m, 5m, 9.5m, 15m and up to 18 m) and the temperature distribution in the field.

Five experiments were taken with man made fire field simultaneously observed by FY-1D ，EOS TERRA、AQUA respectively (Table 2.5).

Table 2.5 The list of information about the five experiments.

Date of experiment	Data source	Size of field	Time of burning (Beijing time)	Time of satellite scan (Beijing time)
Oct. 20, 2005	TERRA	$100m^2$	22:30	23:04
Oct. 23, 2005	AUQA	$100m^2$	14:00	14:07
Oct. 23, 2005	FY-1D	$200m^2$	19:44	19:59
Oct. 28, 2005	TERRA	$200m^2$	11:06	11:20
Nov. 24, 2005	AQUA	$100m^2$	14:04	14:08

The experiment held at night of Oct. 23, 2005年 using FY-1D

Time of start burning ：19:44；

Time of satellite scanned： 19:59'30"；

Size of man made fire field： 200m^2

Fig..2.21 Live picture of fire field when satellite scans

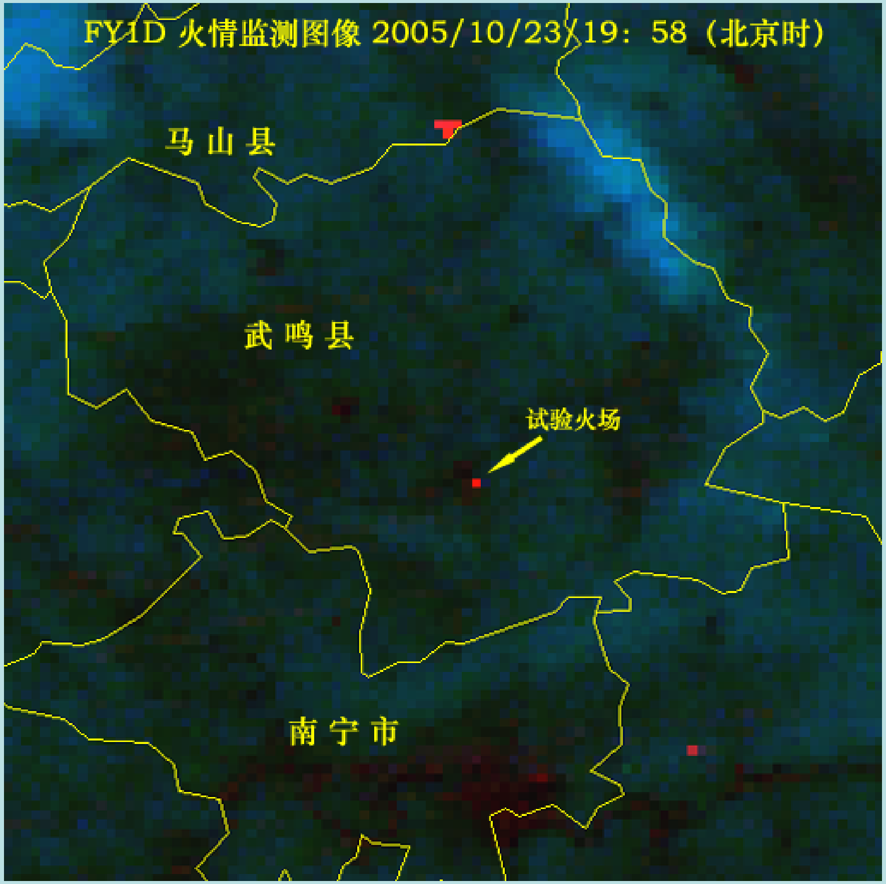

Fig. 2.22 FY-1D image CH.3,2,1 RGB

2005/10/23/19:58（Beijing time）

Brightness temperature increment in 3.7μm and 11μm in the mixed pixel.

T_{3mix} = 295.8K, T_{3bg} = 289.1K, ΔT_{3mix} = **6.7K** (night)

T_{4mix} = 288.4K, T_{4bg} =288.3K, **ΔT_{4mix} = 0.1K**

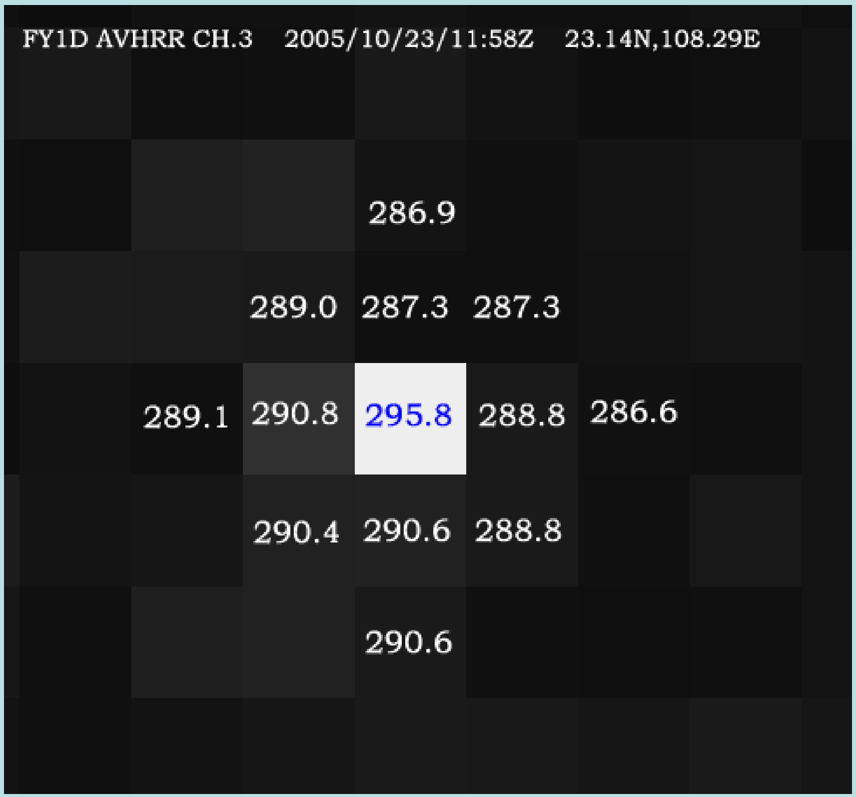

CAVHRR CH.3

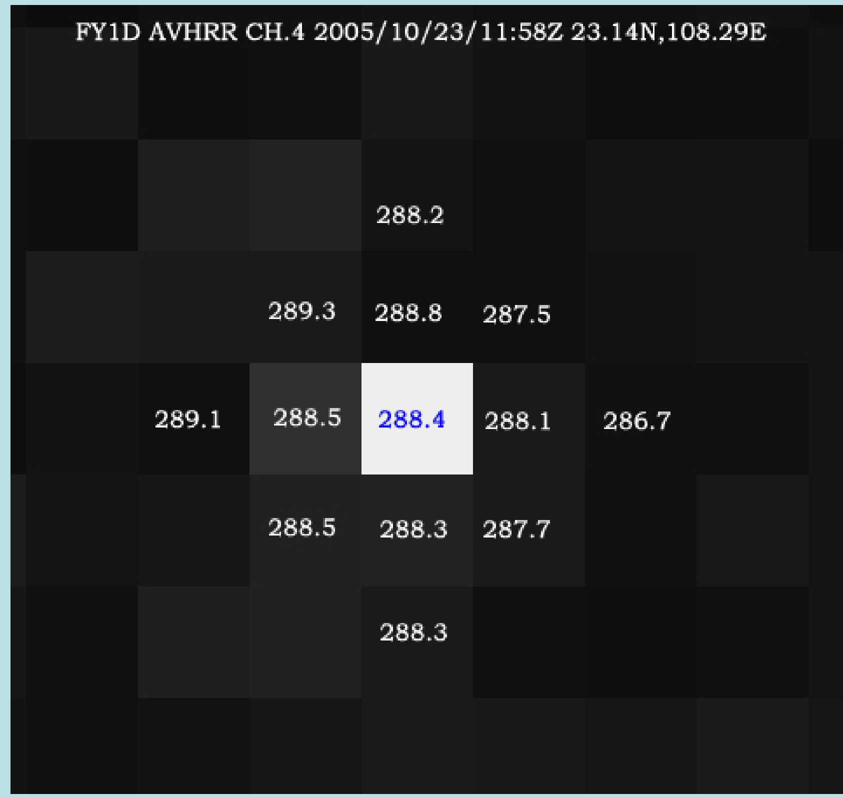

CAVHRR CH.4

Fig. 2.23 The brightness temperature in the mixed pixel and adjacent pixels in CH3,and CH4 of FY-1D 2005/10/23/11:58Z)

The experiment hold in Oct. 28, 2005 using TERRA

Time of start burning ： 11:06；
Time of satellite scanned： 11:20
Size of man made fire field： 200m^2

Fig. 2.24 Live picture of fire field when satellite scans

Fig. 2.25 TERRA MODIS image CH.20,2,1 RGB
2005/10/28/11:20（Beijing time ）

Brightness temperature increment in 3.7μm and 11μm in the mixed pixel.

T_{20mix} = 317.9K, T_{20bg} = 306.8K, **ΔT_{20mix} = 11.1K**,

T_{31mix} = 299.2K, T_{31bg} =297.8K, **ΔT_{31mix} = 1.4K**,

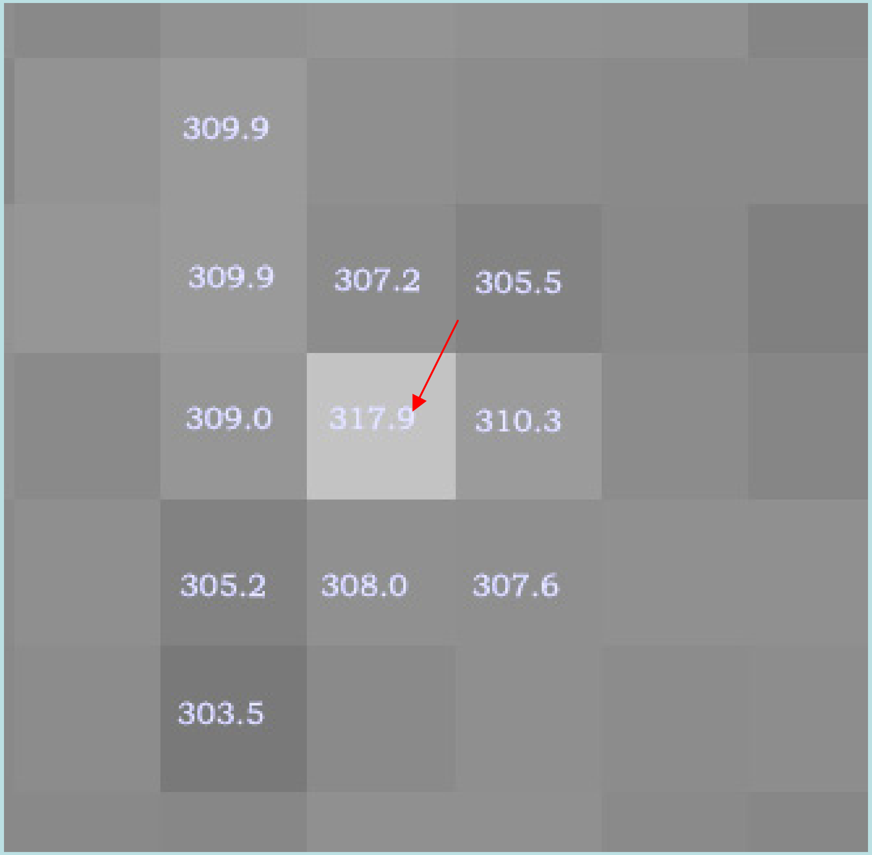

MODIS CH.20

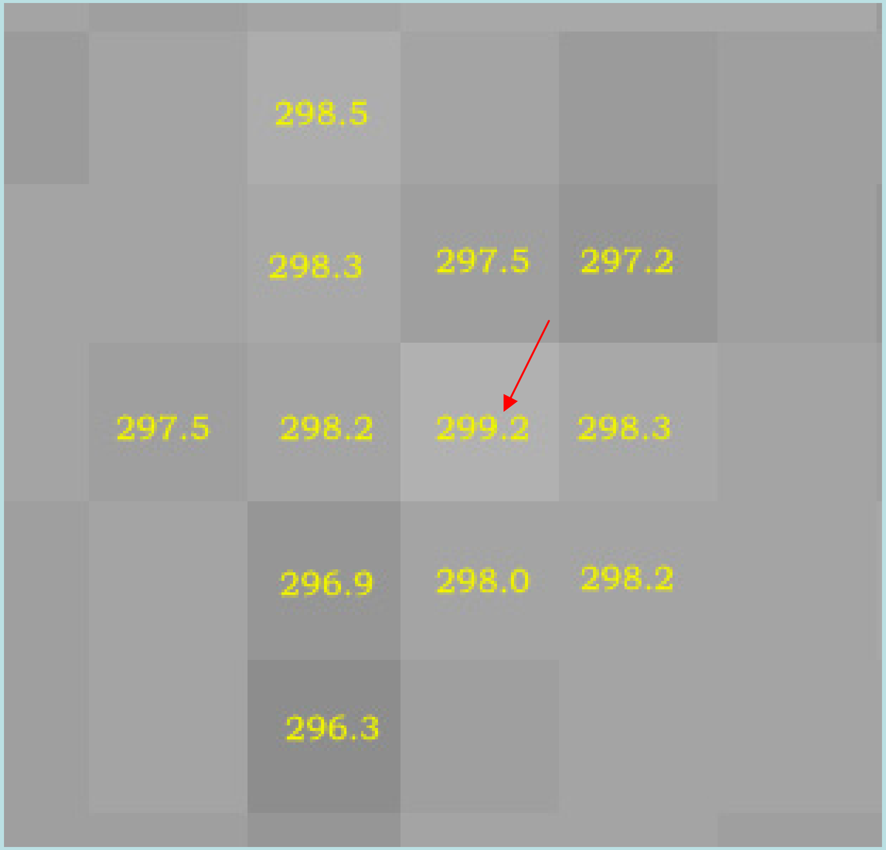

MODIS CH.31

Fig. 2.26 The brightness temperature in the mixed pixel and adjacent pixels of TERRA (2005/10/28/03:20Z)

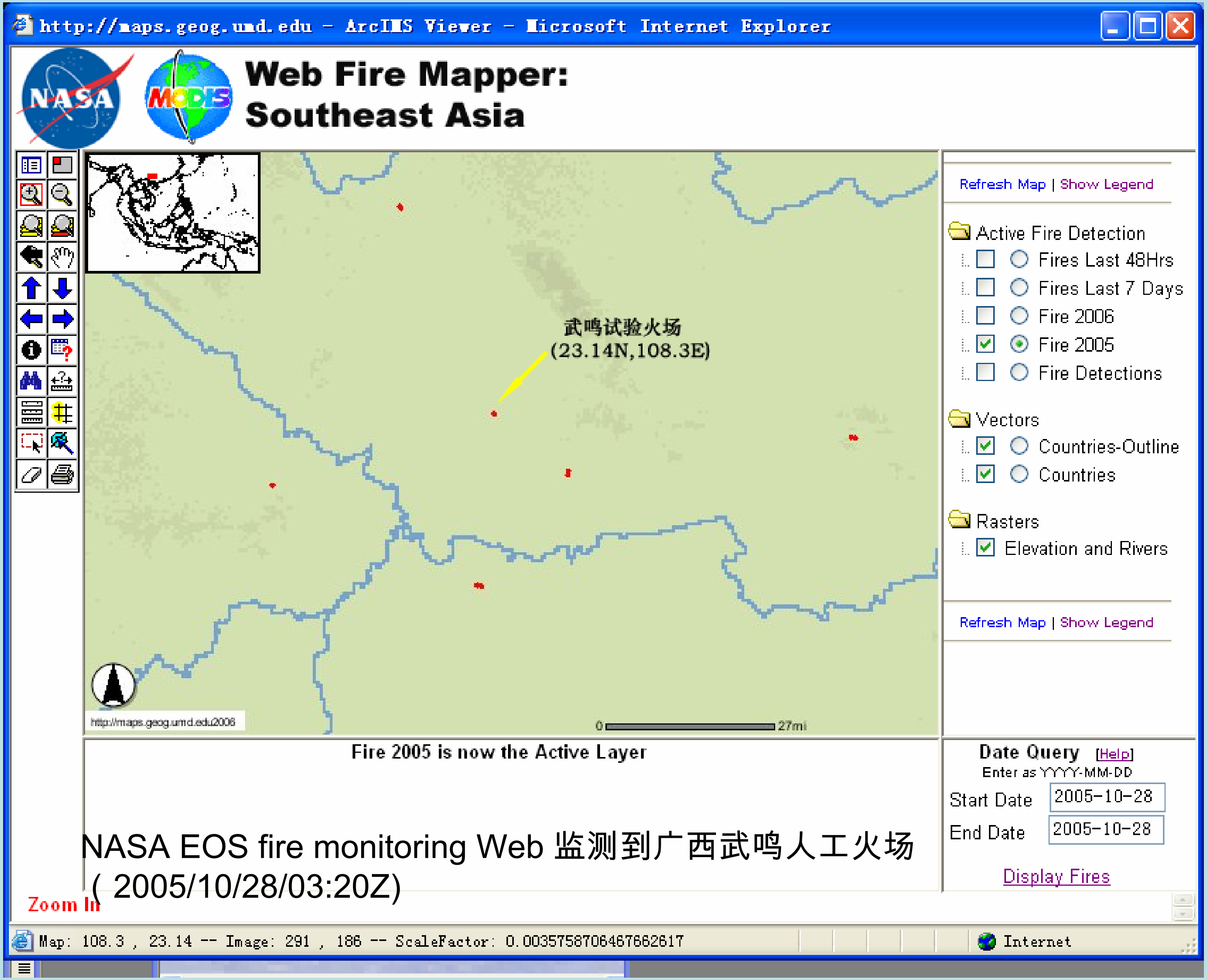

NASA EOS fire monitoring Web 监测到广西武鸣人工火场
(2005/10/28/03:20Z)

Fig. 2.27 Web Fire Mapper shows the manmade fire spot in TERRA data of 2005/10/28/03:20Z

A pilotless plane were used to take a picture to fire field simultaneously with satellite pass over.

Fig. 2.28 The pilotless plane was used in the experiment

Fig. 2.29 The picture was taken by a pilotless plane at 11:16 before the satellite pass when the flame occupied more than half of the field.

Fig. 2.30 the Thermal Imaging System in the altitude of 17.5m.

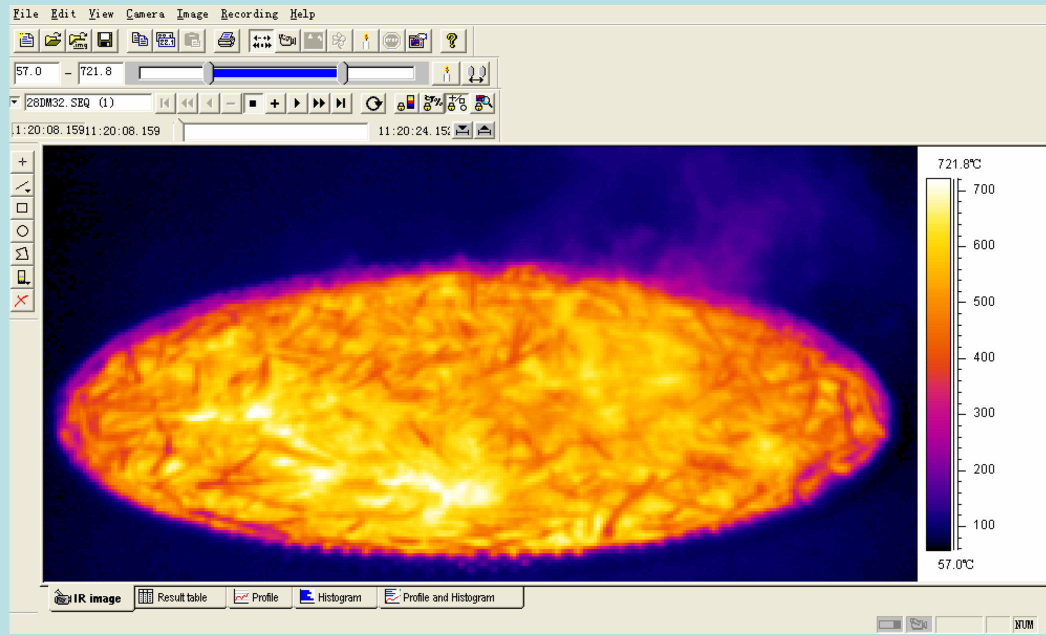

Fig. 2.31Thermal Imaging System instrument were used at 17.5 altitude to measure the temperature distribution in the fire field,

The experiment hold in Nov. 24, 2005 using AQUA

Time of start burning ： 14:04；
Time of satellite scaned： 14:08;
Size of man made fire field： 100m^2

Fig. 2.32 Live image of fire field when satellite scans

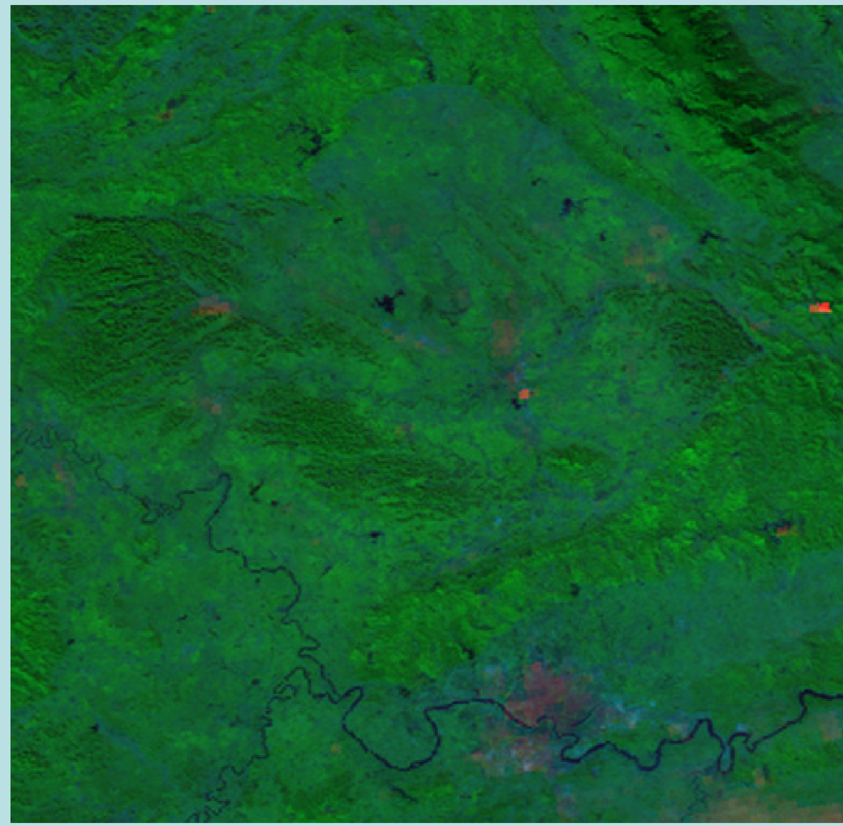

Fig. 2.33 AQUA MODIS image CH.20,2,1 RGB 2005/11/24/14:02（Beijing time）

Brightness temperature increment in 3.7μm and 11μm in the mixed pixel.

T_{20mix} = 311.3K, T_{20bg} = 302.9K, ΔT_{20mix} = **8.4K**,

T_{31mix} = 297.8K, T_{31bg} =296.5K, ΔT_{31mix} **= 1.3K**

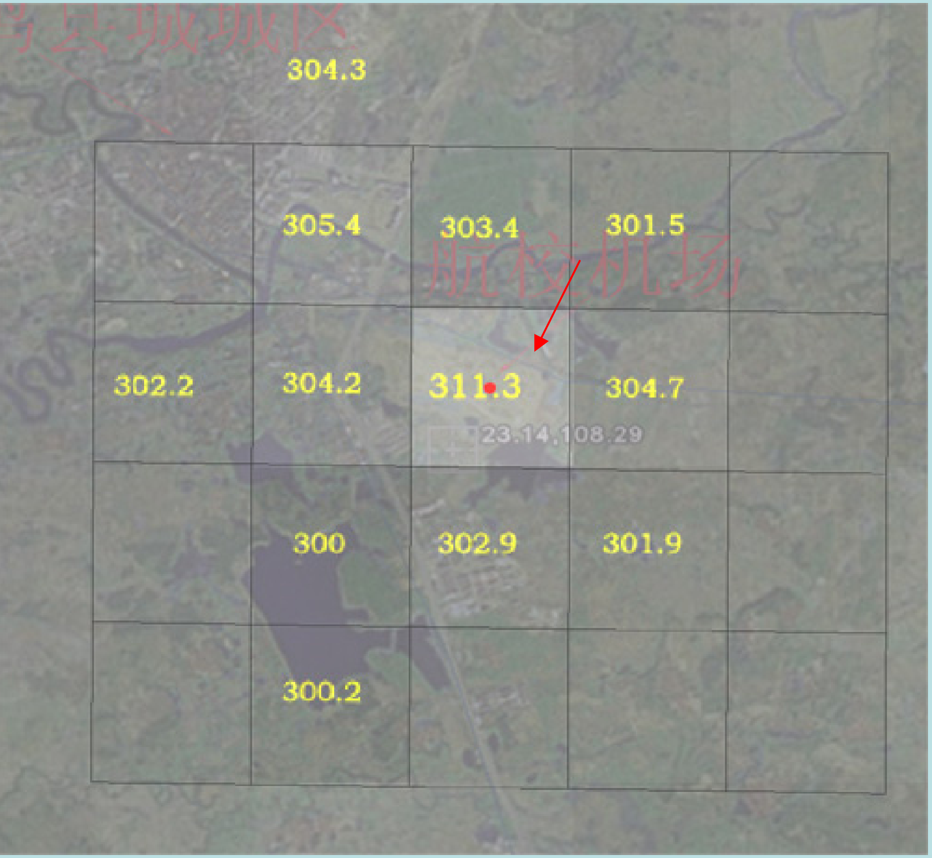

MODIS CH.20 MODIS CH.31

Fig. 2.34 The brightness temperature in the mixed pixel and adjacent pixels of AQUA (2005/11/24/06:02Z)

As surface features of the mixed pixel containing the airport is different from adjacent pixels, the temperature will be relatively different usually. To delete this influence, the satellite data received in Oct. 8, 2005, before the experiment, were used as the background.(Fig.2.35) The airport located in 23.14°N,108.29°E.

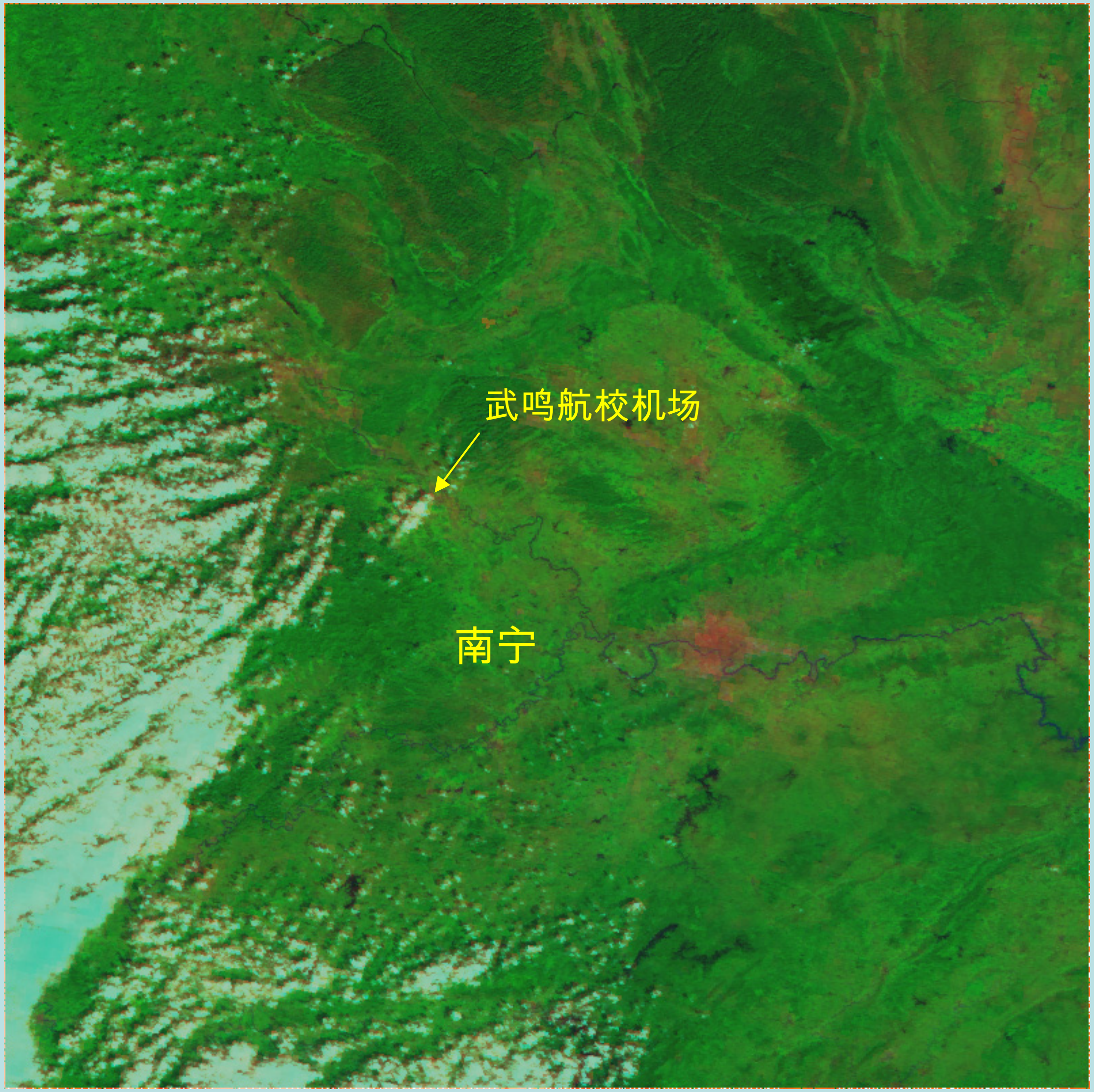

Fig.2.35 TERRA / MODIS CH 20，2，1（250m）
2005/10/08/11:39（Beijing time）

Brightness temperature increment in 3.7μm and 11μm in the mixed pixel.
$\Delta T20mix = 3.1K$,
$\Delta T31mix = 1.4K$

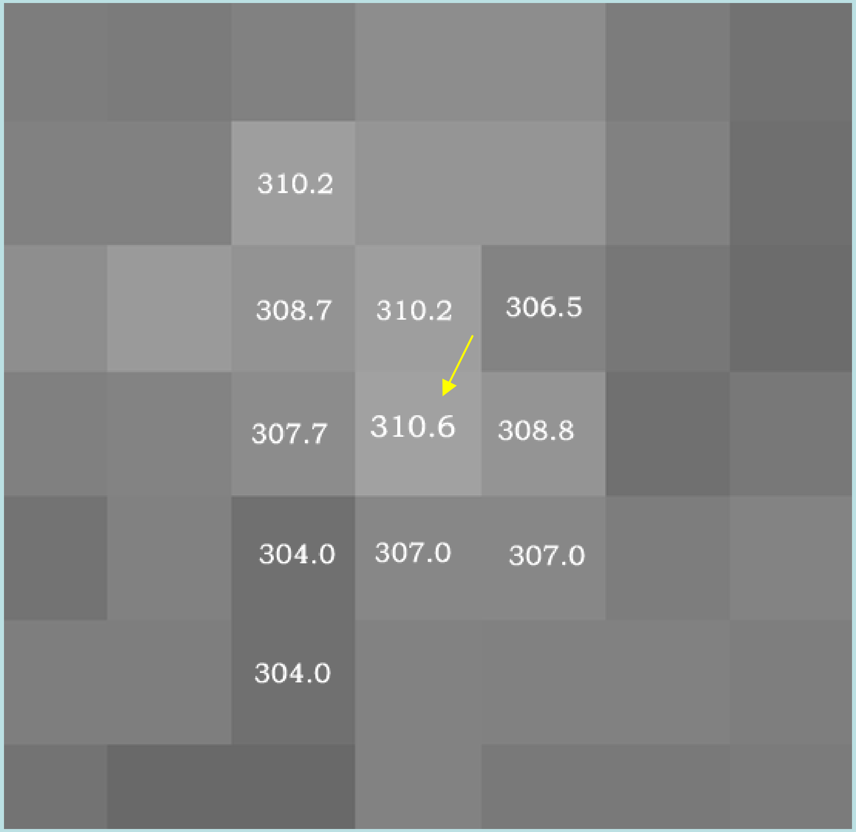

MODIS CH 20

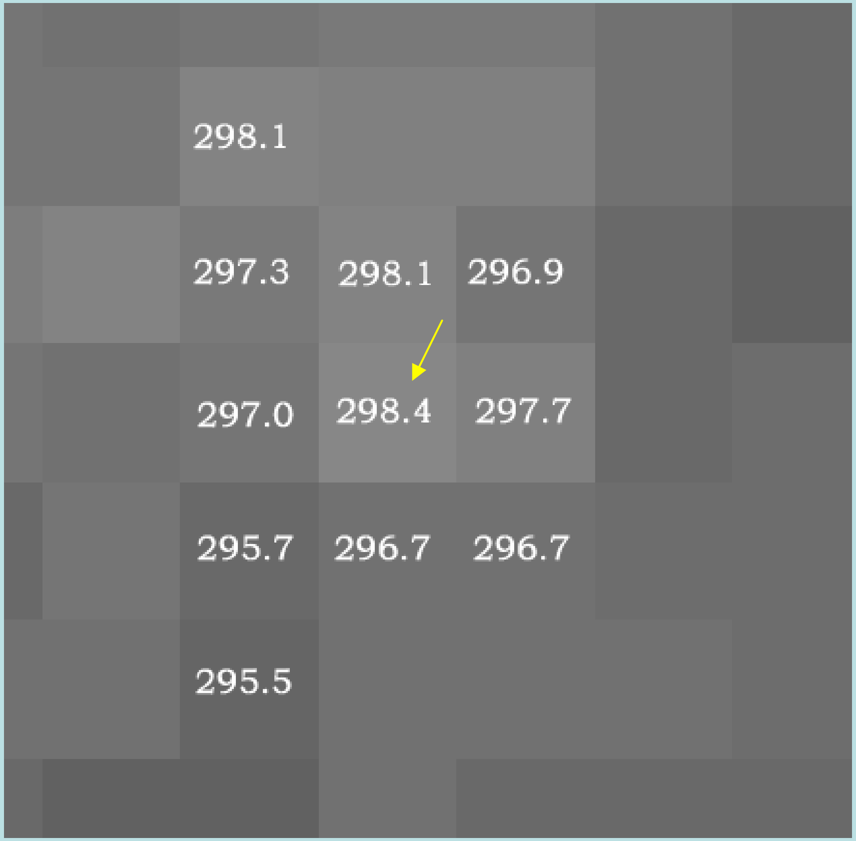

MODIS CH 31

Fig. 2.36 The brightness temperature in the mixed pixel and adjacent pixels of TERRA (2005/10/08/11:39Z)

Fig. 2.37 shows that a fire spot with 100 m^2 size and 800K (flame) temperature only cause about 0.13K brightness temperature increment in 11μm channel and 600K only cause 0.06K increment with background temperature of 300 K. As the surface features in the mixed pixel is relatively different from adjacent, it is very difficult to get the accurate background temperature in 11 μm. As the background temperature of small fire spot in 11μm Channel has some influence in sub pixel size evaluation, we substitute three background temperature in calculation respectively with 0.1k, 0.2k, 0.3K difference from mixed pixel in 11 μm to see the difference, ie: $T_{bg} = T_{31mix} - \Delta T$, ΔT = 0.1k, 0.2k, 0.3k

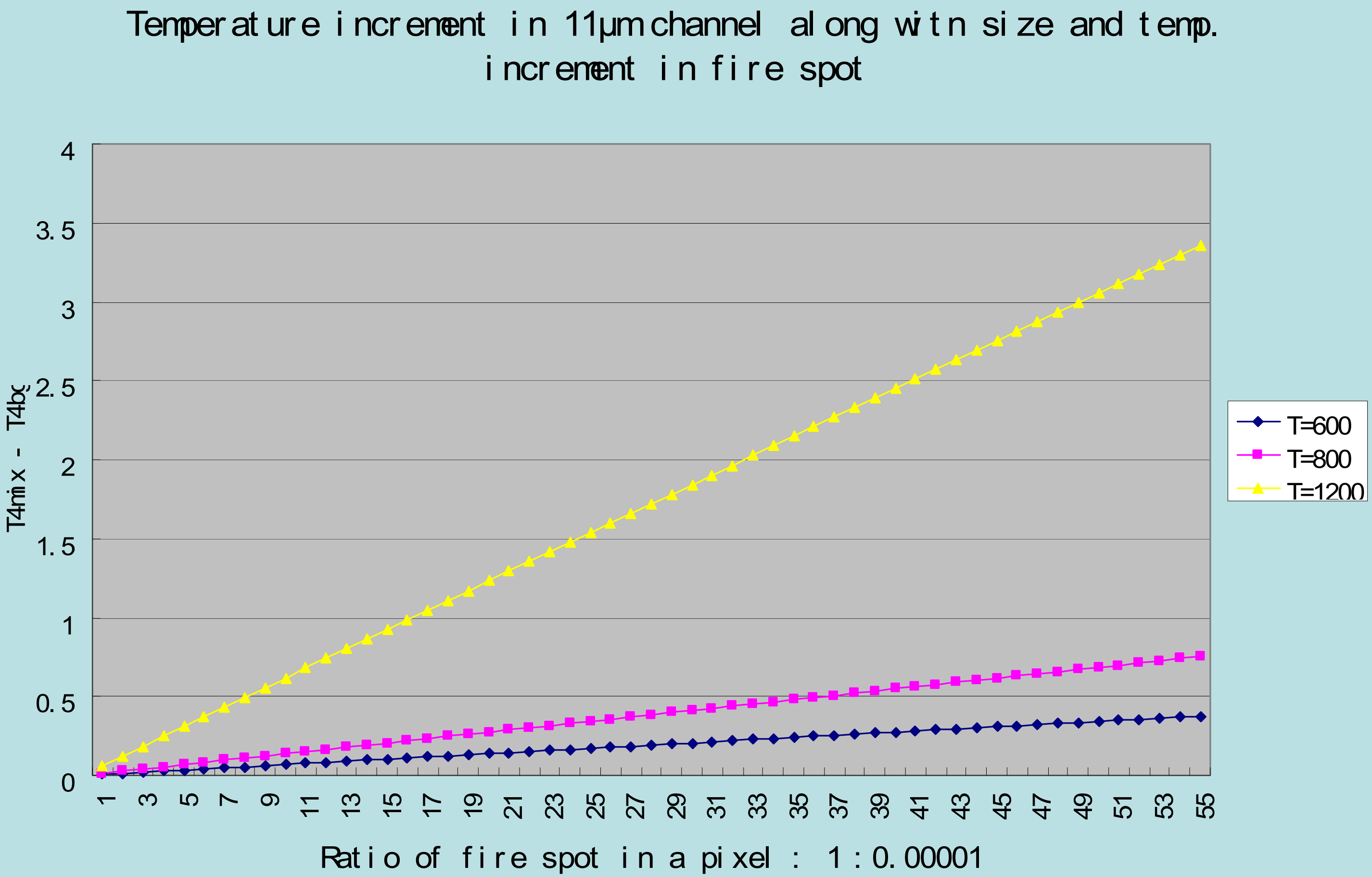

Fig. 2.37 The temperature difference between mixed pixel and background (assuming 300K) increment along with the size of fire spot increasing in 11 μm channel.

Sub pixel size and temperature evaluation

FY-1D data 2005/10/23/19:58(Beijing time)

Size of fire field：200 km^2

T3mix = 295.8K, T3bg = 289.1K, **ΔT3mix = 6.7K** （night）
T4mix = 288.4K, T4bg =288.3K**, ΔT4mix = 0.1K**
Tbg = T4mix - ΔT= 288.4K - ΔT, ΔT = 0.1k, 0.2k, 0.3k

Table 2.6 The list of results in the sub pixel evaluation to fire spot.

Background temperature (K)	The difference of temperature between background and mixed pixe l(K）	Percentage of fire field size in the mixed pixel（%）	Evaluated sub pixel size of fire spot（m^2）	Evaluated temperature of fire spot （K）
288.3	0.1	0.00649	76.3	844
288.2	0.2	0.022	249	666
288.1	0.3	0.04435	502	595

The evaluated sub pixel size and temperature is relatively close to the real case when the background temperature is 0.2 K different from mixed pixel.

Sub pixel size and temperature evaluation

TERRA data 2005/10/28/11:20(Beijing time)

Size of fire field：200 km2

T20mix = 317.9K, T20bg = 306.8K, ΔT20mix = 11.1K, ΔT20bg = 3.1K

T31mix = 299.2K, T31bg =297.8K, ΔT31mix = 1.4K, ΔT31bg = 1.4K

T*20mix = Tbg + ΔT20mix - ΔT20bg = 307.2K

Tbg = T31mix - ΔT, = 299.2K - ΔT, ΔT = 0.1k, 0.2k, 0.3k

Table 2.7 The list of results in the sub pixel evaluation to fire spot.

Background temperature (K)	The difference of temperature between background and mixed pixe l(K)	Percentage of fire field size in the mixed pixel（%）	Evaluated sub pixel size of fire spot （m^2）	Evaluated temperature of fire spot （K）
299.1	0.1	0.005118	58	1004
299.0	0.2	0.018245	206	756
289.9	0.3	0.037195	420	664

The evaluated sub pixel size and temperature is relatively close to the real case when the background temperature is 0.2 K different from mixed pixel.

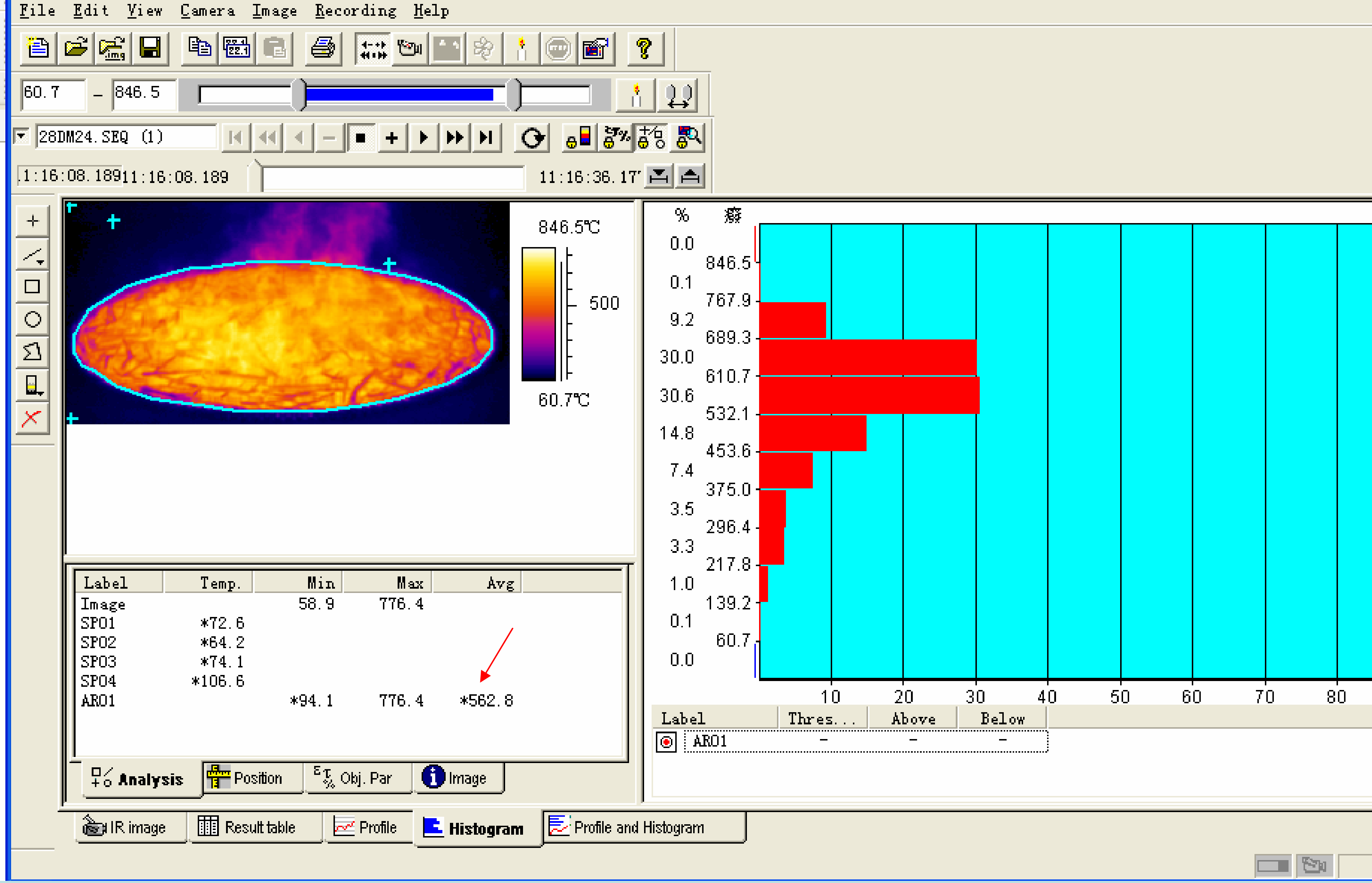

Fig. 2.38 the result figure measured and processed by Thermal Imaging System.

The average temperature of fire field when satellite scans is 562 ºC (835K) measured by Thermal Imaging System, and the size of fire field is 200 m^2.

Sub pixel size and temperature evaluation

AQUA data 2005/11/24/14:02(Beijing time)

Size of fire field：100 km2
T20mix = 311.3K, T20bg = 302.9K, **ΔT20mix = 8.4K**, ΔT20bg = 3.1K
T31mix = 297.8K, T31bg =296.5K, **ΔT31mix = 1.3K**, ΔT31bg = 1.4K
T*20mix = Tbg + ΔT20mix - ΔT20bg = 303.1K
Tbg = T31mix - ΔT, = 297.8K - ΔT, ΔT = 0.1k, 0.2k, 0.3k

Table 2.8 The list of results in the sub pixel evaluation to fire spot.

Background temperature (K)	The difference of temperature between background and mixed pixe l(K)	Percentage of fire field size in the mixed pixel (%)	Evaluated sub pixel size of fire spot (m^2)	Evaluated temperature of fire spot (K)
297.7	0.1	0.0078	88	807
297.6	0.2	0.02648	299	644
297.5	0.3	0.05325	603	577

The evaluated sub pixel size and temperature is relatively close to the real case when the background temperature is 0.1K different from mixed pixel.

3. The operation and service of fire monitoring system in NSMC/CMA

3.1 The daily operational system of fire monitoring

The major data source in fire monitoring including:

Polar orbiting meteorological satellite: FY-1D ,NOAA-12, 16 ,17,18

Geostationary meteorological satellite: FY-2C, MTSAT

EOS/MODIS : Terra and Aqua

Polar-orbiting meteorological satellite are currently mainly used for forest and grassland fire monitoring:

Real time data received from FY-1 satellite data receiving system

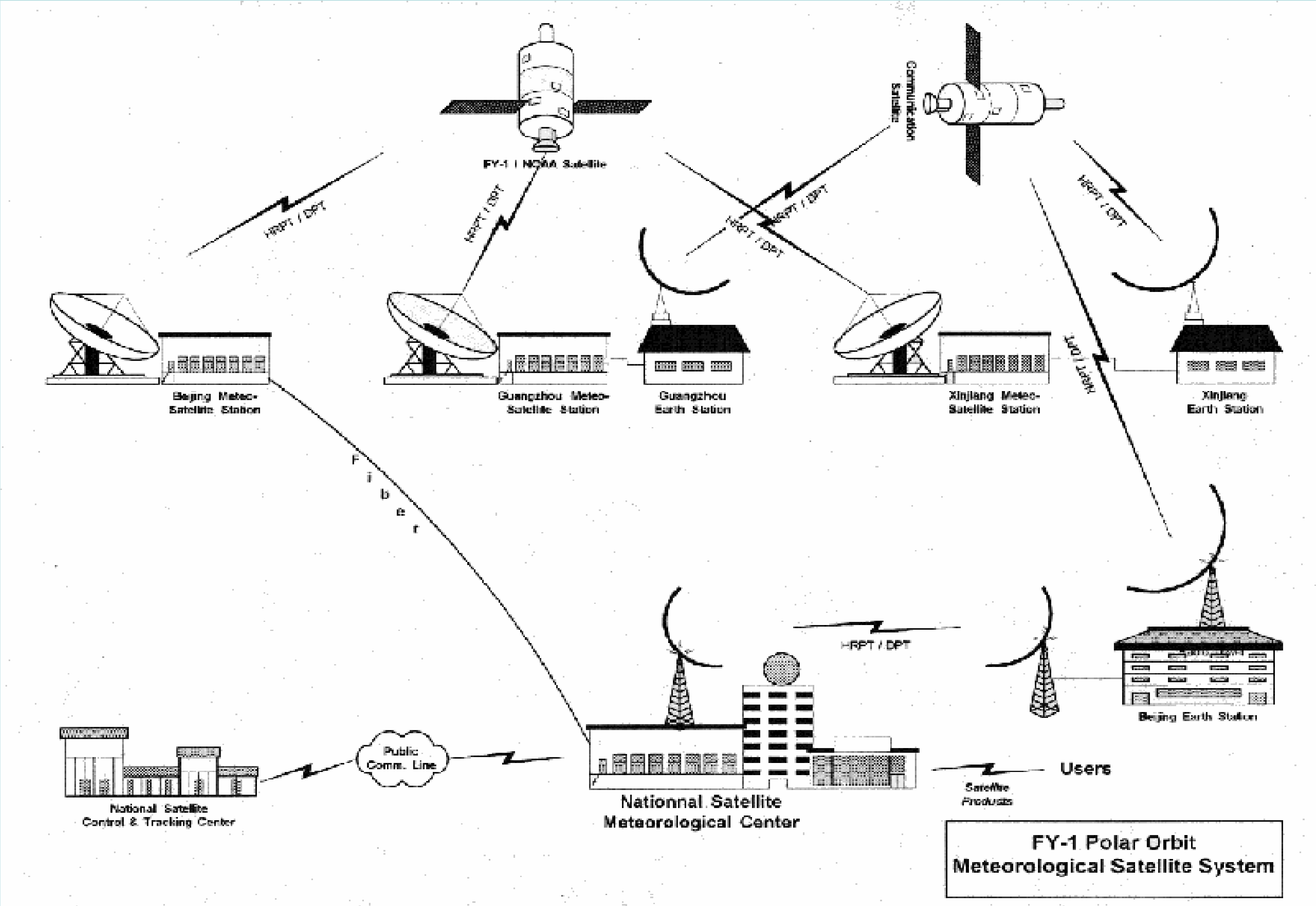

Fig.5.1 FY-1 satellite data receiving system

Daily Operational Service System of Meteorological Satellite Natural Disaster and Environment Monitoring

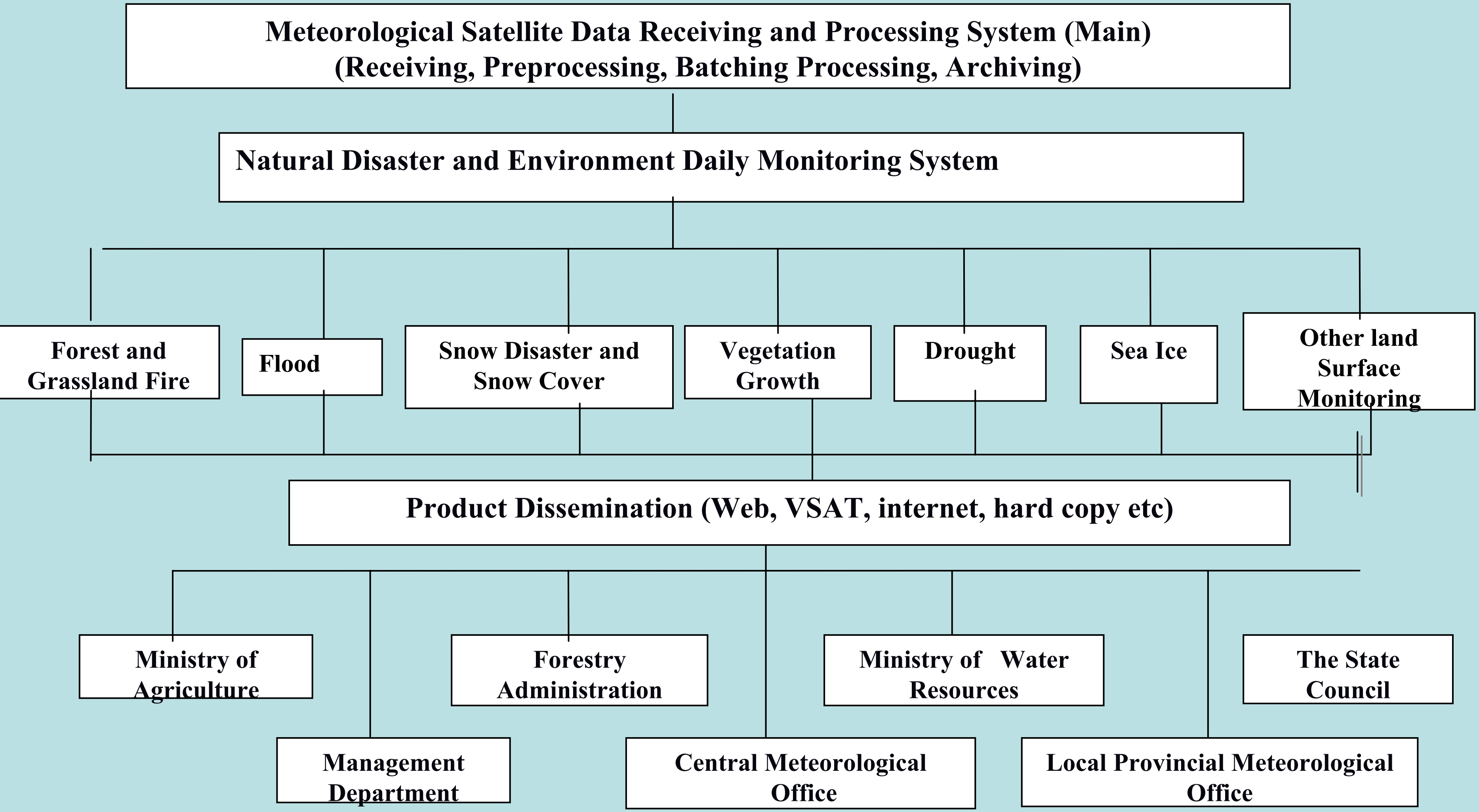

Fig. 3.2 The diagram of **Daily Operational Service System of Meteorological Satellite Natural Disaster and Environment Monitoring**

Daily Forest Fire Monitoring Sketch Map

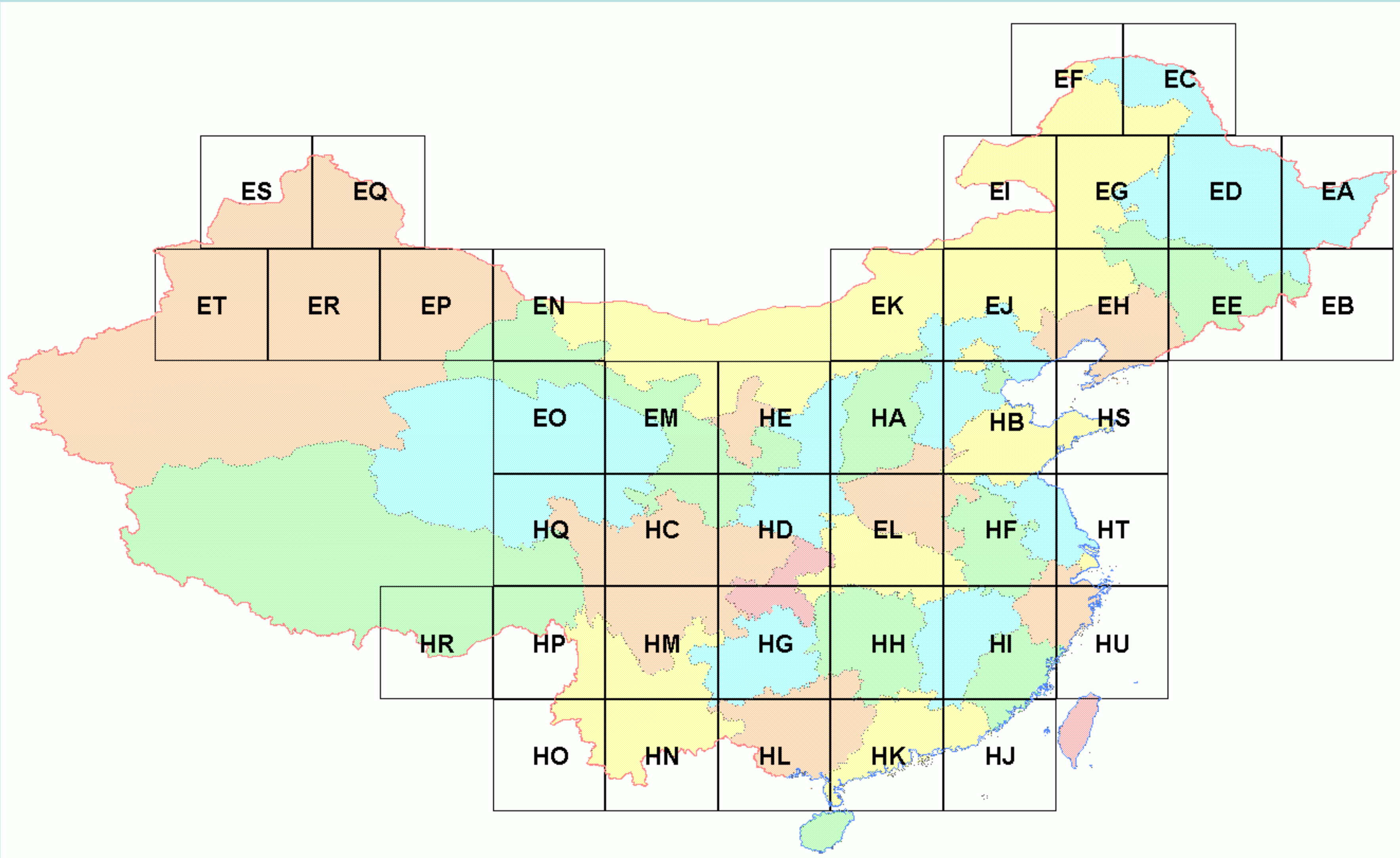

Fig. 3-3 Daily Forest Fire Monitoring Sketch Map for data processing in fire monitoring

Products： Fire Monitoring Image

Hot Spot Map

Hot Spot Detection Information List

Hot Spot Extent Map

Hot Spot Distribution Sketch Map

Hot Spot Frequency Statistics

Burned Size Evaluation

Users： Ministry of Agriculture,

National Forestry Administration,

National Remote Sensing Center

The State Council,

Local Provincial Meteorological Office

Fire Monitoring System by Meteorological Satellite

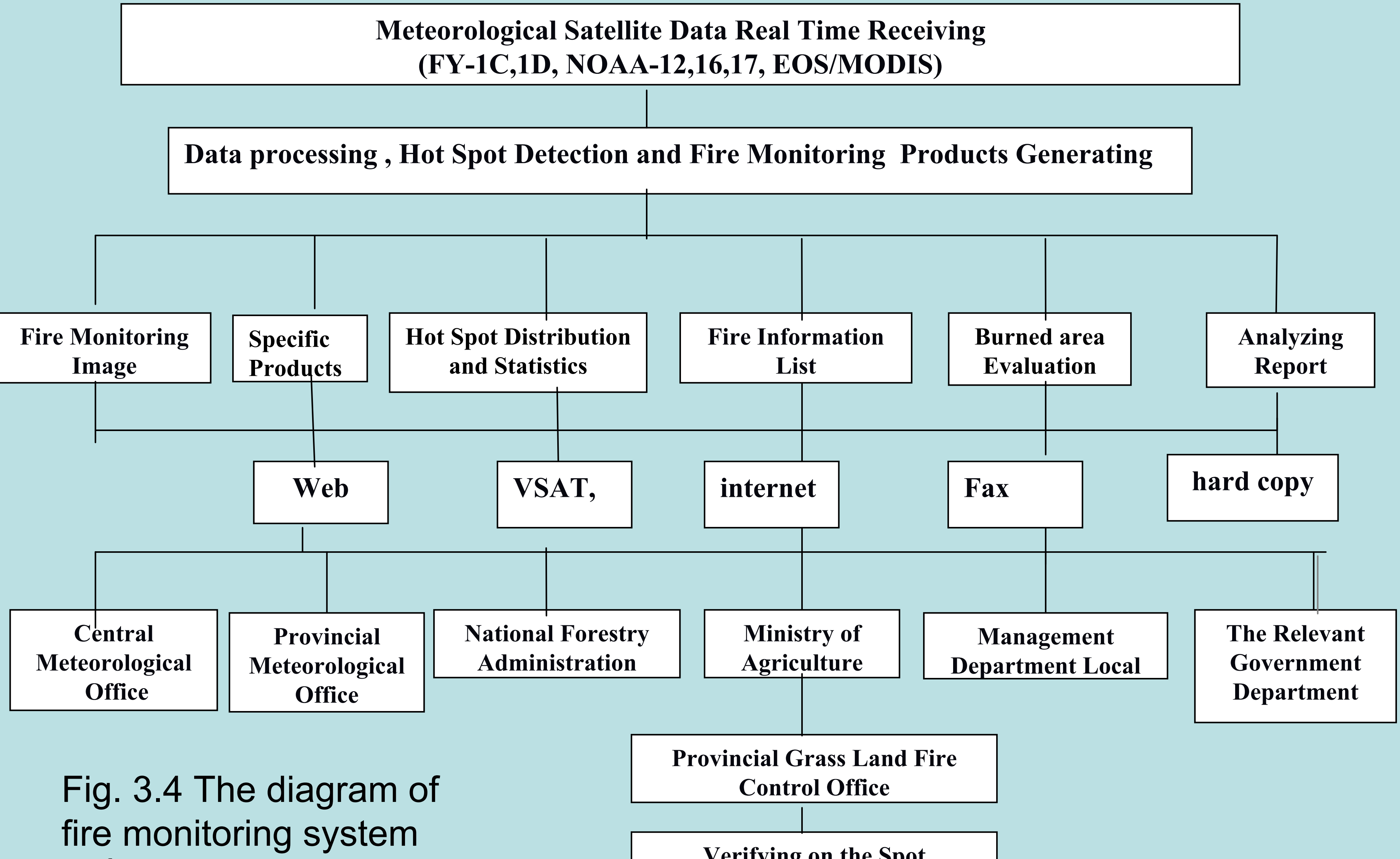

Fig. 3.4 The diagram of fire monitoring system

Fig.3.5 Website for Natural Disaster and Environment Monitoring Products Dissemination

Daily hot spot distribution map

2006-05-28 01:00:00 -2006-05-28 23:00:00 hot spot statistics in province

Fig. 3.6 Daily hot spot distribution map 2006/05/28/01:00-23:00

The regional fire monitoring image by FY-1D in Daxinganling Forest Region

2006/05/28/07:55(Beijing time)

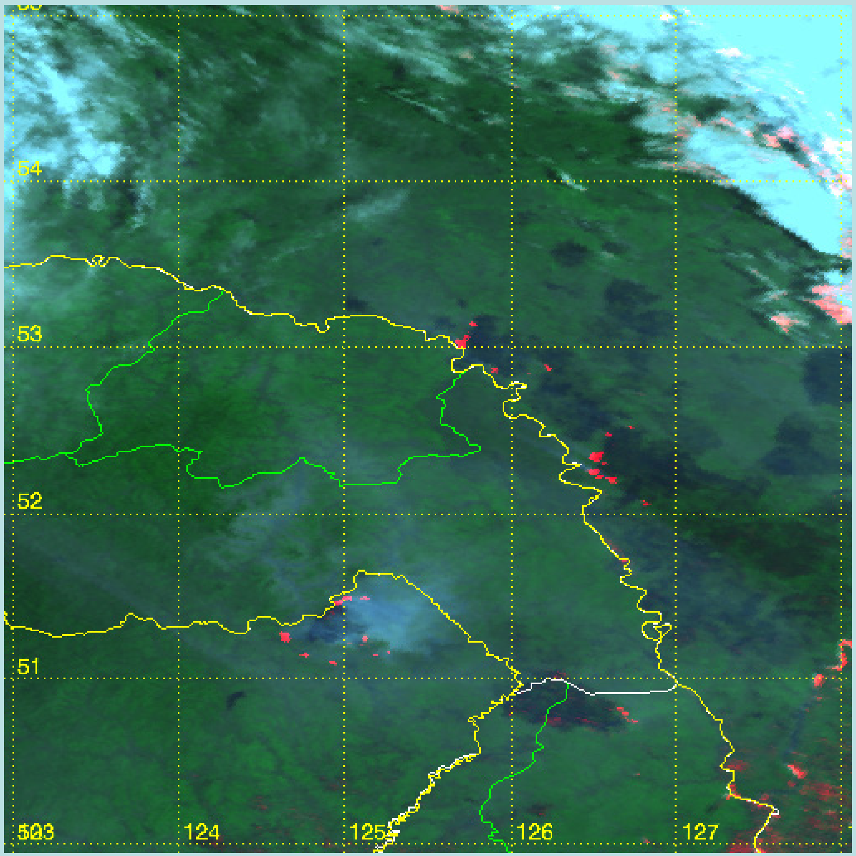

Fig. 3.7 Fire Monitoring Image

Fig.3.8 Hot Spot Map

Fire monitoring information list

Table 3.1 FY-1D fire monitoring list 2006/05/28/ 7:55:00/

省 (province)	地区 (district)	县 (county)	纬度 (latitude)	经度 (longitude)	火点像素数 (No. of pixels)	是否有烟 (smoke)	土地类型 (land type)
黑龙江省	黑河市	黑河市	50	126.82	4	False	
黑龙江省	黑河市	黑河市	50.74	126.75	4	False	
黑龙江省	黑河市	黑河市	50.78	126.68	4	False	
黑龙江省	黑河市	黑河市	50.81	126.65	3	False	
内蒙古自治区	呼伦贝尔盟	鄂伦春旗	51.08	124.93	6	True	
内蒙古自治区	呼伦贝尔盟	鄂伦春旗	51.13	124.75	5	True	
内蒙古自治区	呼伦贝尔盟	鄂伦春旗	51.13	125.18	3	False	
内蒙古自治区	呼伦贝尔盟	鄂伦春旗	51.15	125.26	1	False	
内蒙古自治区	呼伦贝尔盟	鄂伦春旗	51.22	125.12	2	False	
内蒙古自治区	呼伦贝尔盟	鄂伦春旗	51.24	124.63	24	True	
内蒙古自治区	呼伦贝尔盟	鄂伦春旗	51.46	124.98	18	True	
内蒙古自治区	呼伦贝尔盟	鄂伦春旗	51.47	125.12	3	False	

The regional fire monitoring image in Daxinganling Forest Region

2006/05/28/13:03(Beijing time)

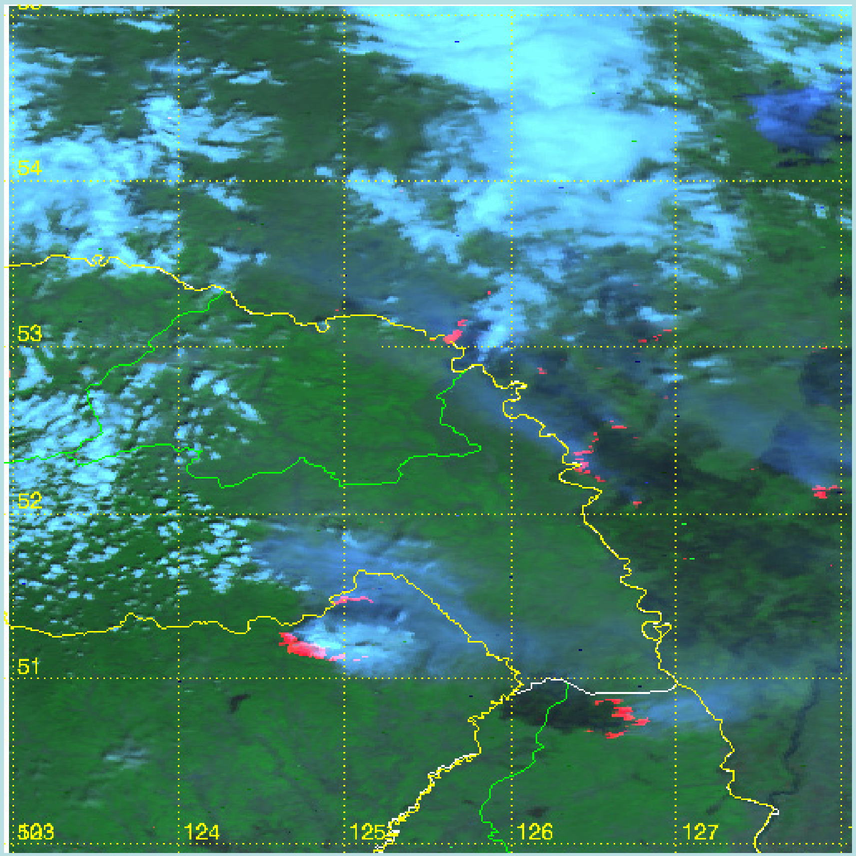

Fig. 3.9 Fire Monitoring Image

Fig. 3.10 Hot Spot Map

Fire monitoring information list

Table 3.2 NOAA-18 fire monitoring list 2006/05/28/ 13:93(Beijing time)

省 (province)	地区 (district)	县 (county)	纬度 (latitude)	经度 (longitude)	火点像素数 (pixel No.)	是否有烟 (smoke)	土地类型 (land type)
黑龙江省	黑河市	黑河市	50.65	126.63	18	True	
黑龙江省	黑河市	黑河市	50.68	126.46	2	False	
黑龙江省	黑河市	黑河市	50.74	126.79	27	True	
黑龙江省	黑河市	黑河市	50.78	126.68	68	True	
黑龙江省	黑河市	黑河市	50.85	126.53	7	False	
黑龙江省	黑河市	黑河市	50.86	126.61	16	True	
内蒙古自治区	呼伦贝尔盟	鄂伦春旗	51.11	125.07	4	False	
内蒙古自治区	呼伦贝尔盟	鄂伦春旗	51.13	124.94	25	True	
内蒙古自治区	呼伦贝尔盟	鄂伦春旗	51.13	125.11	4	False	
内蒙古自治区	呼伦贝尔盟	鄂伦春旗	51.19	124.74	184	True	
内蒙古自治区	呼伦贝尔盟	鄂伦春旗	51.47	125.03	47	True	

5.2 The features of different satellite in fire monitoring application

Polar-orbiting meteorological satellite fire monitoring:

1) **Sensitive to the hot spot. The minimum size of active fire detected can be smaller than 200 m^2.**

2) **More satellites can be used in operational fire monitoring. Currently there are at least five satellites can be used in fire monitoring.**

3) **Fast data processing. The fire monitoring product can be generated in 20 minutes after satellite data received.**

Table 3.3 Channel Characteristics and purpose of NOAA AVHRR

CH. No.	Wavelength (μm)	Resolution (km)	Dynamic range	Primary usage
1	0.58-0.68	1.1	0-100%	Daytime cloud, ice/snow
2	0.7-1.1	1.1	0-100%	Daytime cloud, ice/snow, vegetation
3A	1.58-1.64	1.1	0-100%	Ice/snow distinguishing
3B	3.55-3.95	1.1	190K-330K	Hot spot, nighttime cloud
4	10.3-11.3	1.1	190K-330K	Sst, day/night time cloud
5	11.5-12.5	1.1	190K-330K	Sst, day/night time cloud

Table 3.4 Channel Characteristics and purpose of MVISR of FY-1C/1D

CH. No.	wavelength	Resolution (km)	Primary usage
1	0.58-0.68	1.1	Daytime cloud, ice, snow
2	0.84-0.89	1.1	Daytime cloud, ice/now, vegetation
3	**3.55-3.95**	**1.1**	**Heat source, nighttime cloud**
4	10.3-11.3	1.1	SST, day/night time cloud
5	11.5-12.5	1.1	SST, day/night time cloud
6	1.58-1.64	1.1	Ice/snow distinguishing
7	0.43-0.48	1.1	Ocean color
8	0.48-0.53	1.1	Ocean color
9	0.53-0.58	1.1	Ocean color
10	0.9-0.985	1.1	Water vapor

EOS/MODIS fire monitoring

EOS/MODIS data:

It has more advantages in fire monitoring in accurate positioning, sub-pixel size and burned size evaluating.

Table 3,5 The channels relevant to fire monitoring in EOS/MODIS:

Ch. No.	Wavelength（μm）	Resolution	Usage
CH.1	0.62～0.67	250m	Burned area，smoke
CH.2	0.84～0.87	250m	Burned area，smoke
CH.6	1.62～1.65	500m	Hot spot detection
CH.7	2.10～2.13	500m	Hot spot detection
CH.20	**3.66～3.84**	**1000m**	**Hot spot detection**
CH.21	**3.92～3.98**	**1000m**	**Hot spot detection**
CH.22	3.92～3.98	1000m	Hot spot detection
CH.23	4.02～4.08	1000m	Hot spot detection
CH.24	4.43～4.49	1000m	Hot spot detection
CH.25	4.48～4.54	1000m	Hot spot detection
CH.31	10.7～11.2	1000m	Burned area
CH.32	11.7～12.2	1000m	Burned area

EOS/MODIS

CH.20 is most sensitive to high temperature target in those 6 mid. infrared channels including CH.20 to CH.25.

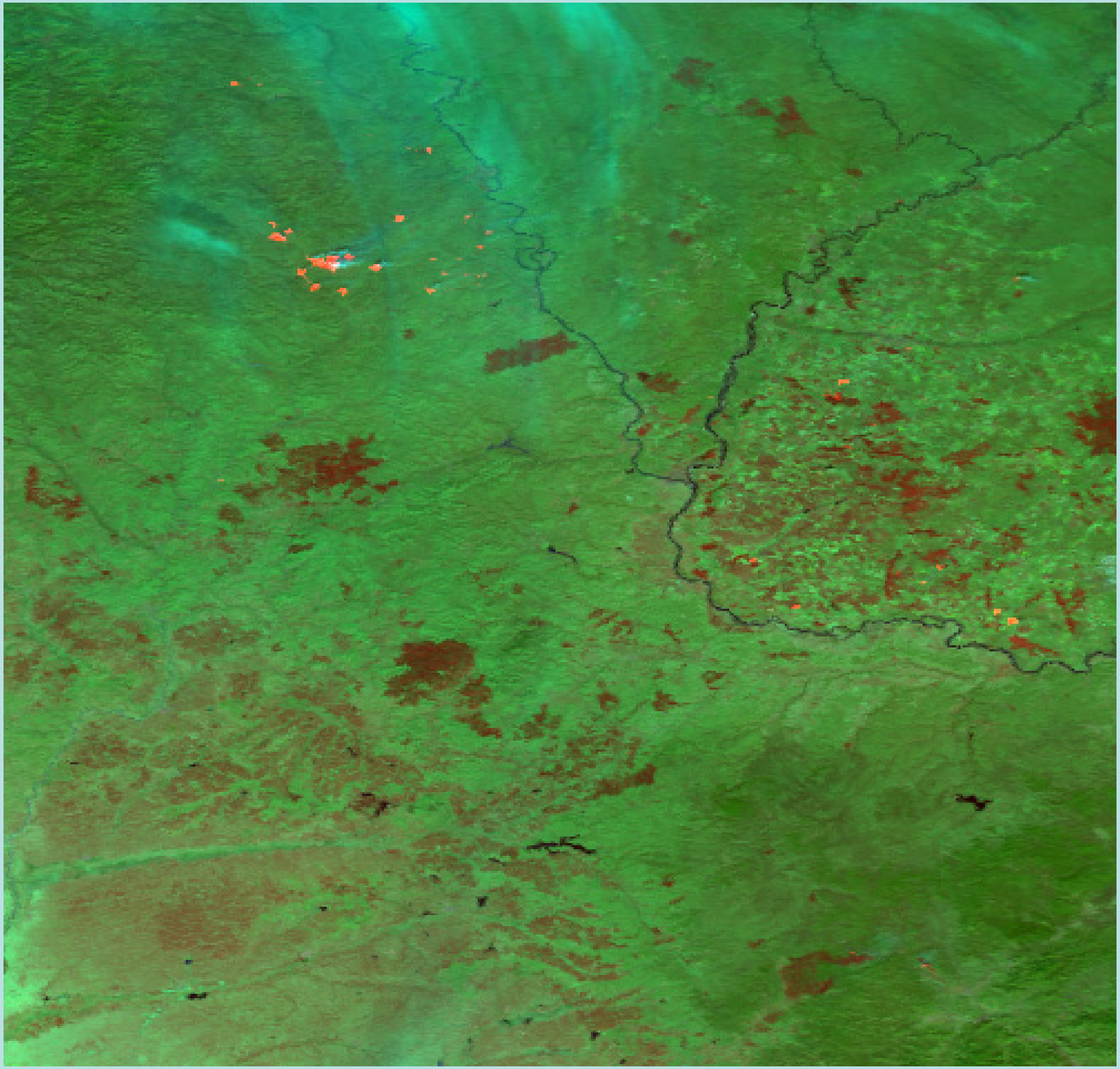

Fig. 3.11 EOS/MODIS CH20 , 2 , 1 RGB 2001/10/14

Using CH.21 to evaluate sub-pixel size and temperature

The dynamic range of brightness temperature of CH.21 is very wide, the upper brightness temperature can be up to 500K above, which gives more advantages in sub-pixel size and temperature evaluation.

In the image, the brightness temperature of CH21 in mixed pixel A,B,C are 401K, 414K, 348K respectively, using Newton's iteration method to solve the P (the percentage of hot spot sub-pixel size within a mixed pixel) and T_f (temperature of the fire) are as following:

A：P = 1.18%， T =725K

B：P = 1.2%， T = 781K

C：P = 0.13%， T = 830K

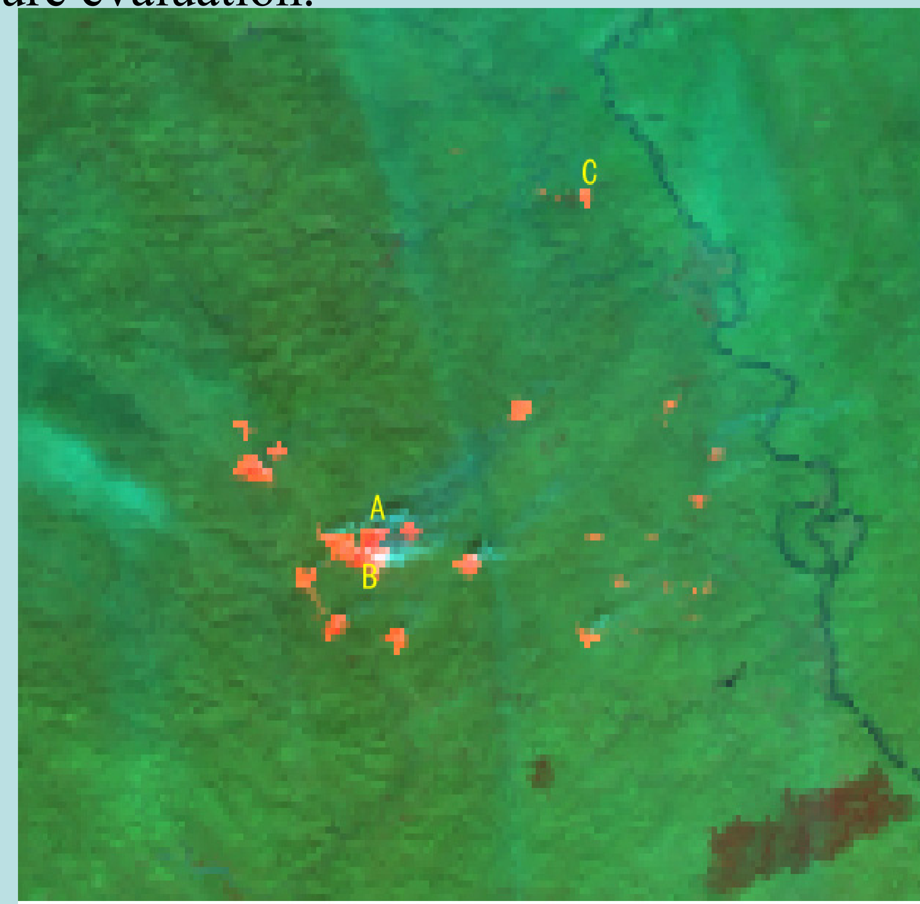

Fig. 3.12EOS/MODIS CH20，2，1 RGB 2001/10/14/10：48（lc）

CH6 and CH7 can be used to detect the hot spot with quite high temperature, and the accuracy of location are improved as the resolution of CH6 and CH7 is 500 m.

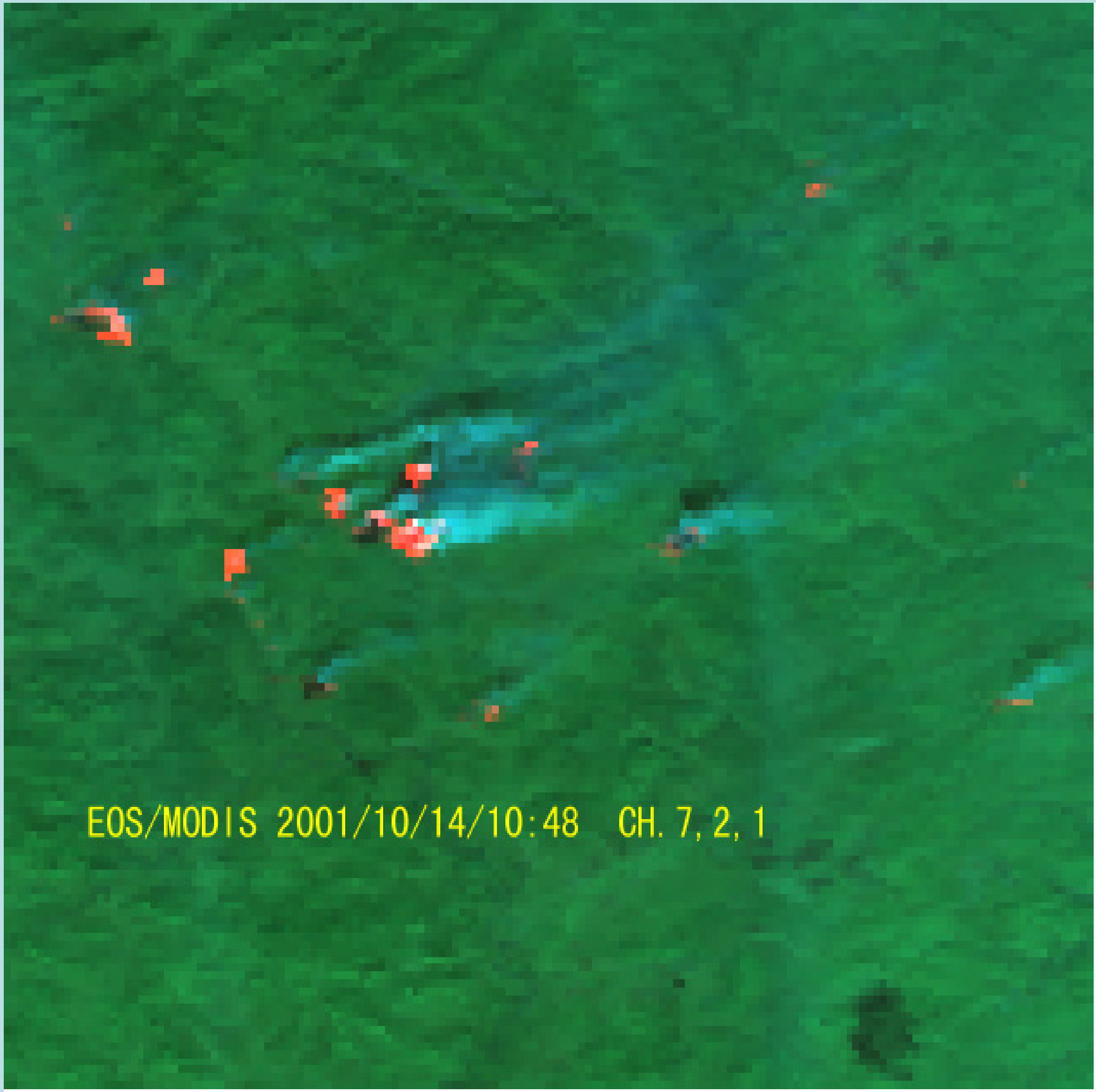

Fig. 3.13 EOS/MODIS CH.7, 2, 1 RGB 2001/10/14/10:48(LC)

The accuracy of burned size evaluation is improved by using EOS/MODIS data.

Fig. 3.14 Using EOS/MODIS 250m data to evaluate the burned size of forest fire is better than polar orbiting meteorological satellite 1 km resolution data.

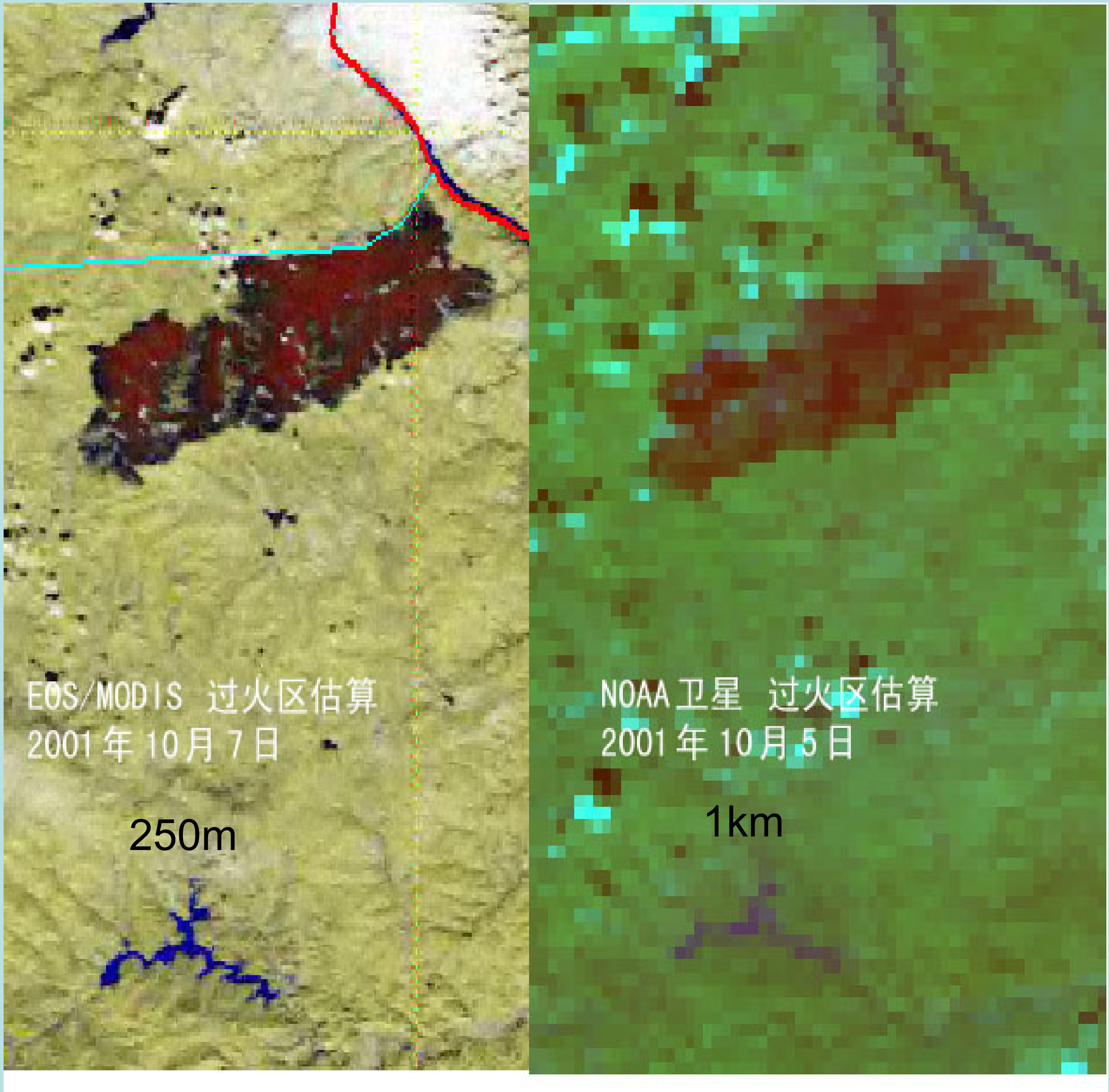

Geostationary Meteorological Satellite Fire Monitoring

(FY-2C, MTSAT, GOES-9 can be used to detect hot spot.)

1) Frequently observation. Once per hour even once per 30 minutes.
2) Widely observation and lower resolution.
3) The stable position in multiple observation.

Table 3.6 Characteristics of **FY-2C** radiometer

Characteristics of **FY-2C** radiometers					
Channel No.	1 (VIS)	2 (IR 1)	3 (IR 2)	4 (IR 3)	5 (WV)
wavelength (um)	0.50-0.75	10.3-11.3	11.5-12.5	3.5-4.0	6.3-7.6
Resolution	1.25 km	5 km	5 km	5 km	5 km

Table 3.7 Characteristics of **MTSAT** radiometers

Characteristics of **MTSAT** radiometers					
Channel No.	1 (VIS)	2 (IR 1)	3 (IR 2)	4 (WV)	**5 (IR 3)**
wavelength (um)	0.55-0.80	10.3-11.3	11.5-12.5	6.3-7.6	**3.5-4.0**
Resolution	1 km	4 km	4 km	4km	**4 km**

Table 3.8 Characteristics of (GOES I-M) radiometers

Characteristics of (GOES I-M)					
Channel No.	1 (Visible)	**2 (Shortwave)**	3 (Moisture)	4 (IR 1)	5 (IR 2)
wavelength (um)	0.55 - 0.75	**3.80 - 4.00**	6.50 - 7.00	10.20 - 11.20	11.50 - 12.50
Resolution	1 km	**4 km**	8 km	4 km	4 km

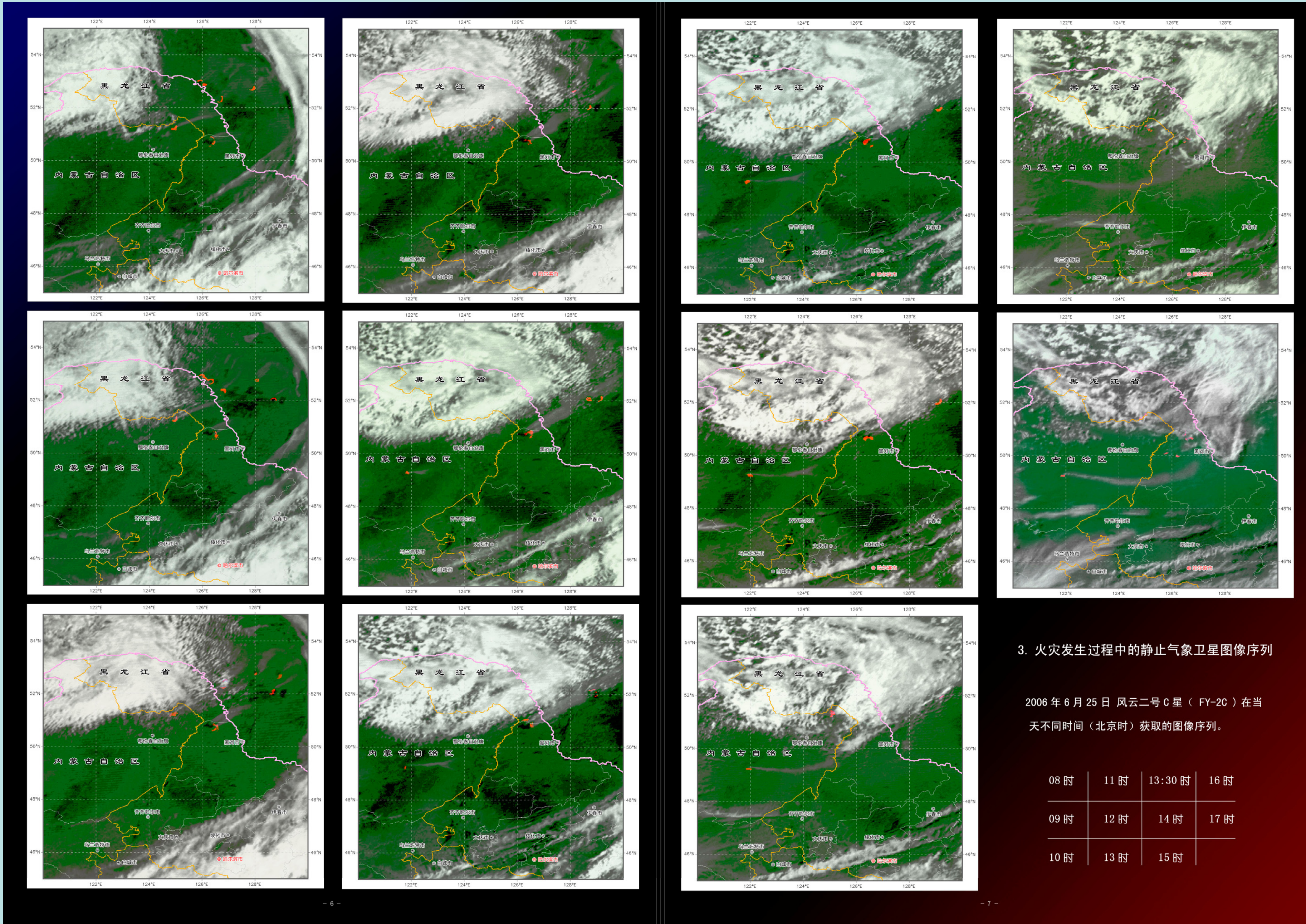

Fig. 3.15 FY-2C fire monitoring image in consecutive hours from 00z to 09z in June 25, 2006

The hot spot intensity product

Using the result of sub-pixel size and temperature evaluation from GOES-9 data to generate a hot spot intensity product.

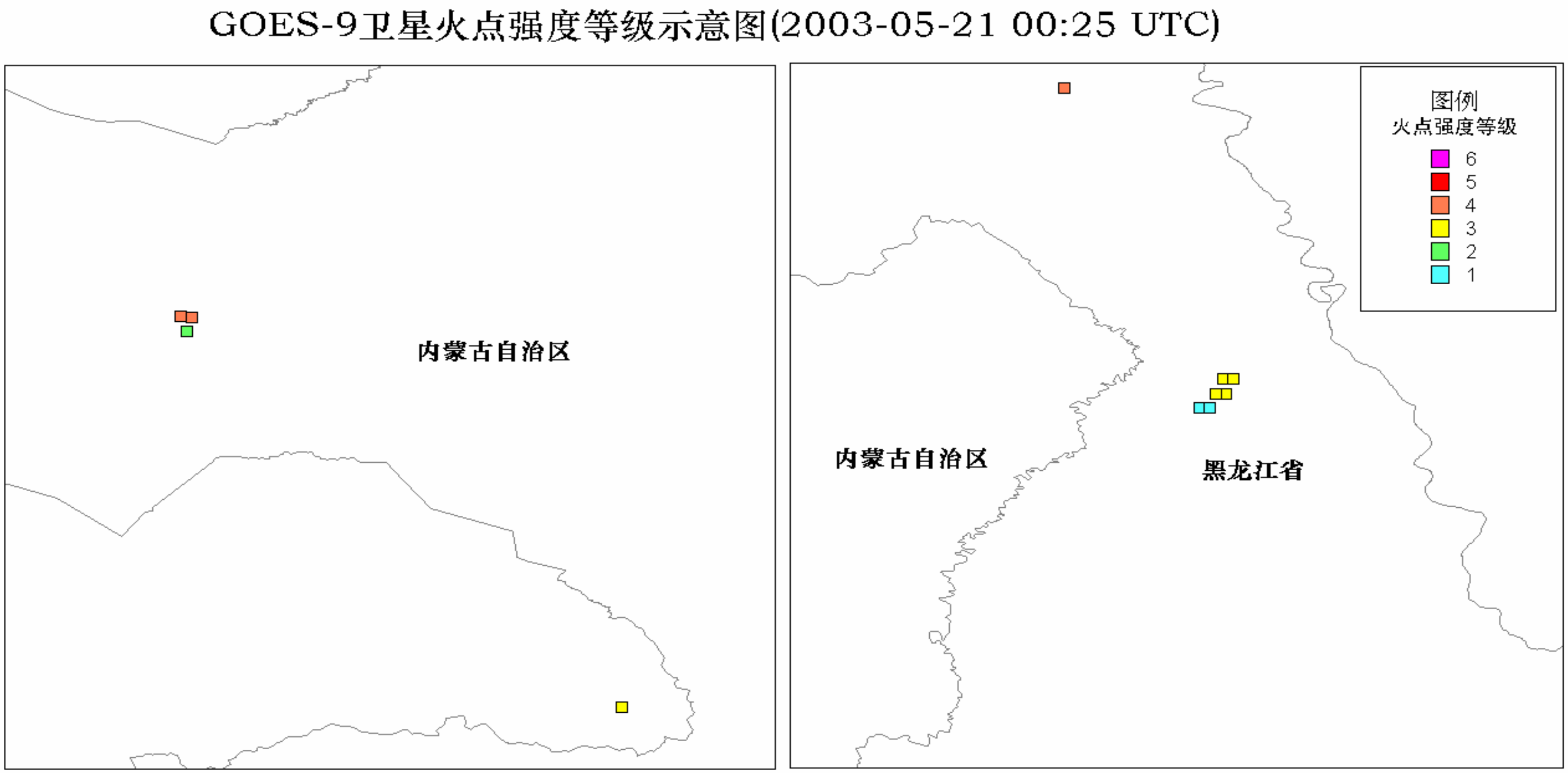

Fig. 3.16 The hot spot intensity using GOES-9 data.

Yellow: 1 or 2
Red: 3 or 4
Blue: more than 5 observations.

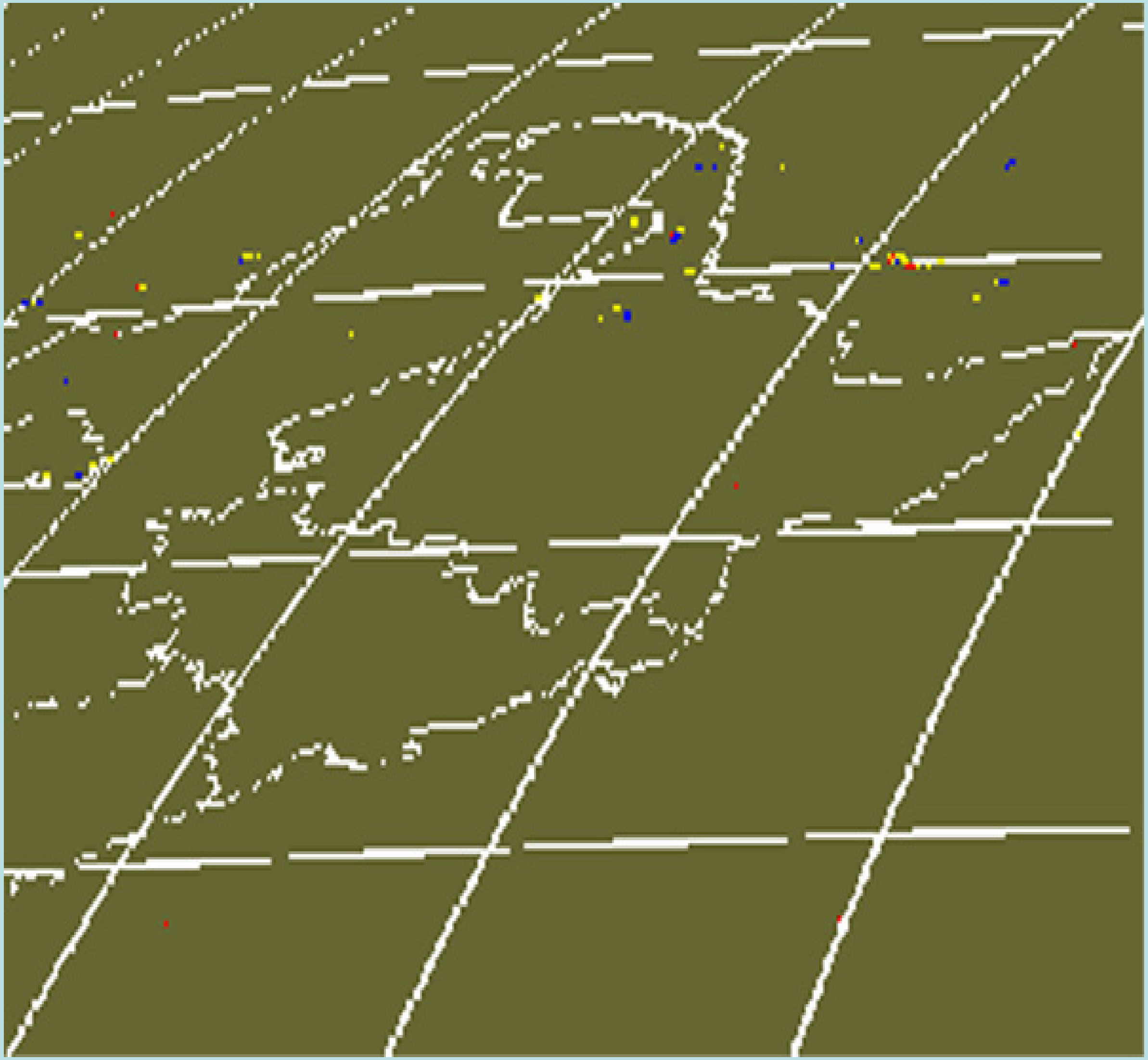

Fig. 3.17 The frequency of hot spots detected from multiple observation of GOES-9

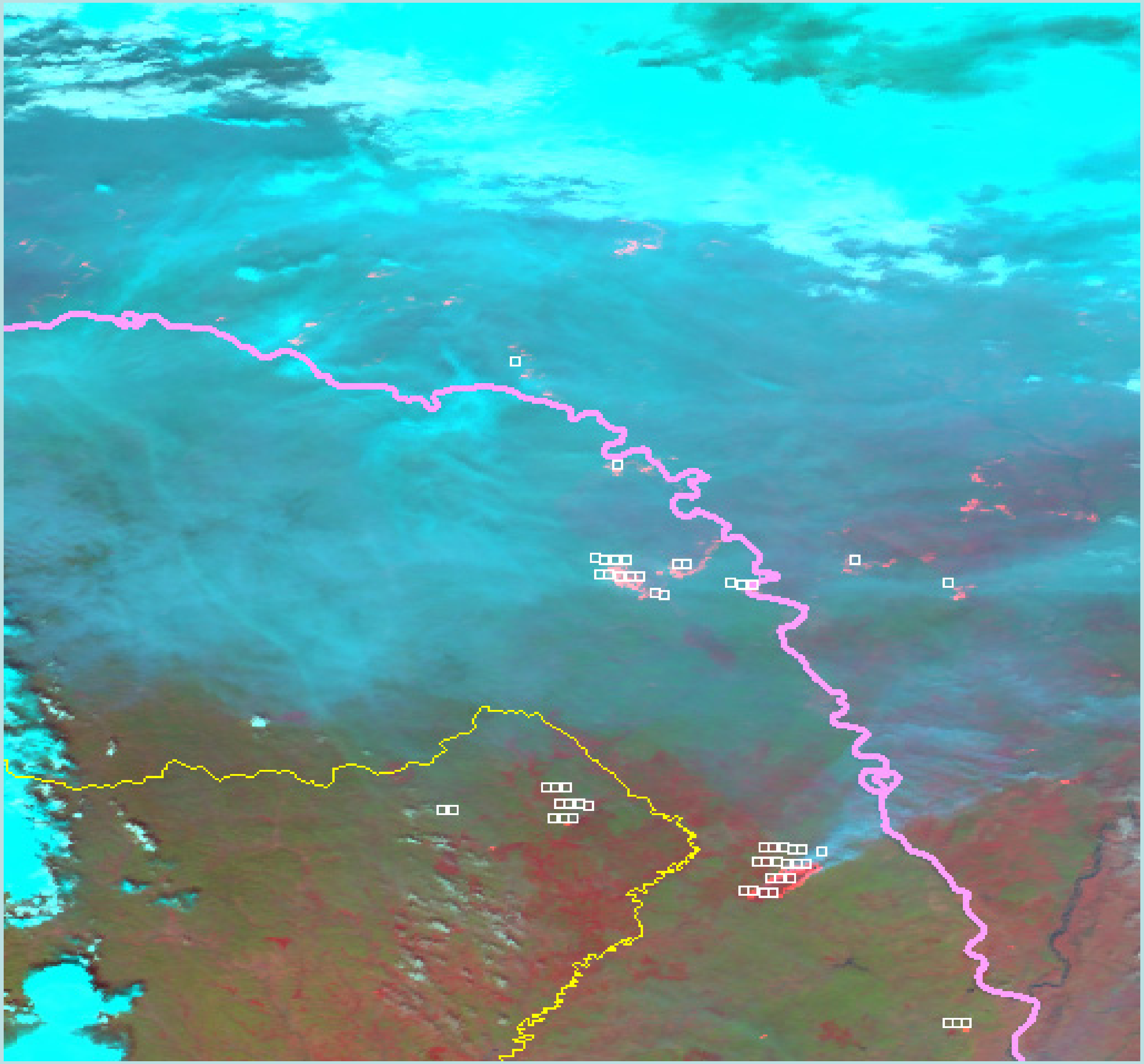

Fig. 3.18The hot spots detected from multiple observation of GOES-9 overlay on polar orbiting satellite image

4.The Aspects of Application of Fire Monitoring

1) Active fire monitoring in real time
2) Evaluation for burned size
3) Prediction for active fire field development
4) Fire dangerous level prewarning
5) Regional fire situation evaluation
6) Weather condition on forest and grass land fire dangerous level forecasting

1) Active fire monitoring in real time

- ● The situation of huge fire with large fire field can be quickly found out .
- ●The grassland fire in the remote area can be monitored. ● The fire whose size is much smaller than a pixel can be detected.
- ● Many fire spots distributed in large area can be quickly found out

• The situation of huge fire with large fire field can be quickly found out .

In the morning of May 6,1987

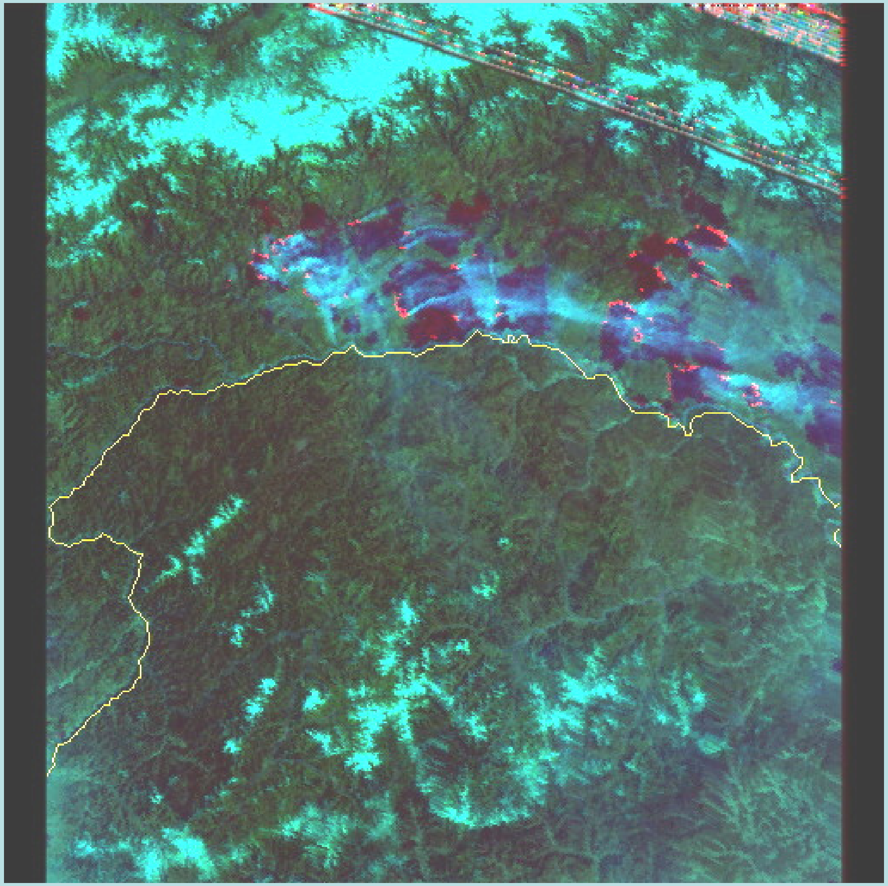

Fig. 4.1 NOAA –8 AVHRR CH.3,2,1

In the afternoon of May 6, 1987

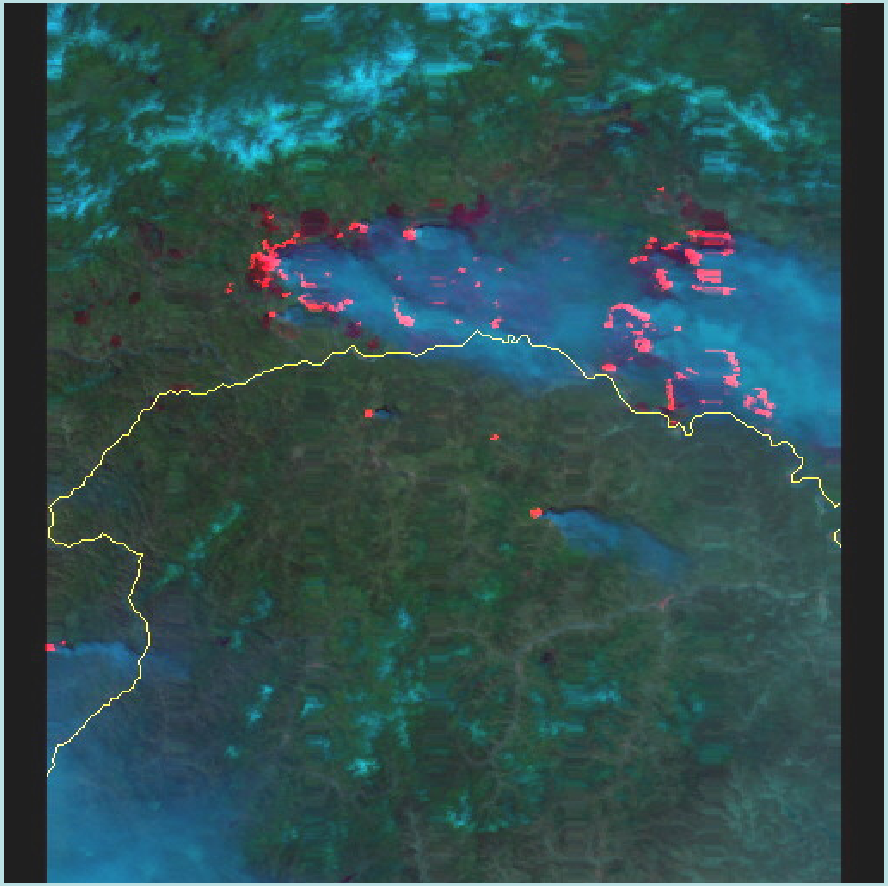

Fig. 4.2 NOAA –9 AVHRR CH.3,2,1

In the morning of May 8, 1987

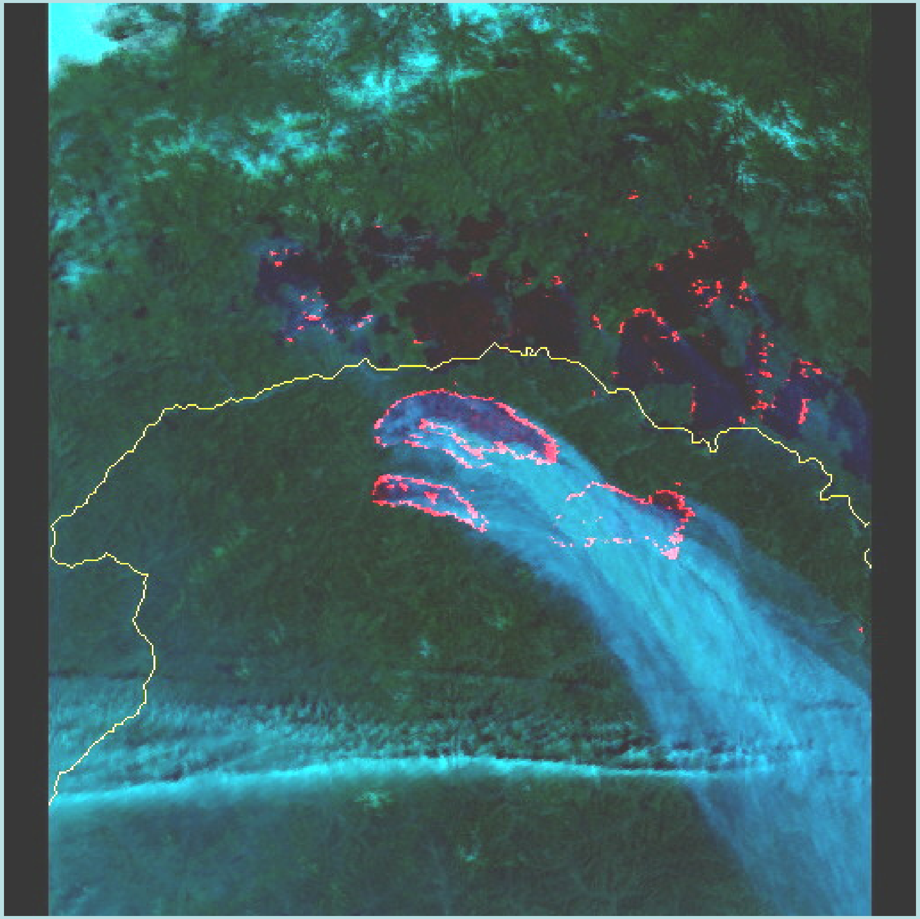

Fig. 4.3NOAA –8 AVHRR CH.3,2,1

In the afternoon of May 20, 1987

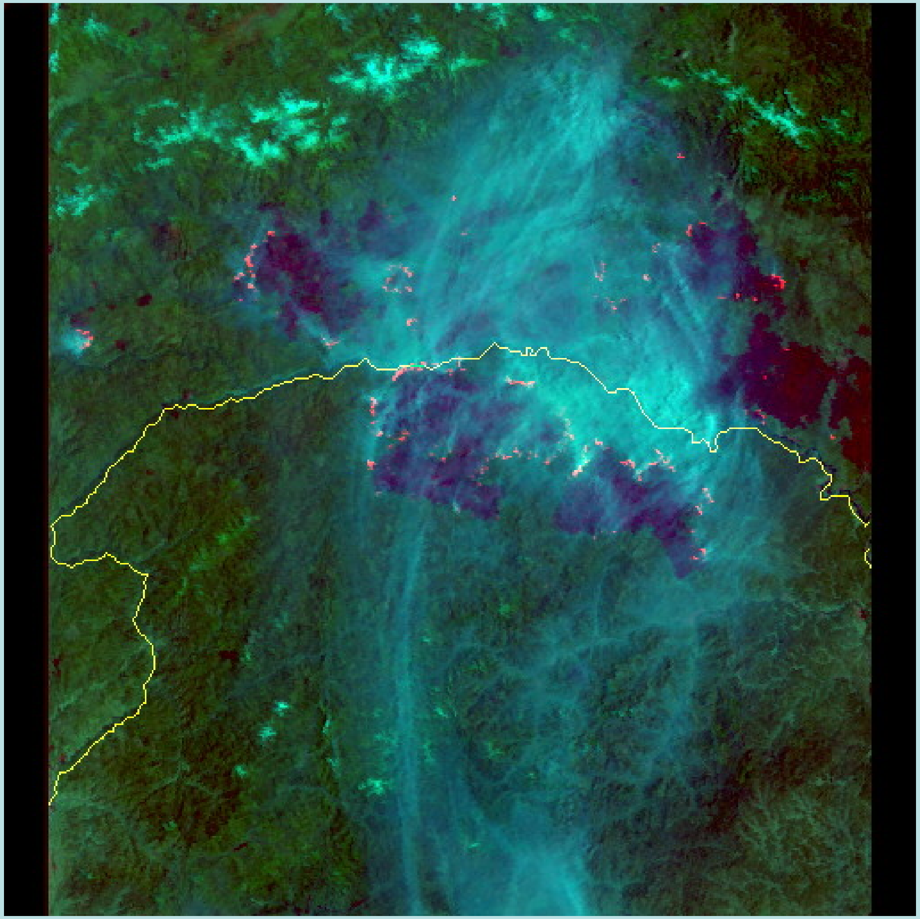

Fig. 4.4 NOAA –9 AVHRR CH.3,2,1

Daxinganling Region Forest Fire Monitoring in the spring of 2006

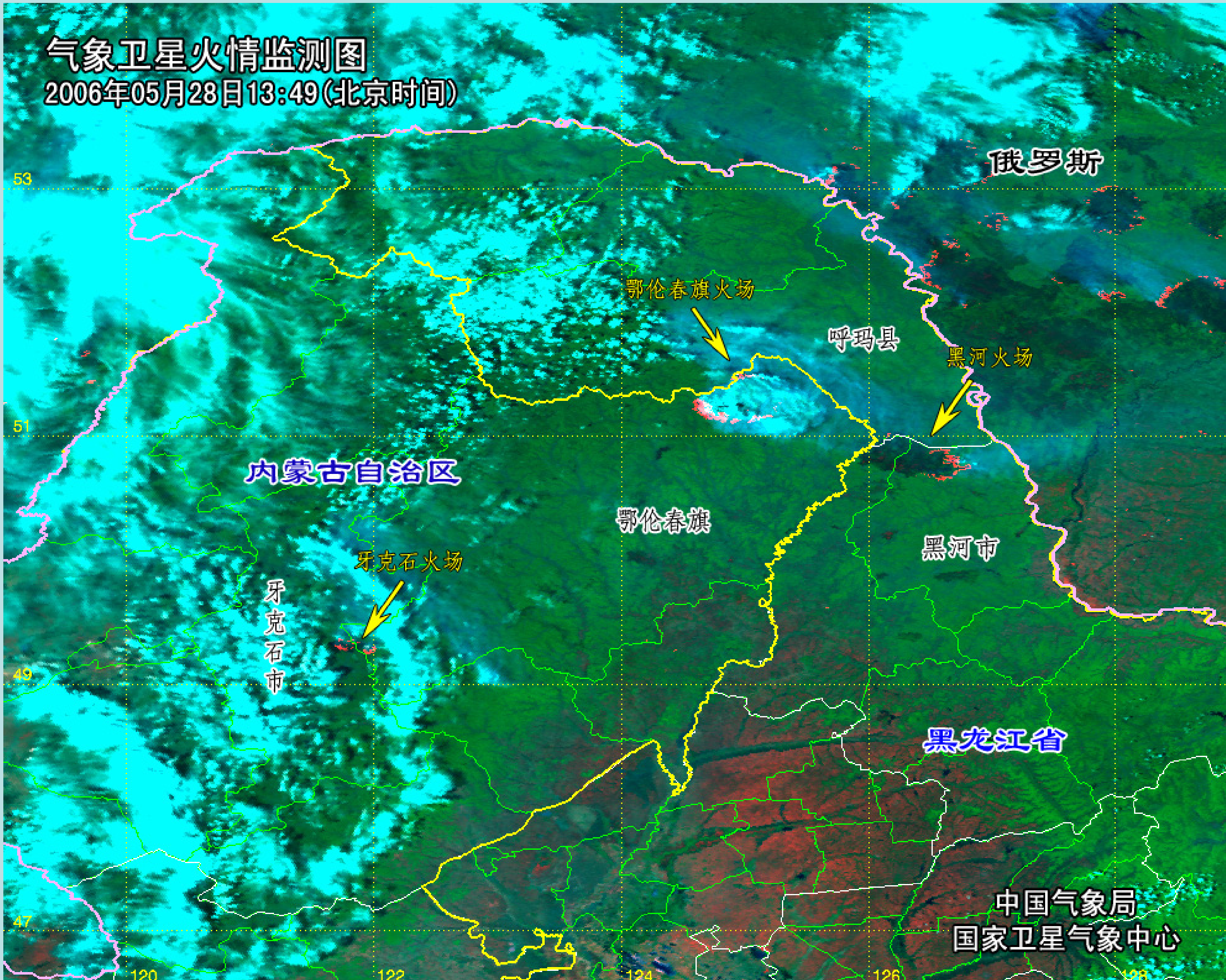

Fig.4.5 NOAA-16 AVHRR CH3,2,1 RGB (2006/05/28/13:49(LO)

Daxinganling Region Forest Fire Monitoring in the spring of 2006

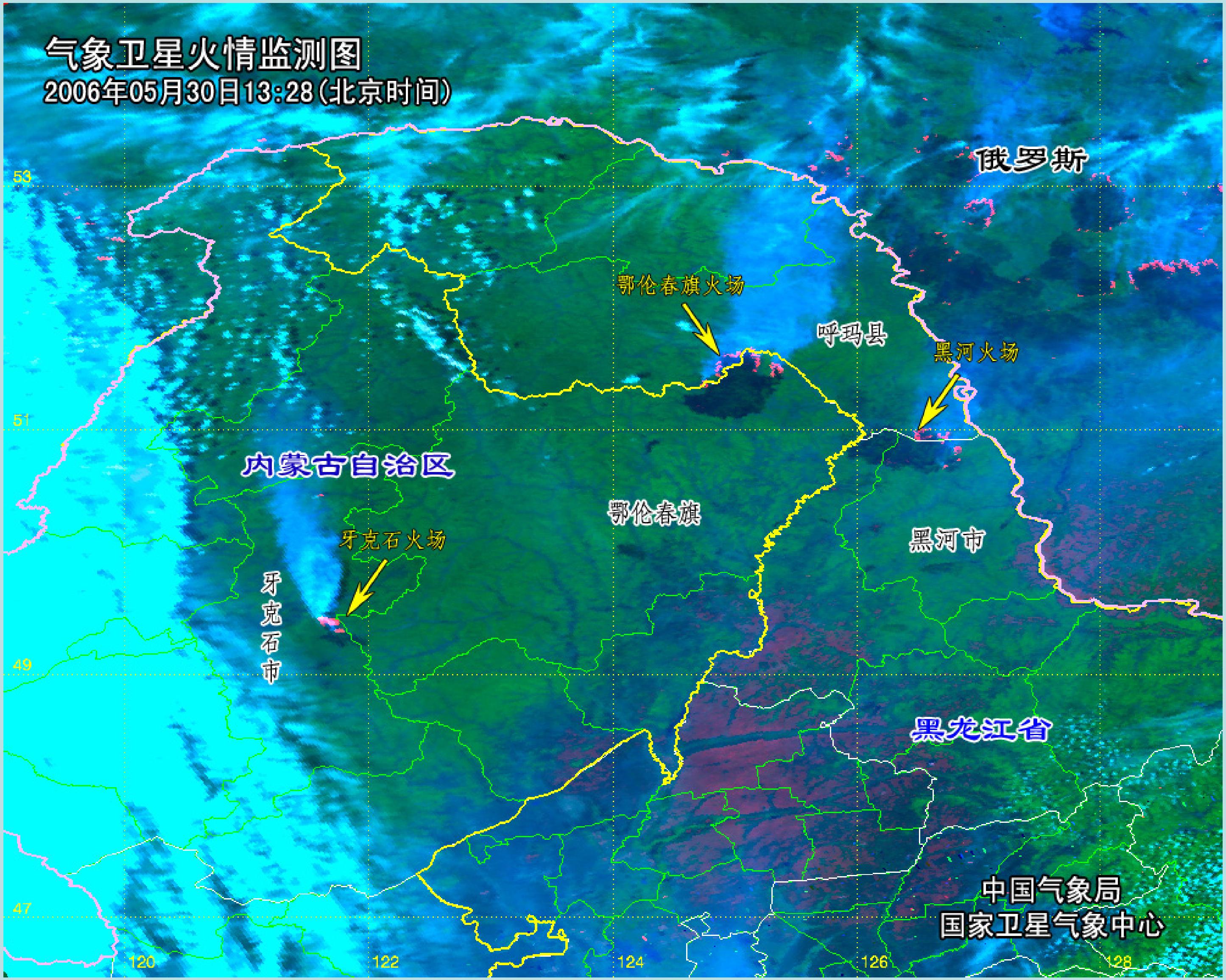

Fig. 4.6 NOAA-16 AVHRR CH3,2,1 RGB (2006/05/30/ 13:28(LC)

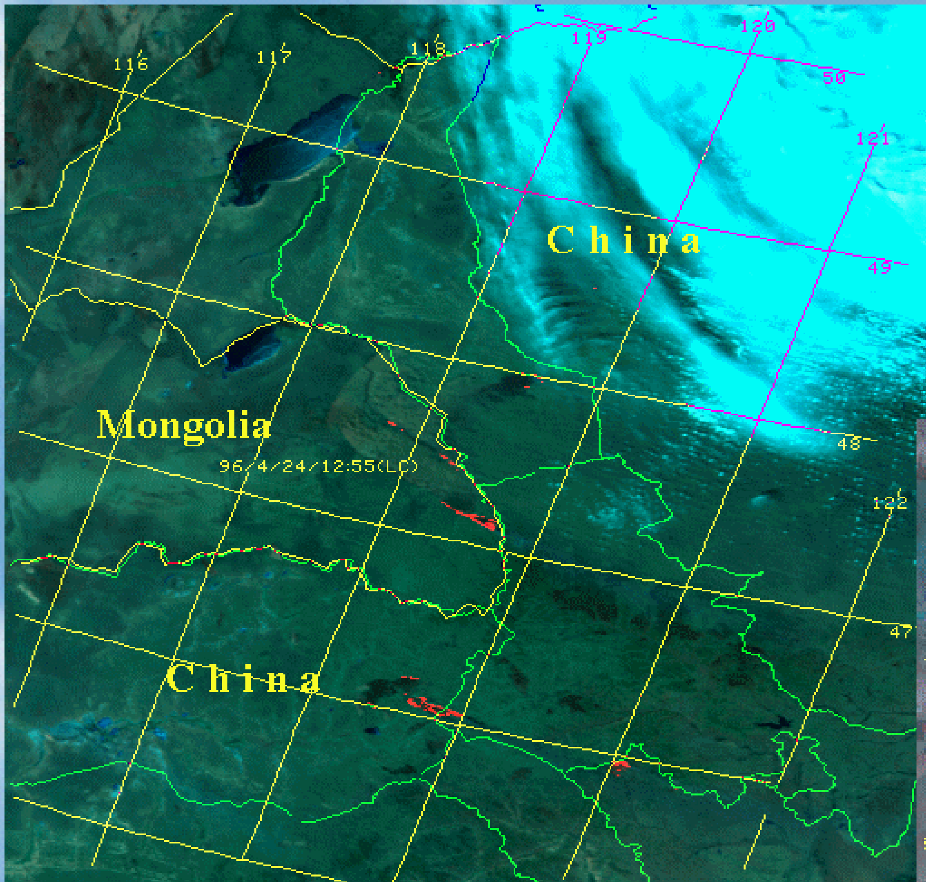

Fig. 4.7 NOAA-14 AVHRR CH.3,2,1
April 24, 1996

The grassland fire in the remote area can be monitored.

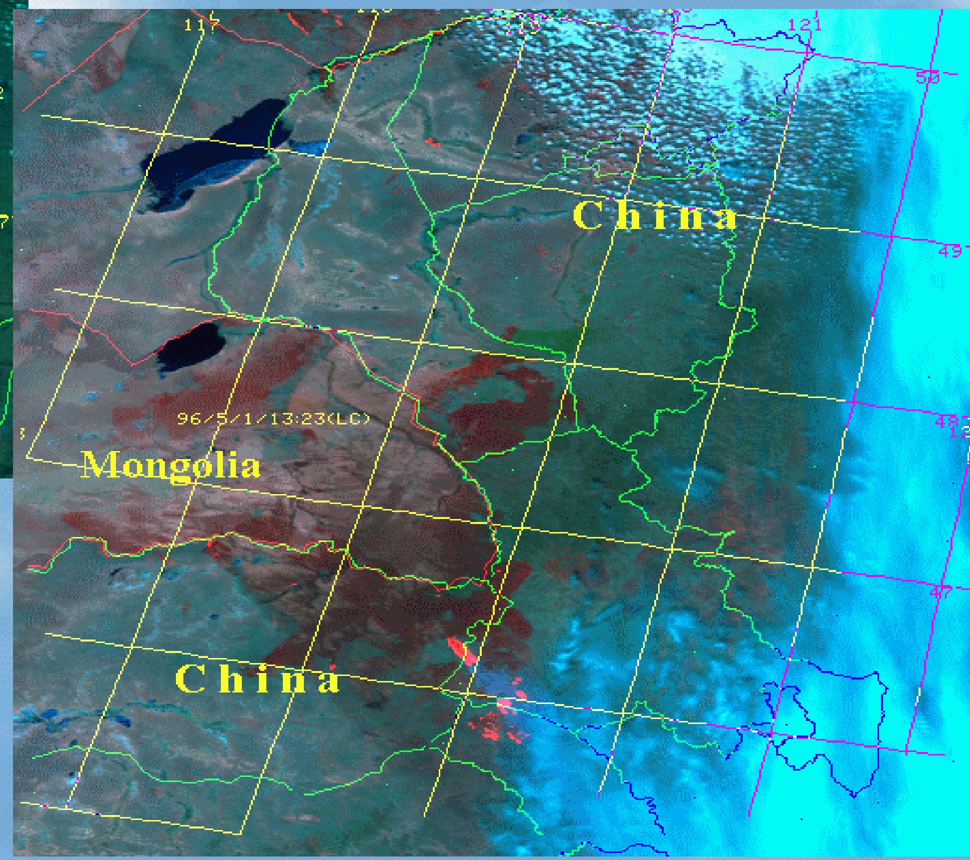

Fig. 4.8 NOAA-14 AVHRR CH.3,2,1
May 1, 1996

- The fire in very small size (much smaller than a pixel) can be detected.

The minimum size of forest fire detected is 0.002 km^2, thus improving the ability of forest fire detection to remote area and natural forest.

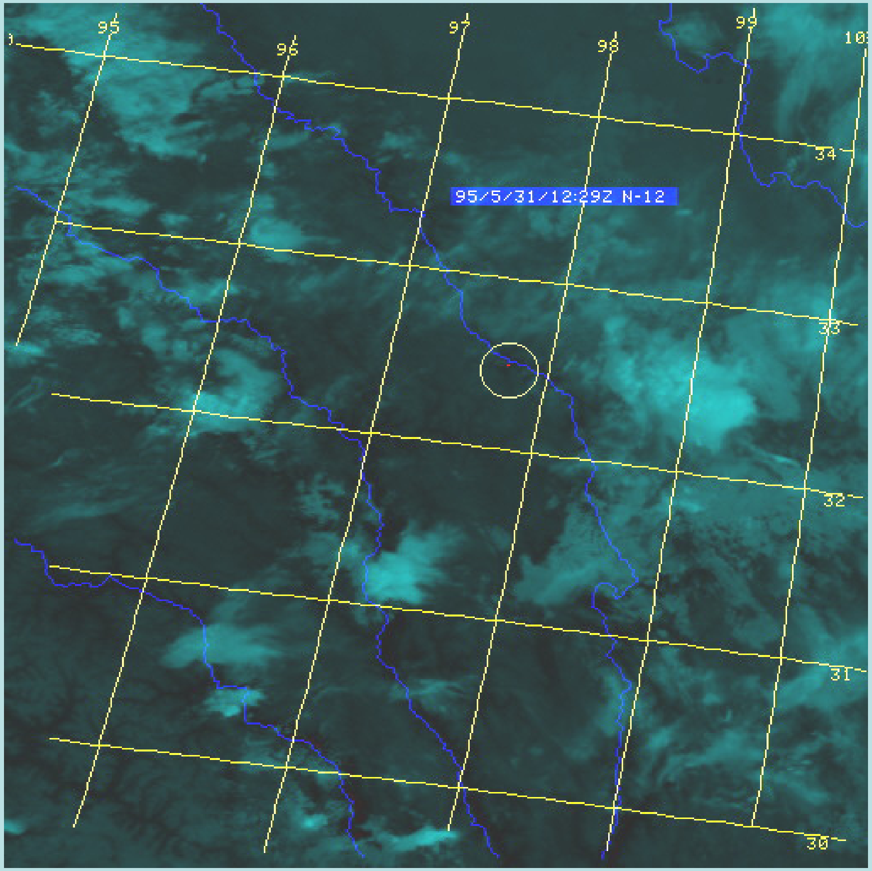

Fig. 4.9 NOAA-11 AVHRR CH3,2,1 RGB (1995/05/31/12:28(LC)

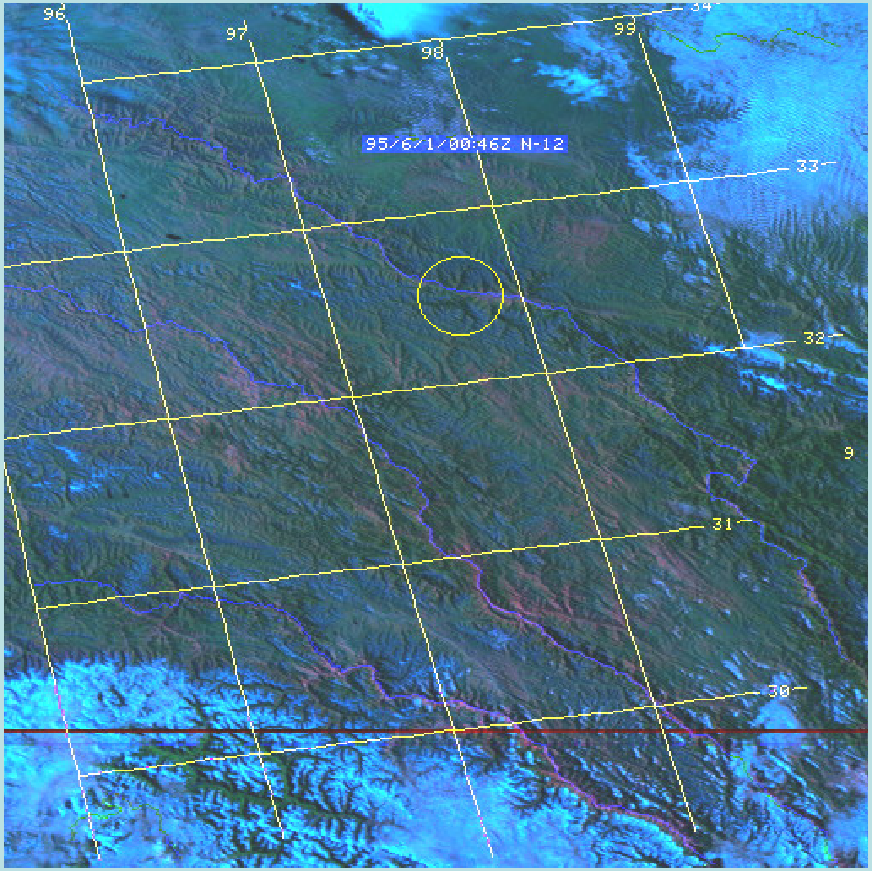

Fig.4.10 NOAA-12 AVHRR CH3,2,1 RGB (1995/06/-1/08:46(LC)

- Large number of fire spots distributed in widly area can be quickly found out

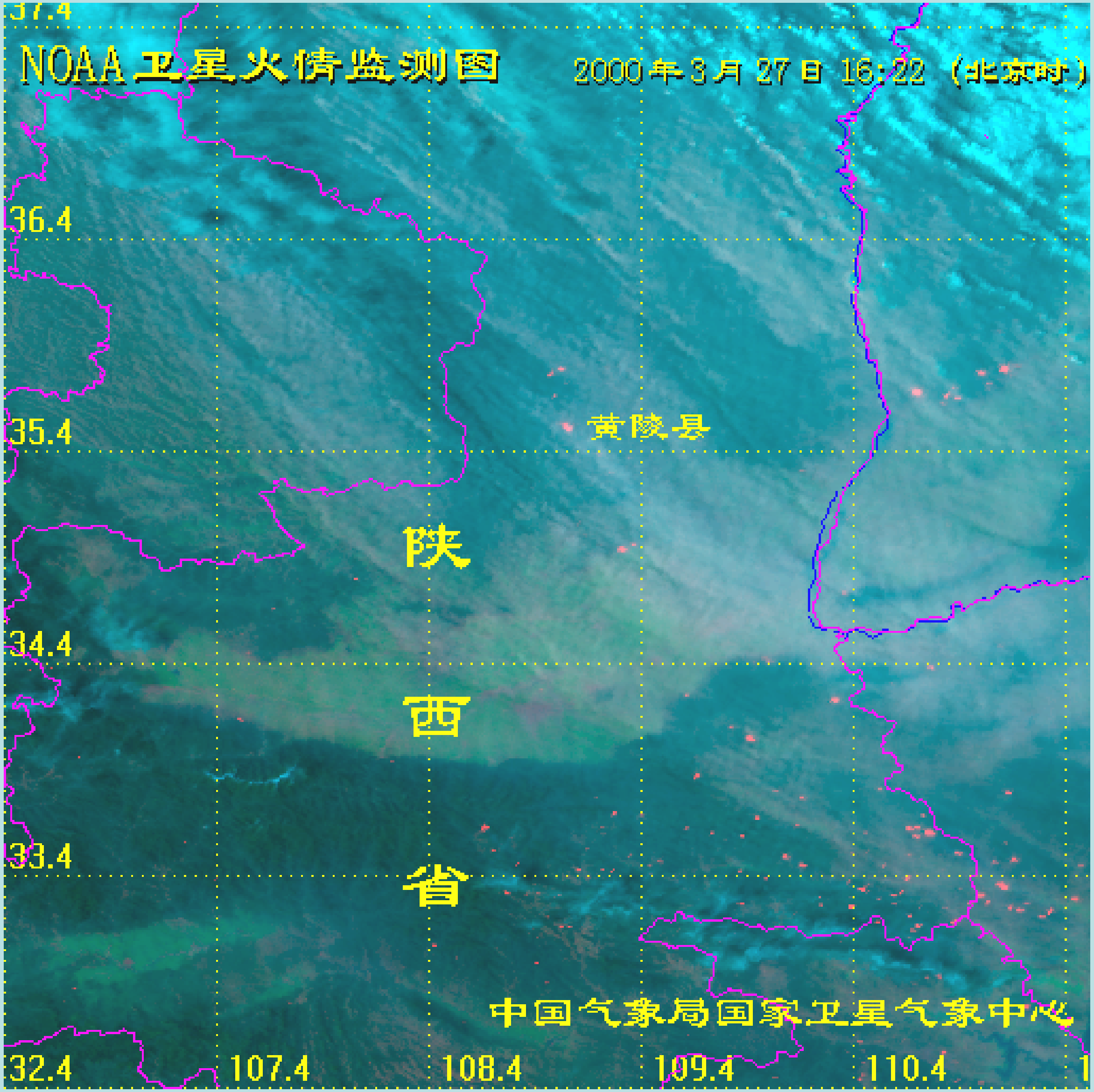

Fig. 4.11 NOAA-14 AVHRR CH.3,2,1 2000/03/27/ 16:22

FY-1C Forest Fire Monitoring (2000/06/22/08:11(lc))

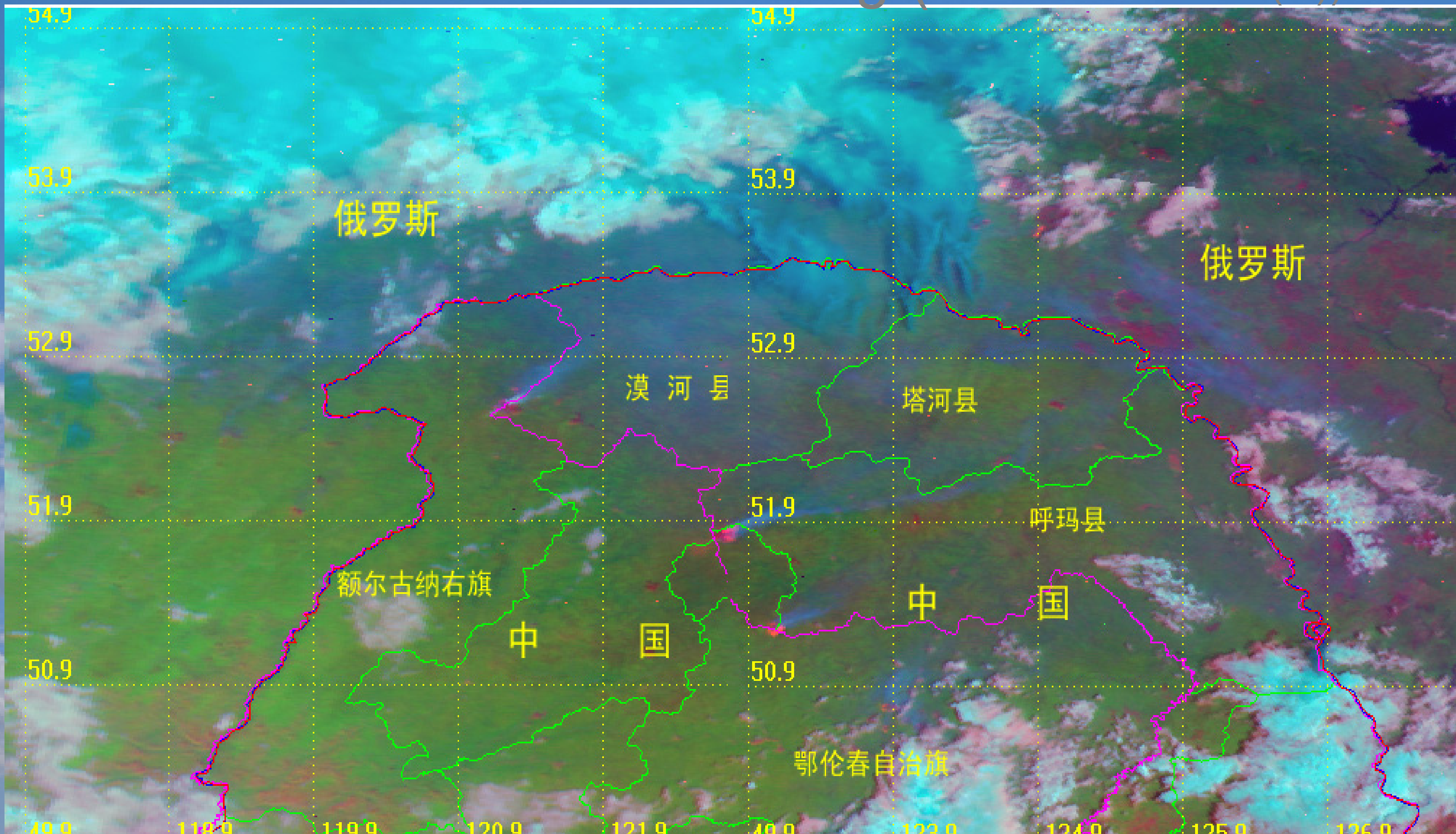

2000年6月22日 8:11(北京时)

Fig. 4.12 FY-1C AVHRR CH.3,2,1 2000/06/22/ 08:11(LC)

2) Evaluation for burned size

The NDVI of burned area will be much lower than before.

The size of stricken area caused by fire can be evaluated quickly.

Using NOAA-8 data we evaluated the stricken area caused by huge forest fire happened in Daxinganling Region in May 1987 is about 10800 km^2.

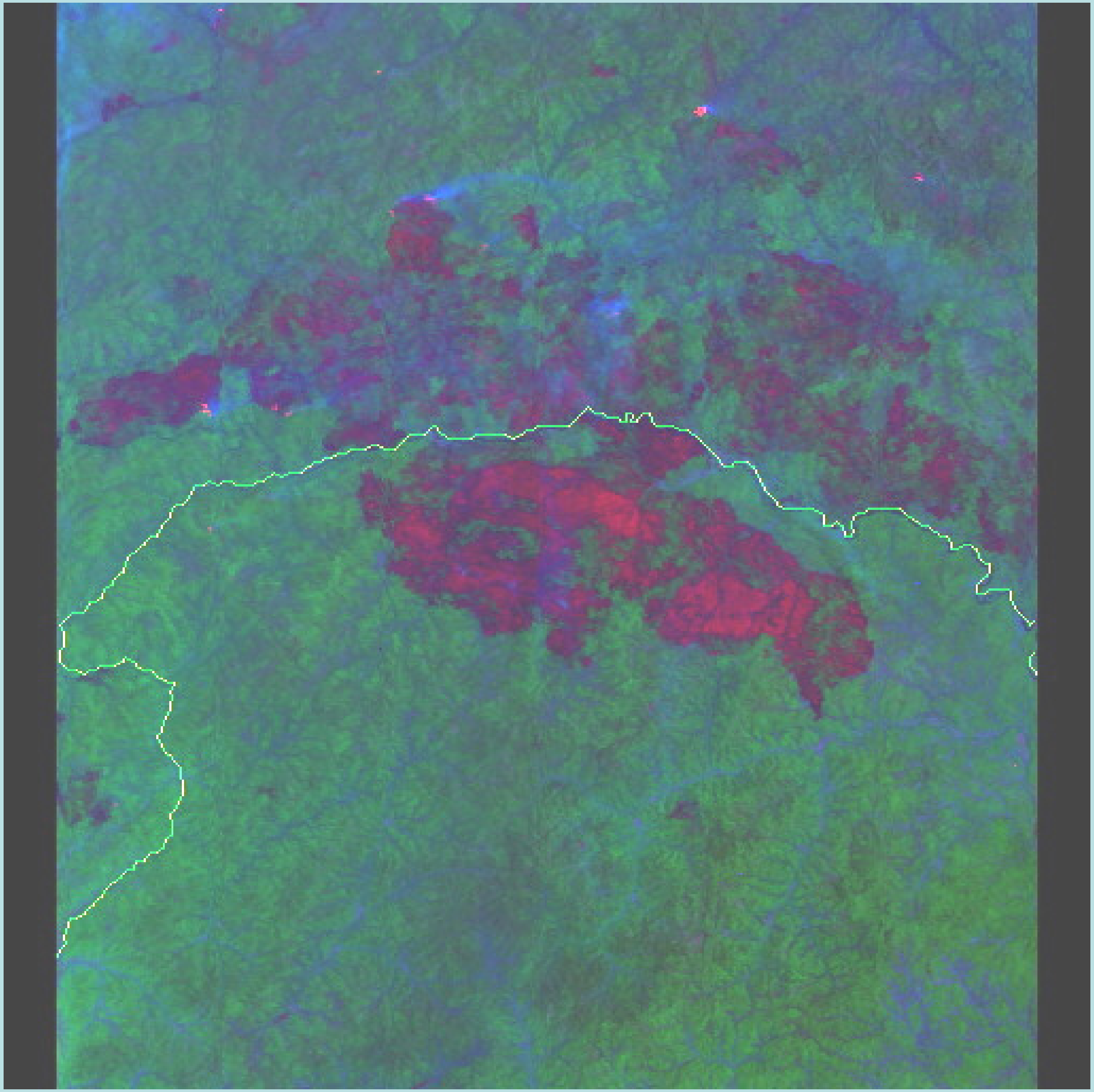

Fig. 4.13 NOAA-8 AVHRR CH.3,2,1 1987/06/03/ 08:40(LC)

Grass Land Fire Monitoring

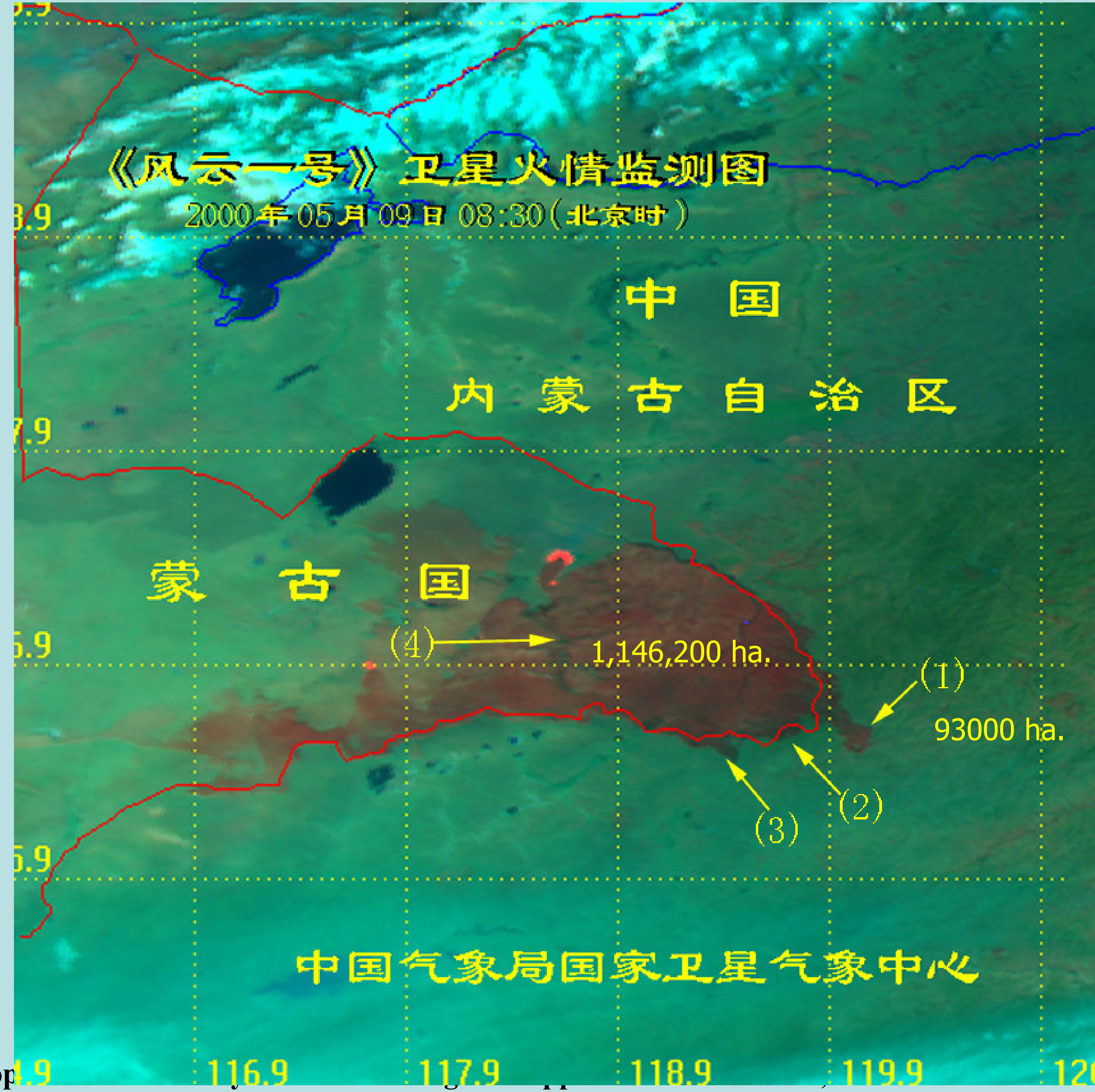

Fig. 4.14 FY-1C AVHRR CH.3,2,1

2000/05/09/08:30(LC)

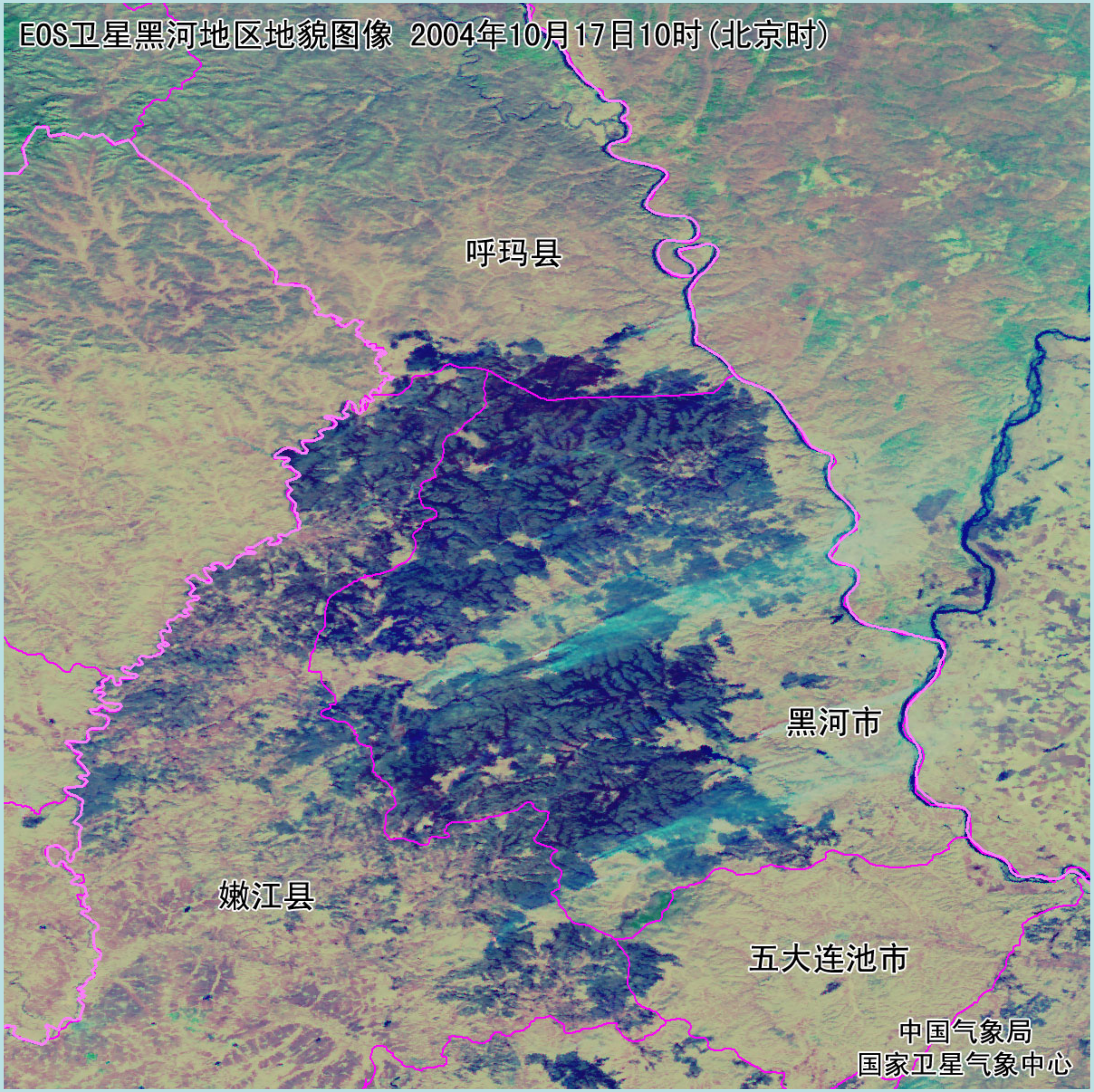

Fig. 4.15 EOS/MODIS data used in burned size evaluation 2004/10/17/10:00(LC)

Evaluating the burned size using CBERS-2

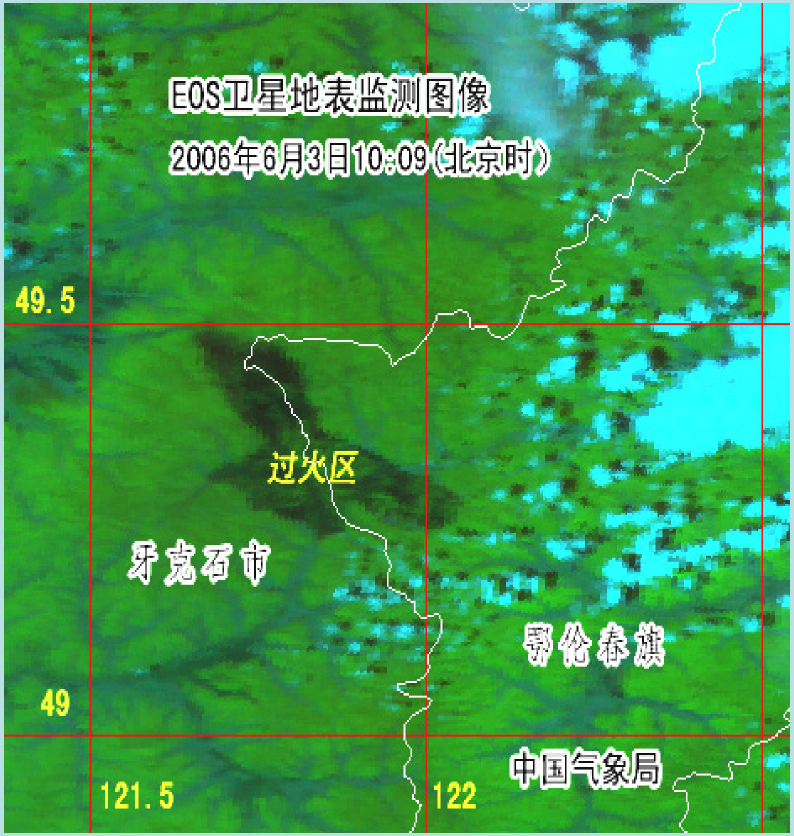

Fig. 4.16 EOS/MODIS 250m (2006/06/03)

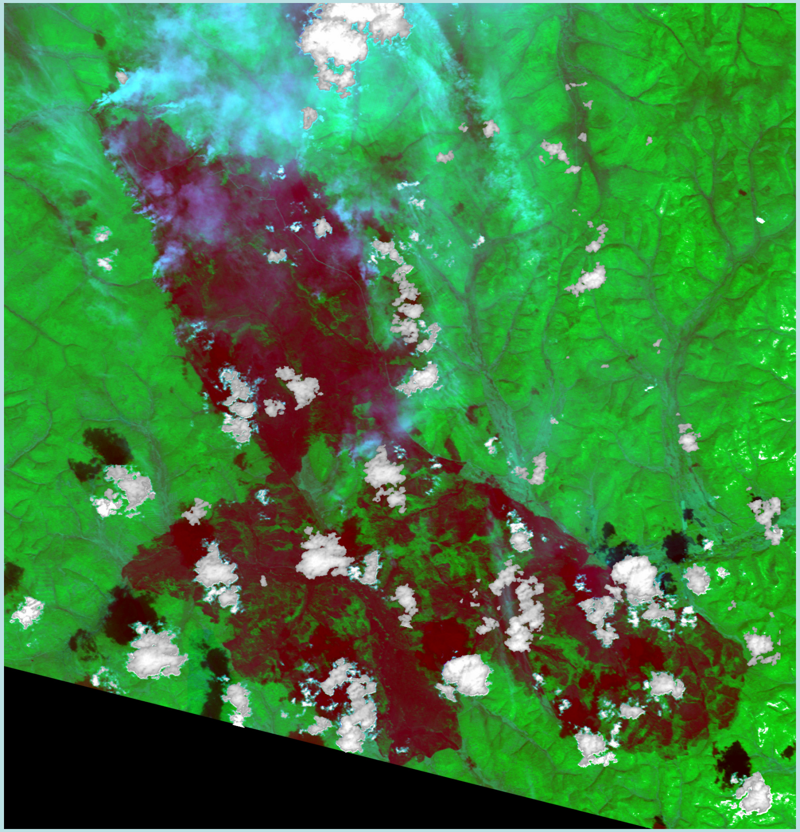

Fig. 4.17 CBERS-2 CCD 19.5m (2006/05/31)

CBERS CCD data can be used evaluating burned size. Its resolution is 19.5m.

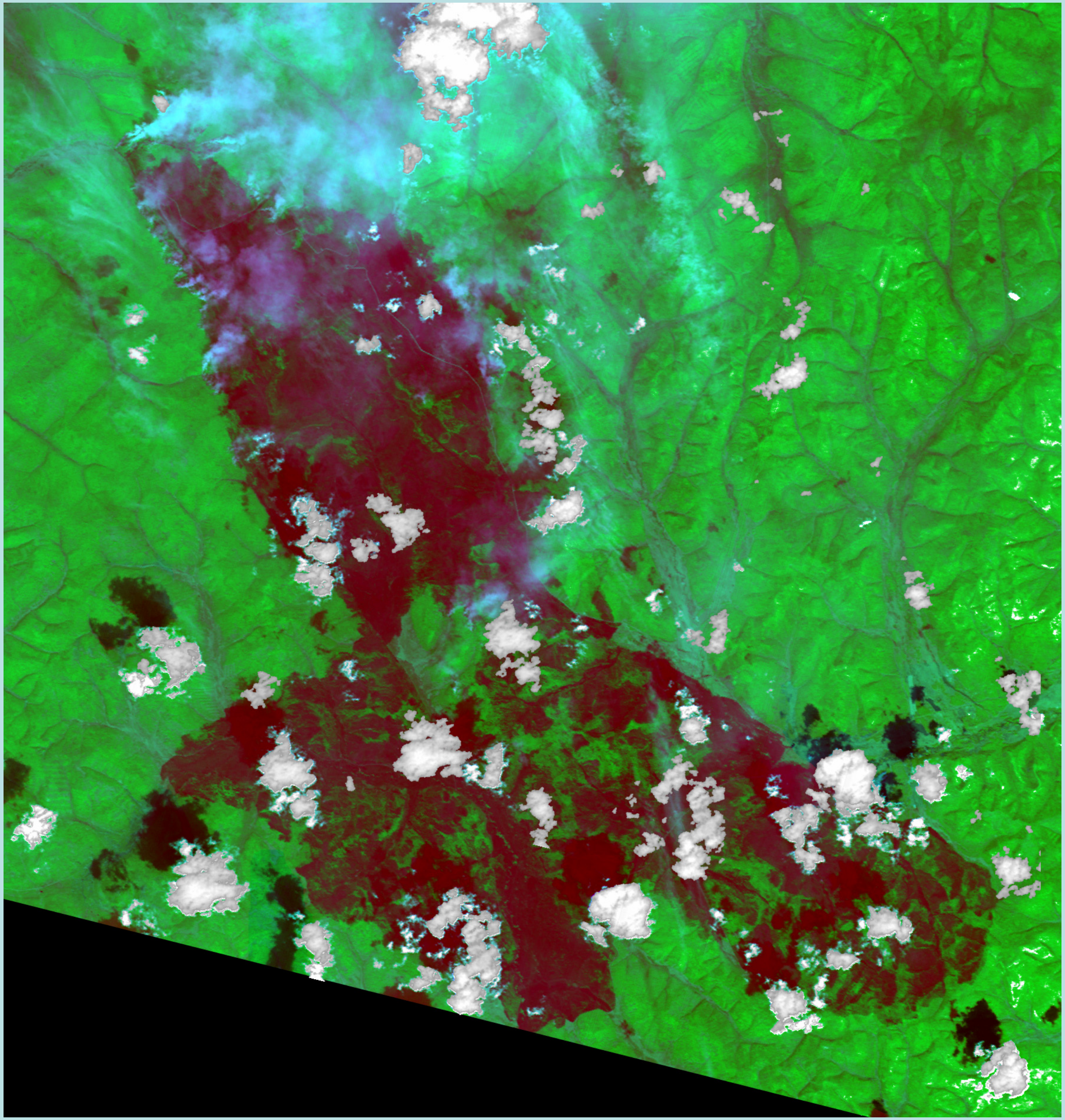

Fig. 4.18 CBERS-2 CCD multiple channel composition 19.5m 2006/05/31

3) Prediction for active fire field developing

2006年卫星遥感监测鄂伦春旗、黑河市过火区发展示意图

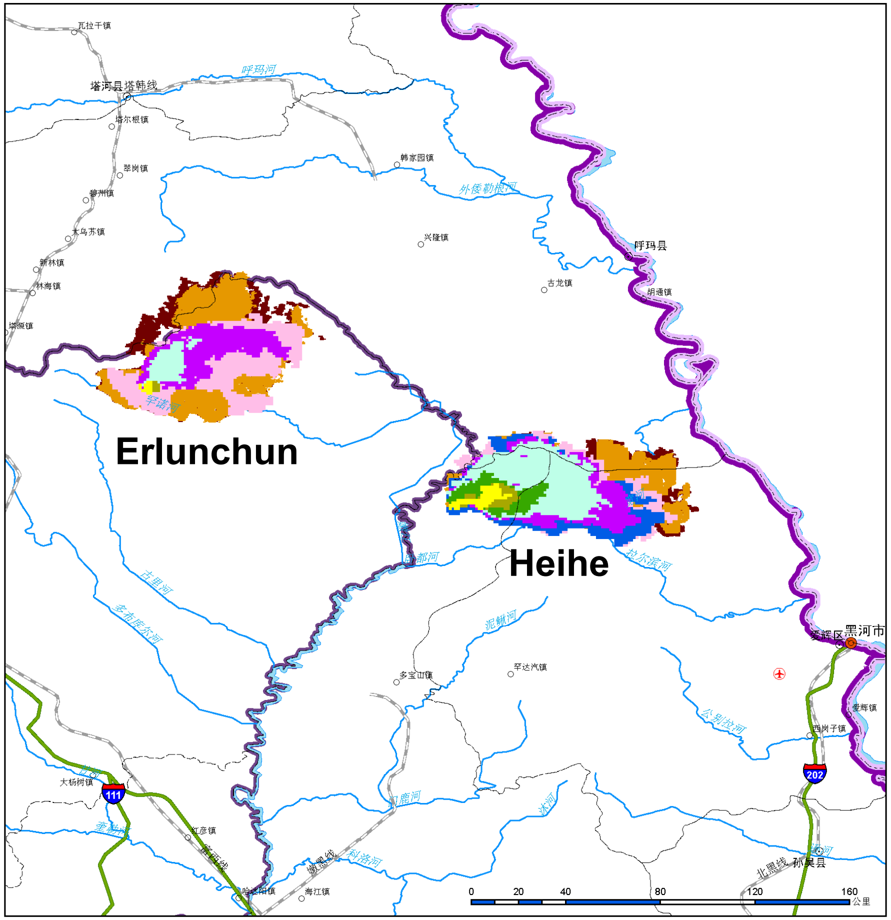

Fig. 4.19 Burned area developing in consecutive days

2006-05-23 06:57 过火区 May,23	2006-05-26 08:12 过火区 May,26	2006-05-29 07:47 过火区 May,29
2006-05-24 06:49 过火区 May,24	2006-05-27 08:04 过火区 May,27	2006-05-30 10:35(MODIS)过火区 May,30
2006-05-25 06:40 过火区 May,25	2006-05-28 13:03 过火区 May,28	2006-06-03 10:09(MODIS)过火区 June,3

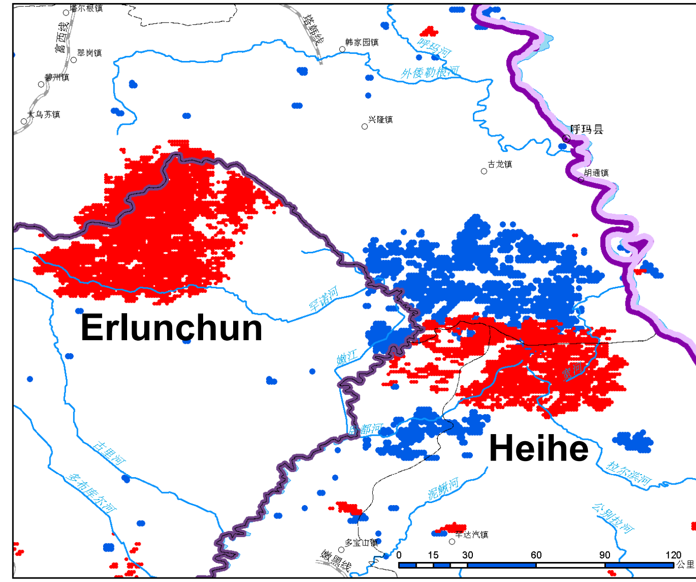

Fig. 4.20 Hot spot distribution · 2005 · 2006

根据各火场过火区逐日发展示意图，各火场发展范围具有以下特点。

1、 黑河市嫩江县火场持续向东蔓延，同时从25日向北蔓延至呼玛县境内，维持数日，未再深入发展。根据2005年和2006年卫星遥感火点分布分析，2005年10月呼玛县邻近黑河市嫩江县区域曾发生大范围火情，当地堆积可燃物已得到有效烧除，因而今年火场蔓延至该地后，火灾蔓延条件降低，没有向北急剧发展。

2、 鄂伦春旗火场主要向东和北方向蔓延，也曾向西部局部蔓延。根据2005年和2006年卫星遥感火点分布分析，鄂伦春旗火场周边地区2005年未发生火情，地面可燃物未得到清除，因而鄂伦春旗火场向呼玛县境内有较多的发展。

3、 牙克石市火场前期向东蔓延，后又转向西北方向发展。

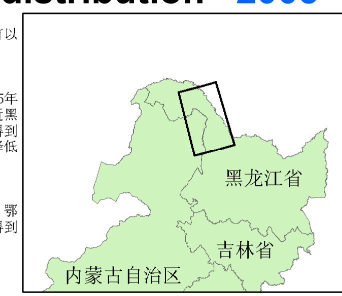

中国气象局
国家卫星气象中心
2006.06.07制作

Two huge forest fire, Heihe and Erlunchun, occurred almost in same period, but their expanding direction were different. Heihe field expanded mainly toward east, and Elunchun in several direction. The hot spot distribution map in 2005 and 2006 give some reasons .

4) Fire dangerous level prewarning

Using the hot spot information detected in the Northeast from 2000 up to May of 2006, we can generate a hot spot frequency grid in 0.5º*0.5º latitude and longitude, than make a hot spot frequency contour lines for these year and get remote sending fire dangerous index map. From this map, we can see that Heihe Region in the Northeast has 6 times per 100 km^2 area each year, so should become a highest fire dangerous level region .

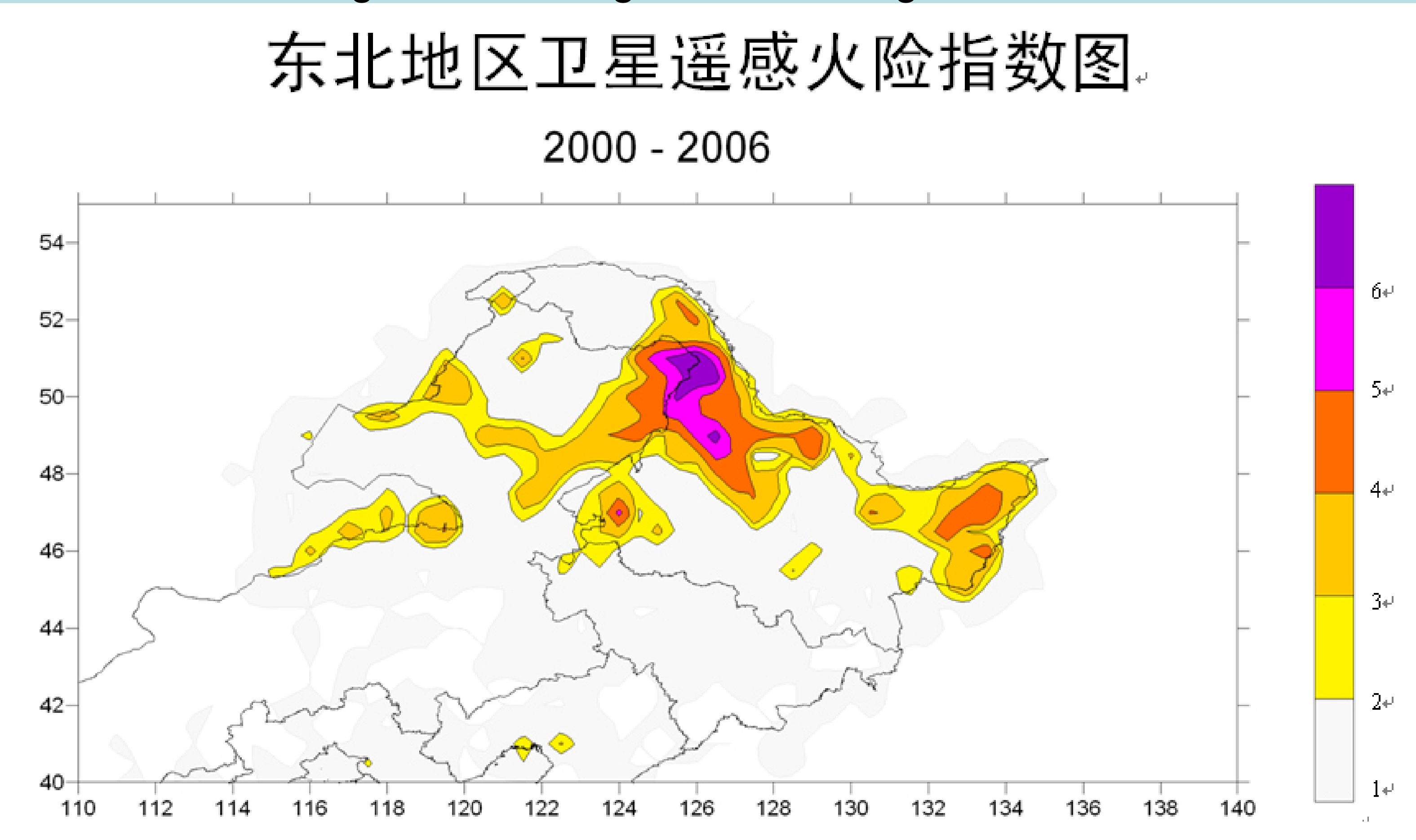

Fig. 4.21 Remote sending fire dangerous index map in 2000-2006

Furthermore, we can get the hot spot frequency contour maps for each month. From these maps, we can see that the high frequency of hot spot in   Heihe Region is in Spring and Autumn when there are 4 times per 100 km^2.

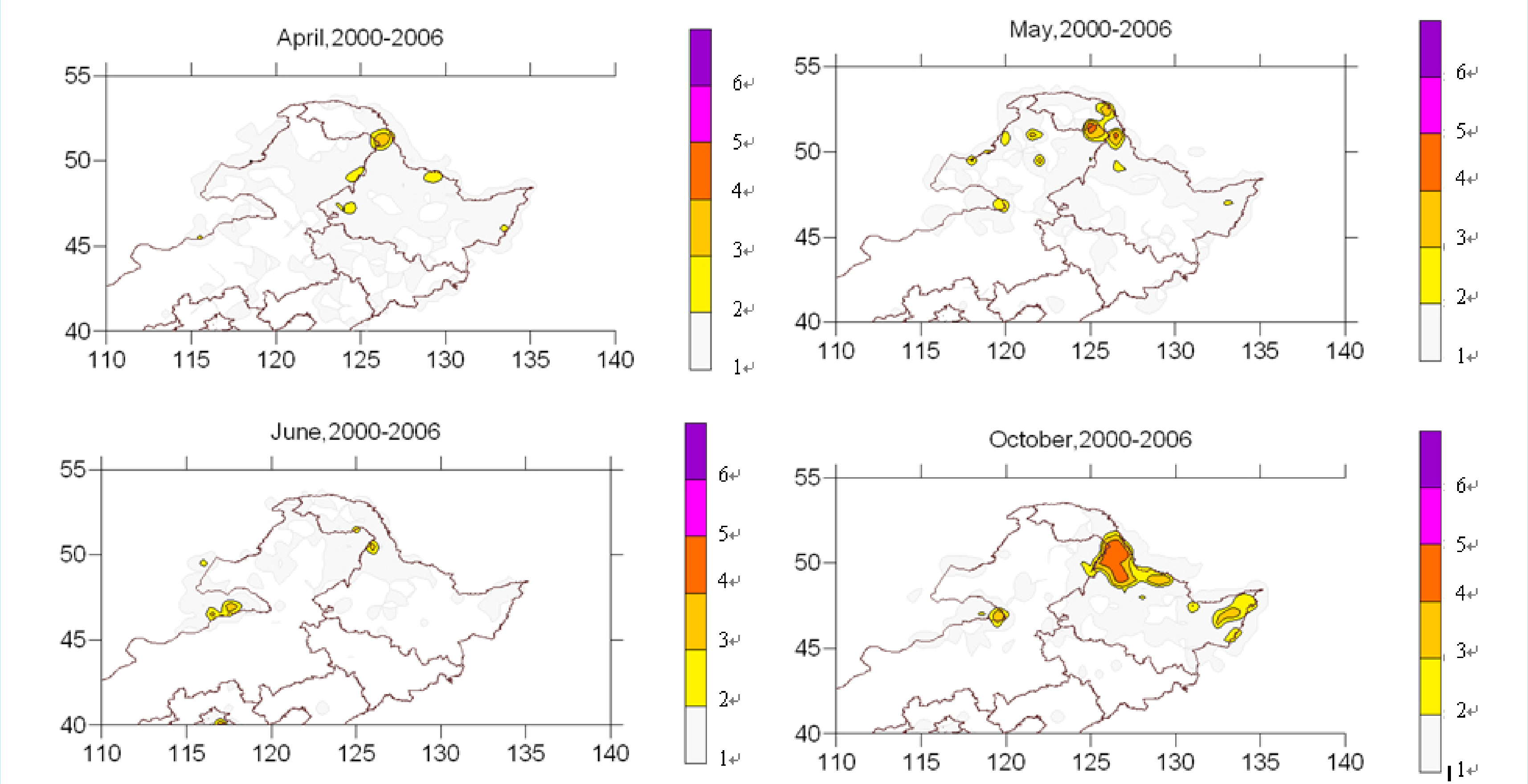

东北地区月火险分布图

Fig. 4.22 remote sending fire dangerous index map in every month.

5) Regional fire situation evaluation

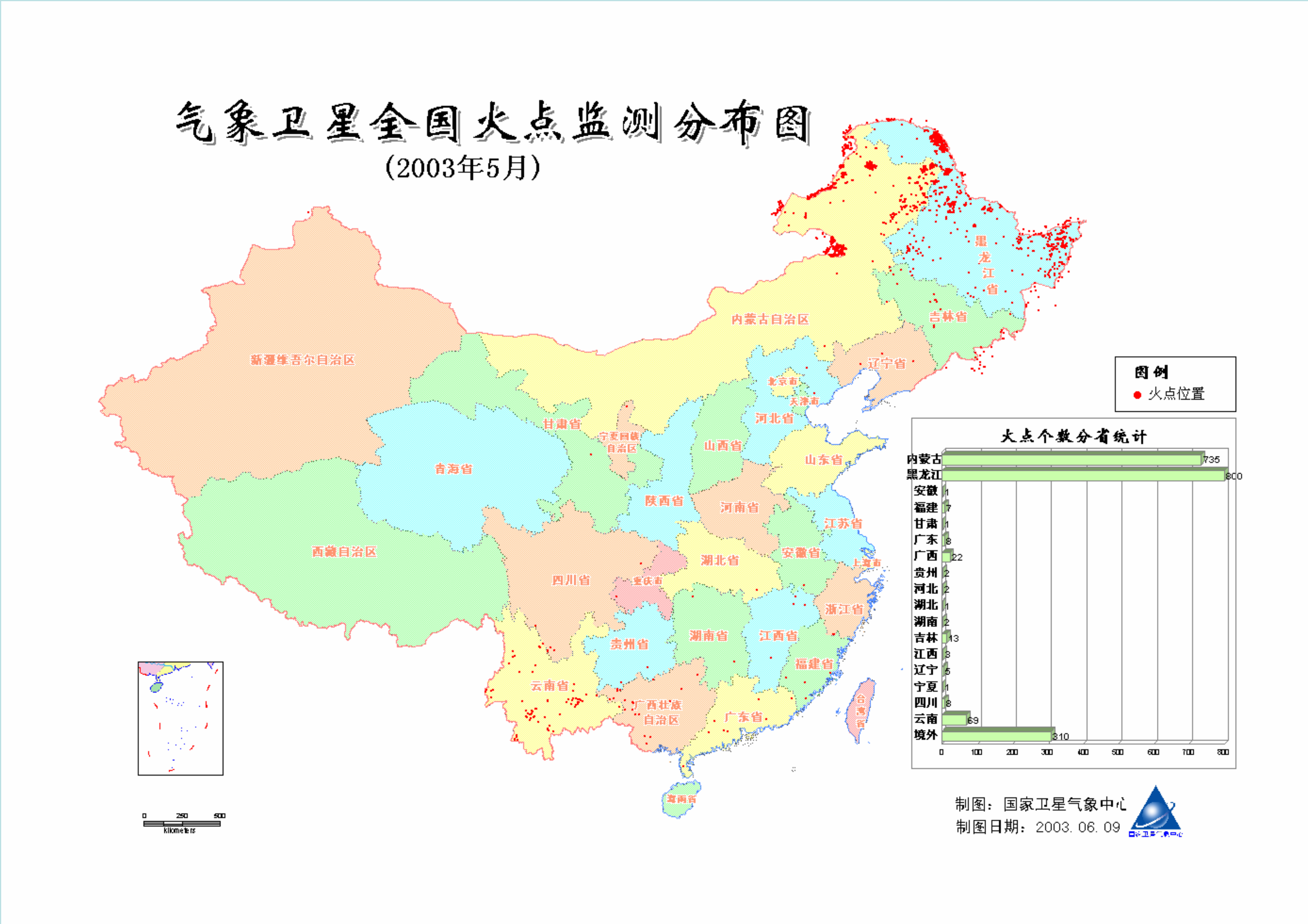

Fig. 4.23 Hot Spot Distribution Statistics in May of 2003

Hot Spot Distribution Statistics in political region Summer season o 2003 vs 2002

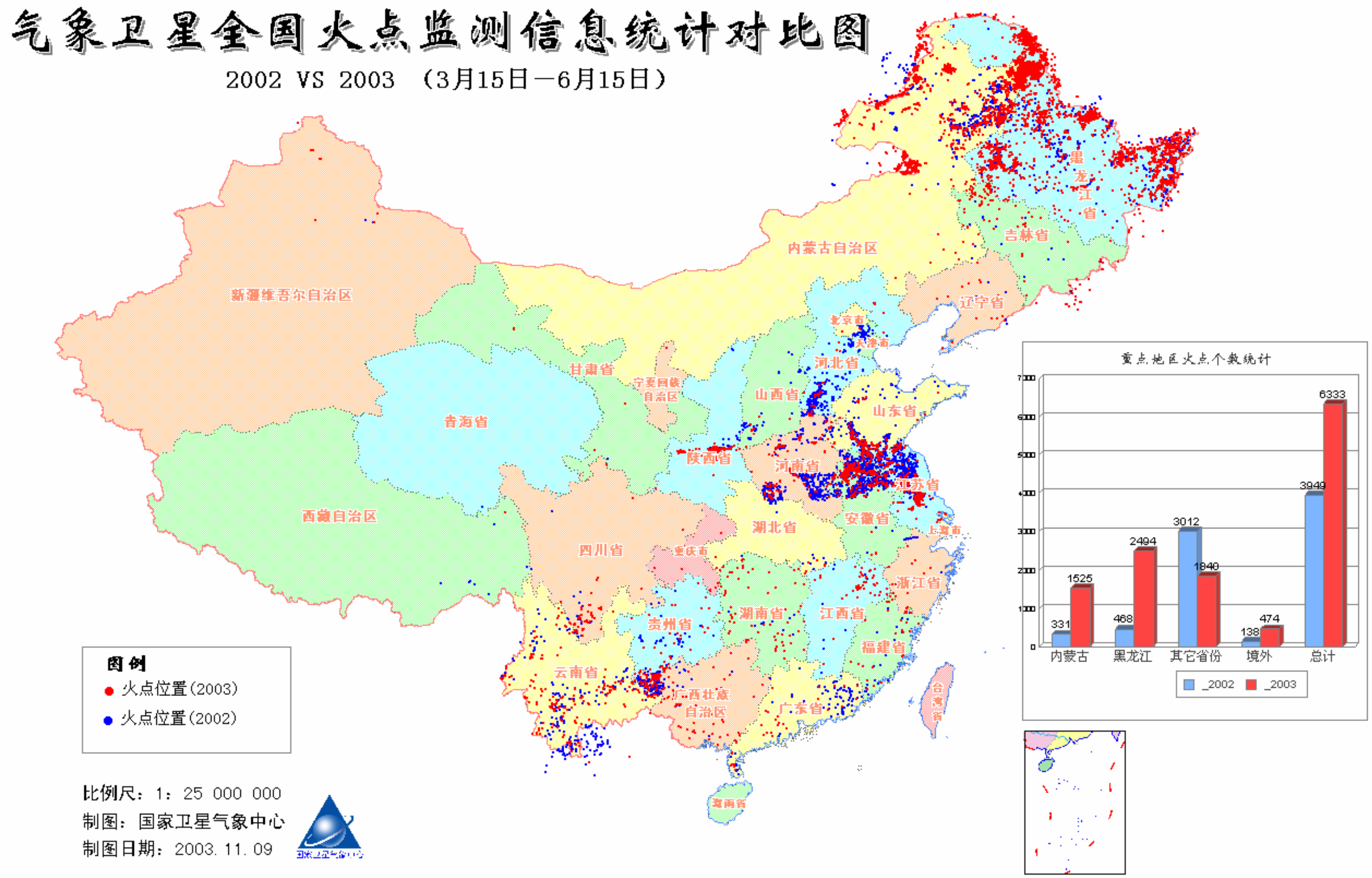

Fig. 4.24 Hot Spot Distribution Statistics in Summer season of 2003 vs 2002

Hot Spot Distribution Statistics in land utilization type Summer season of 2003 vs 2002

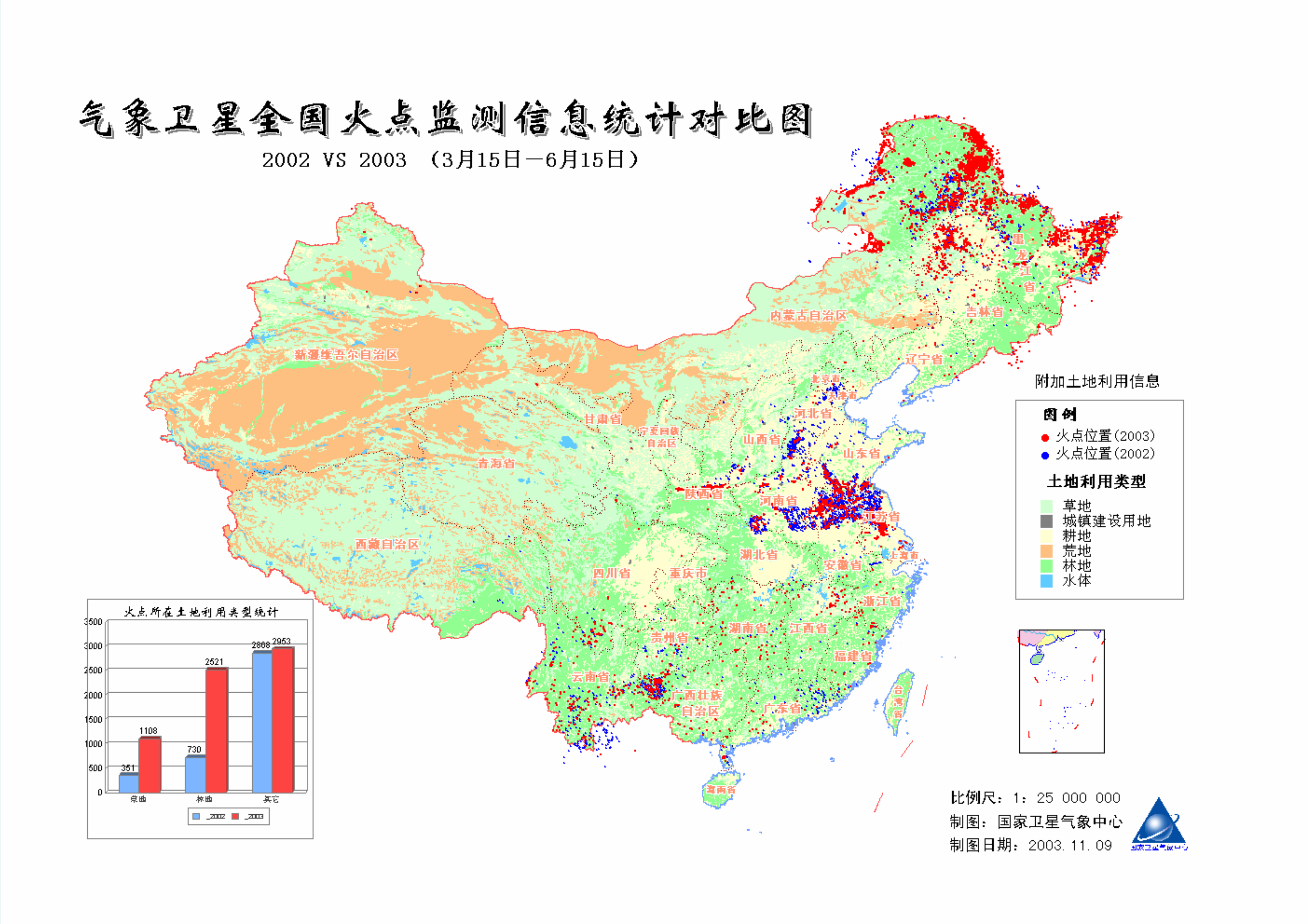

Fig. 4.25 Hot Spot Distribution Statistics in Summer season of 2003 vs 2002

Fig. 6.26 Hot Spot Distribution Statistics (Provincial)

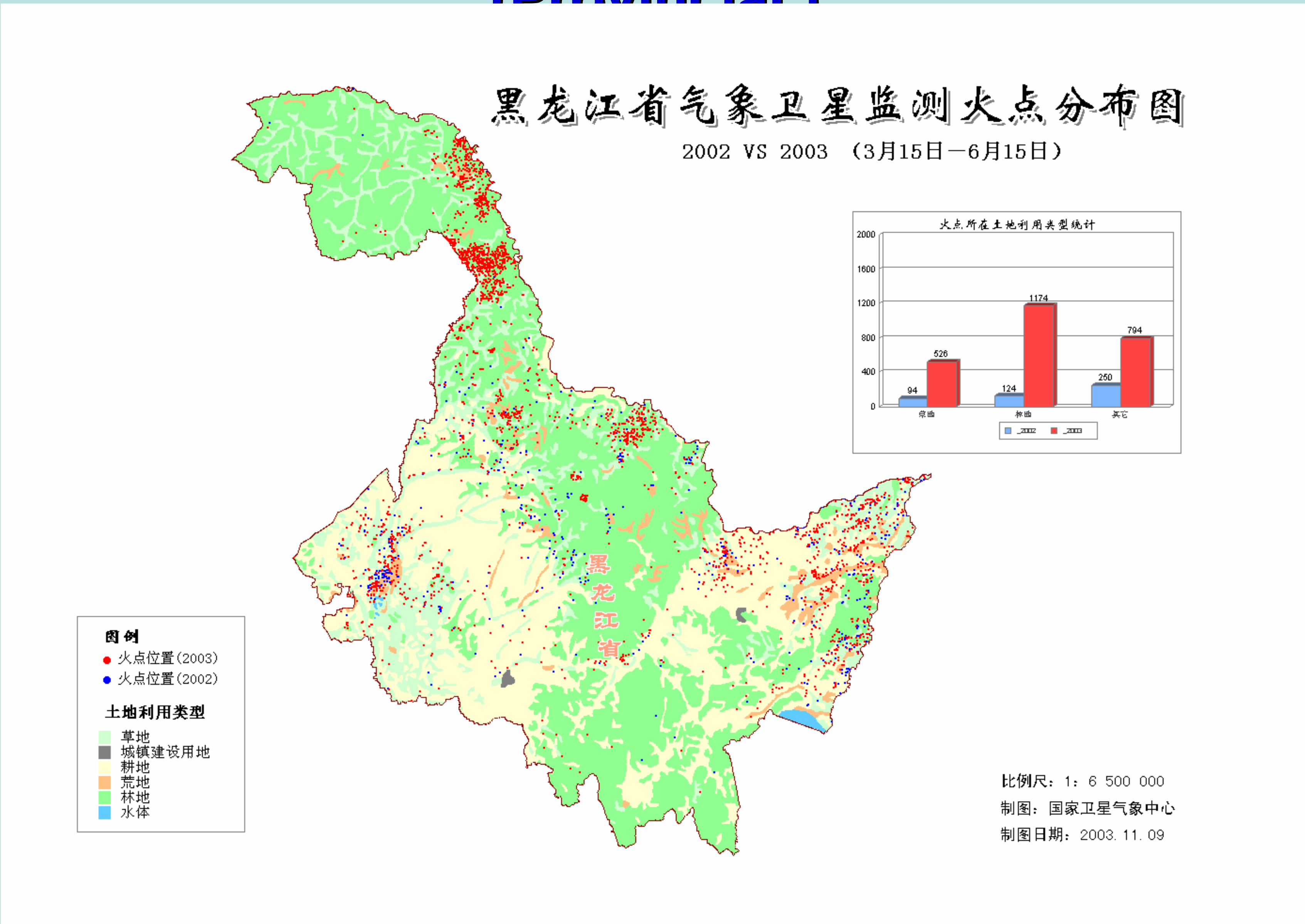

Fig. 4.26 Hot Spot Distribution Statistics (Provincial)

Hot Spot Distribution Statistics (Provincial)

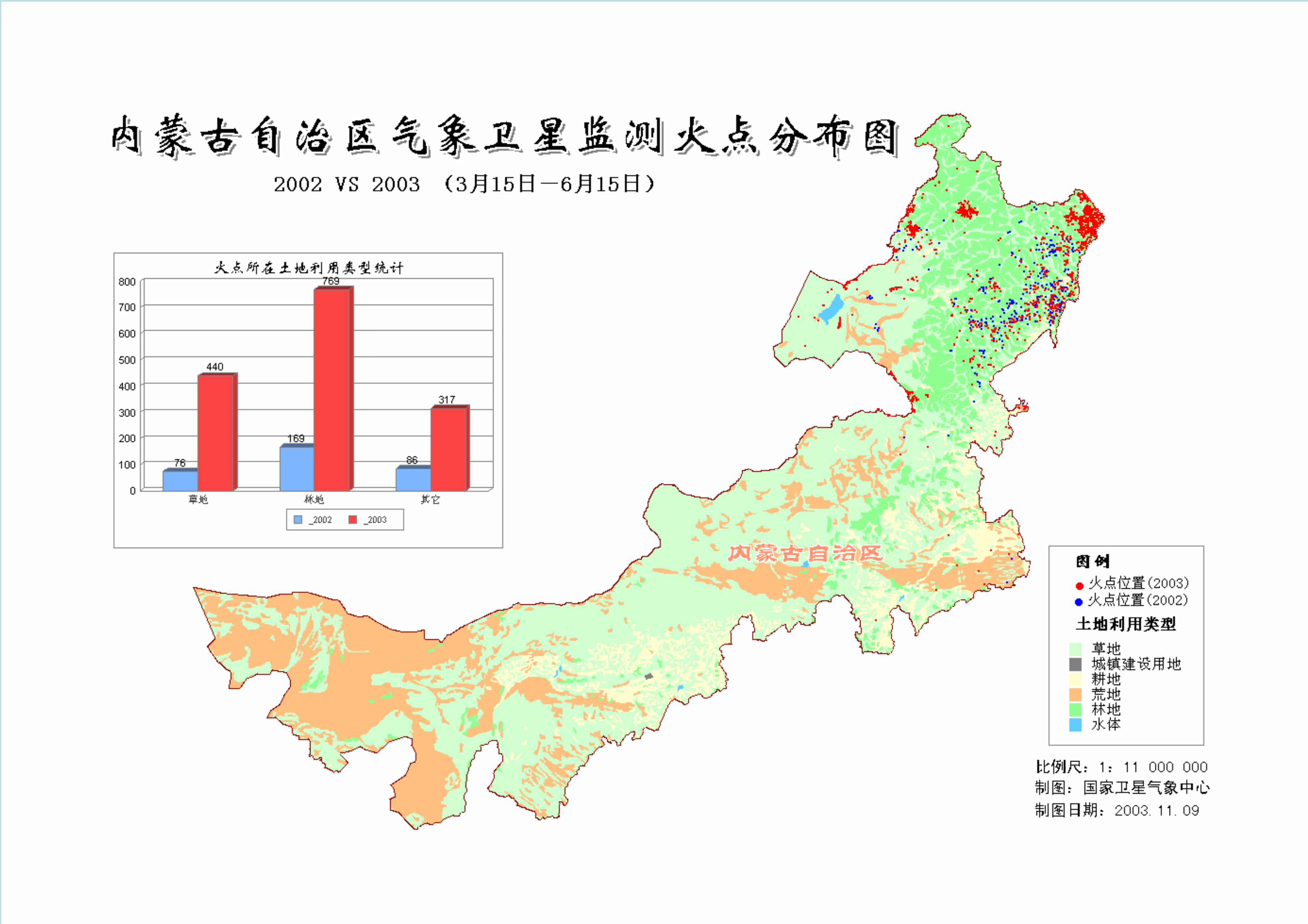

Fig. 4.27Hot Spot Distribution Statistics (Provincial)

6) Weather condition on forest and grass land fire dangerous level forecasting

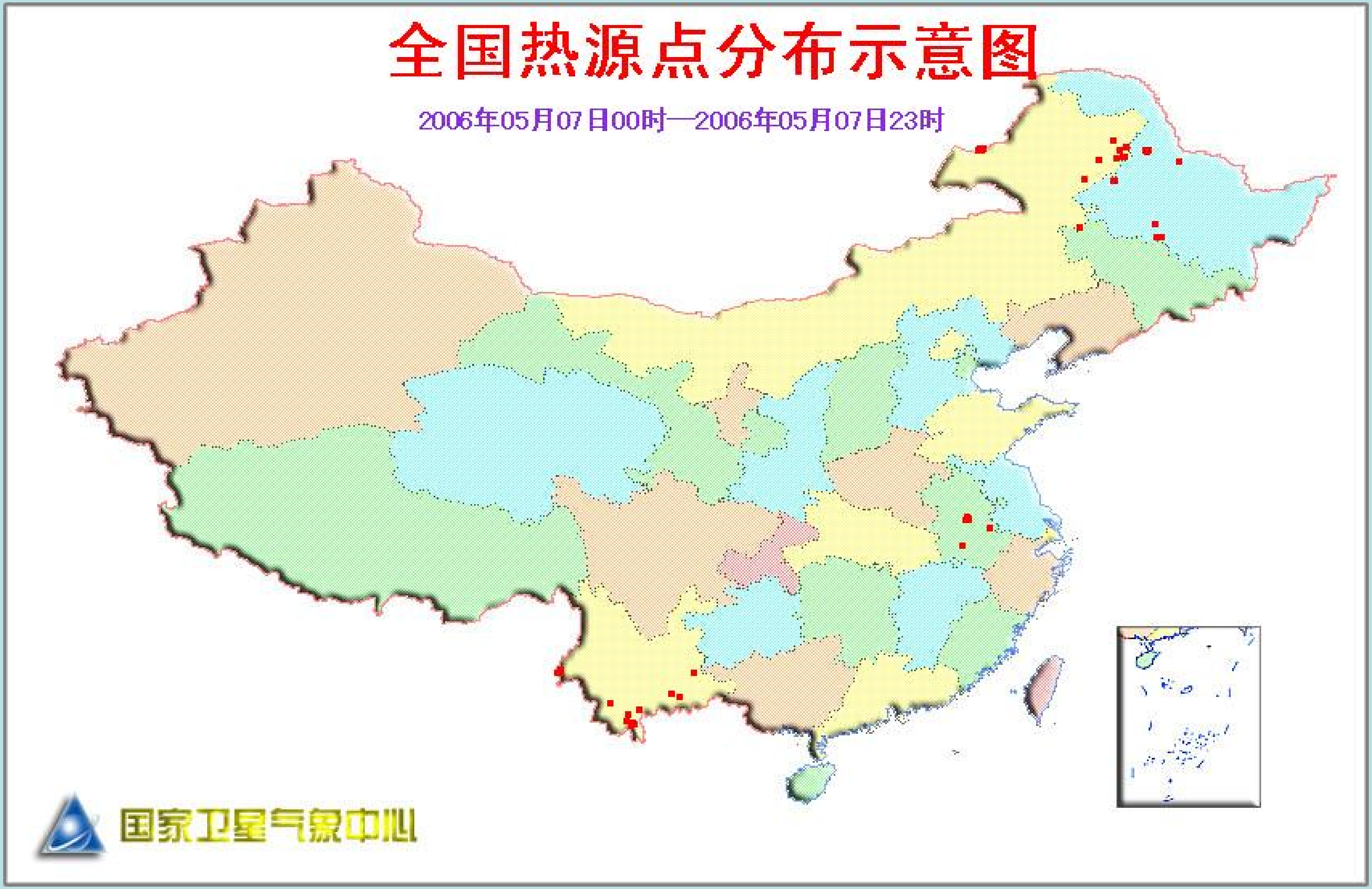

Fig. 4.28 Daily hot spot distribution map generated real time

Thanks for your attention!